Low dimensional materials and their Physical Property

Wei-Li Lee, IoP, Academia Sinica

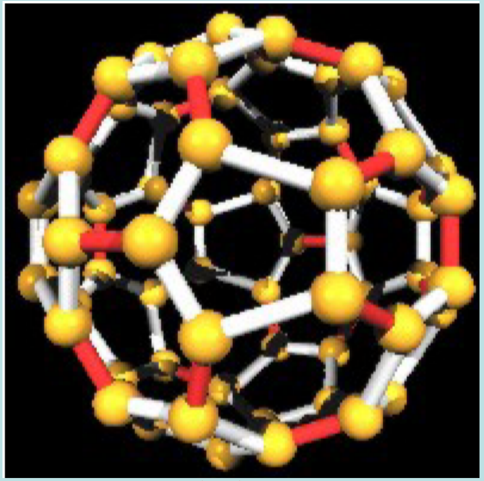

I: Fullerene

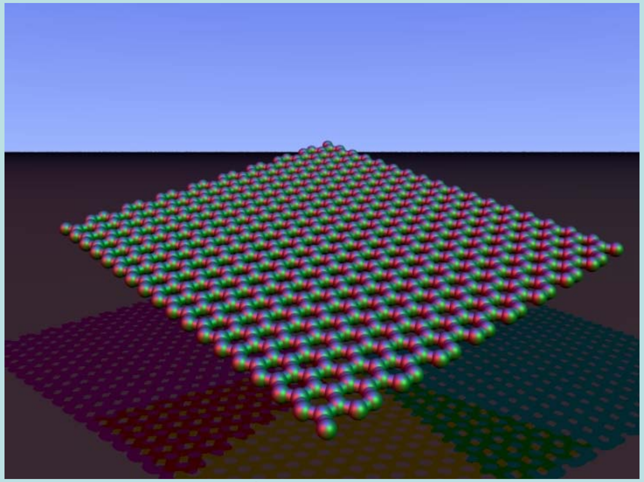

II: Graphene

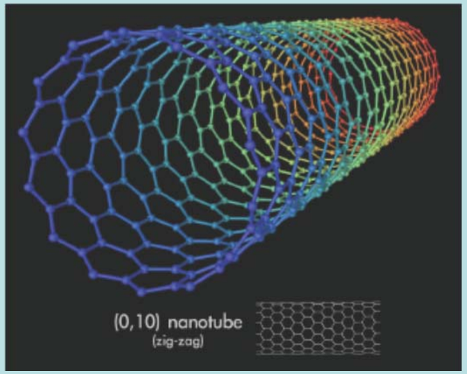

III: Carbon nanotube

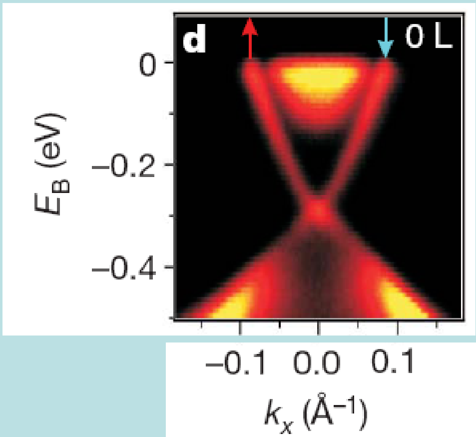

IV:Topological Insulator

Welcome to Carbon World !!

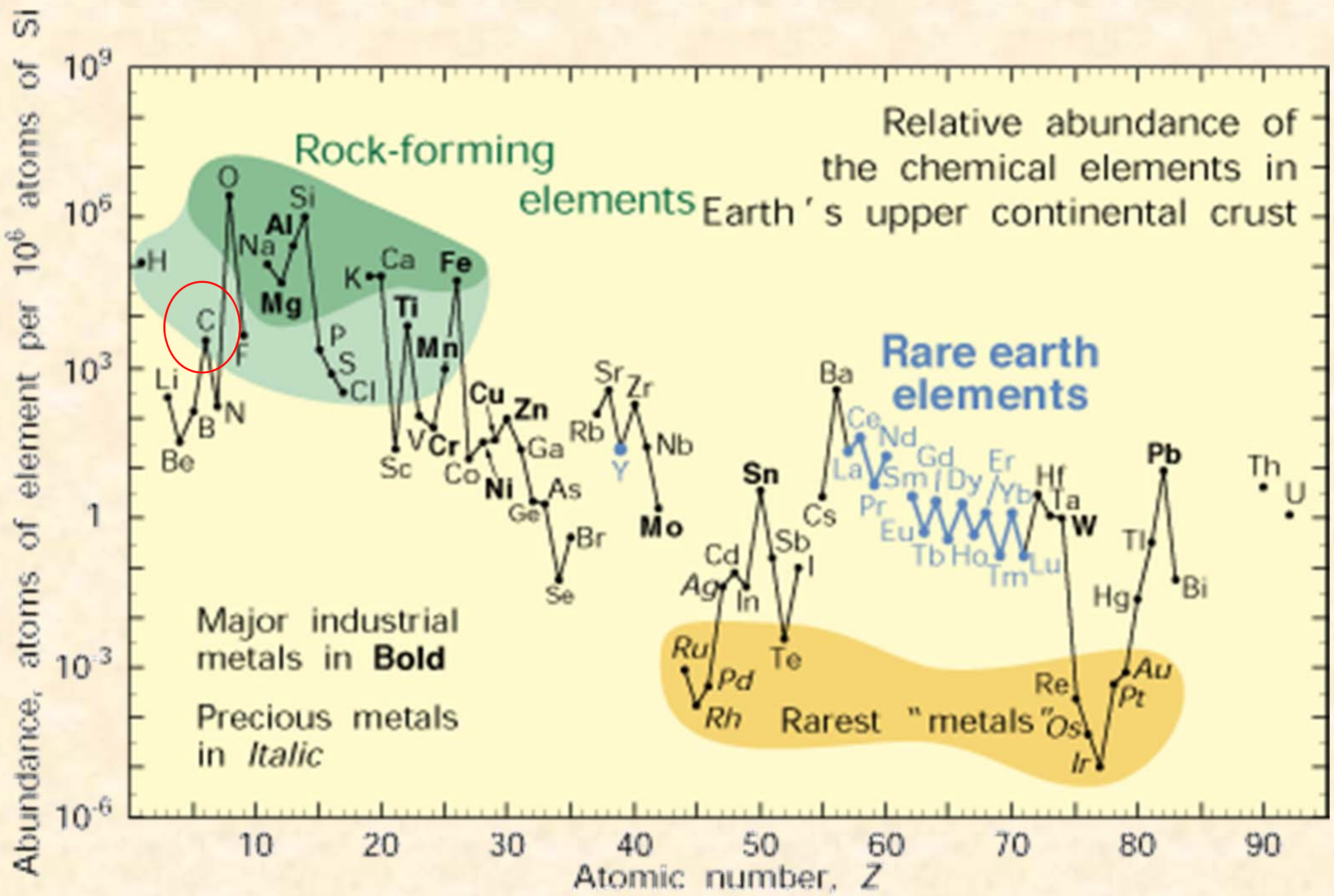

Wilkenson Microwave Anisotropy Probe

WMAP image of CMB (3 Kelvin)

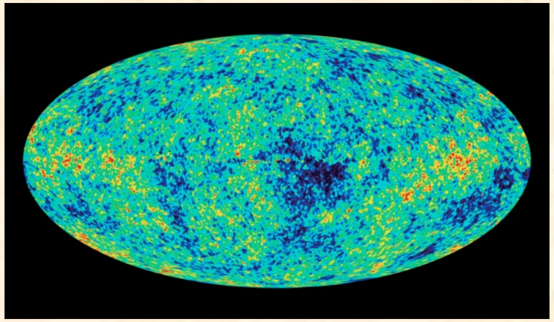

Angular spectrum

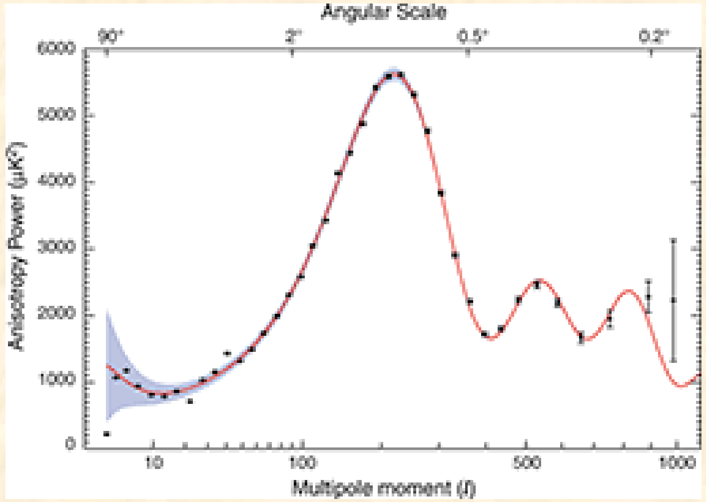

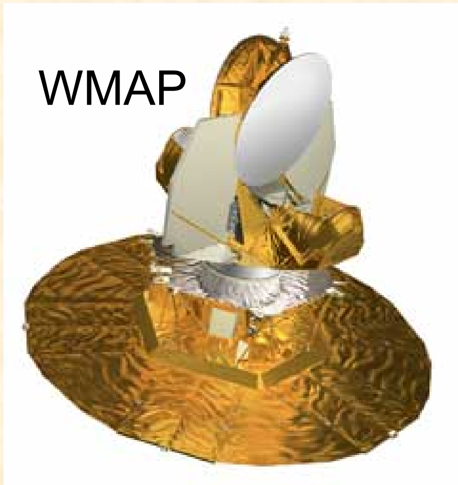

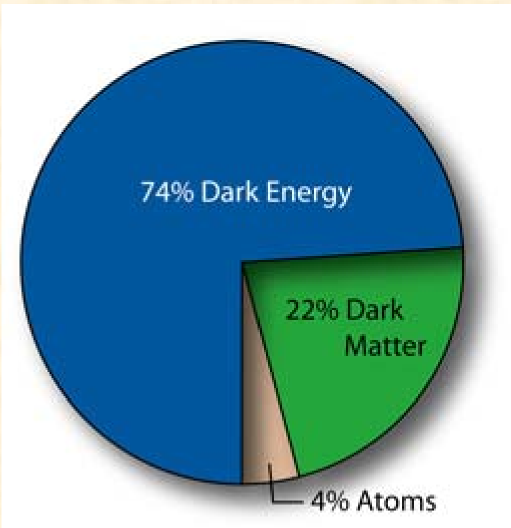

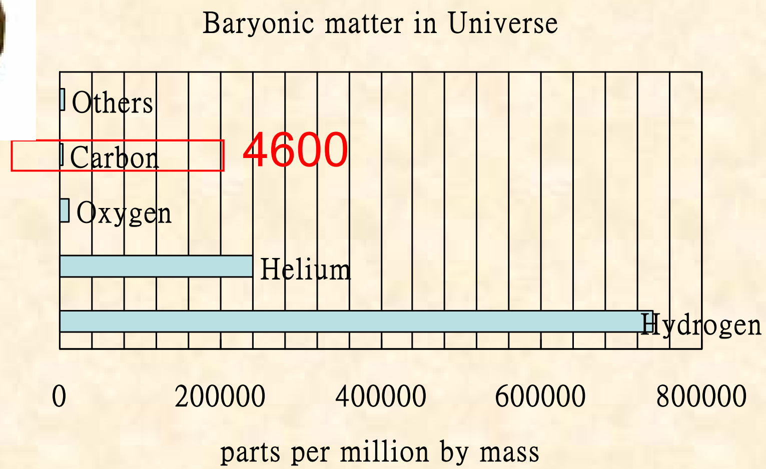

The Nobel Prize in Physics 1978

"for their discovery of cosmic microwave background radiation"

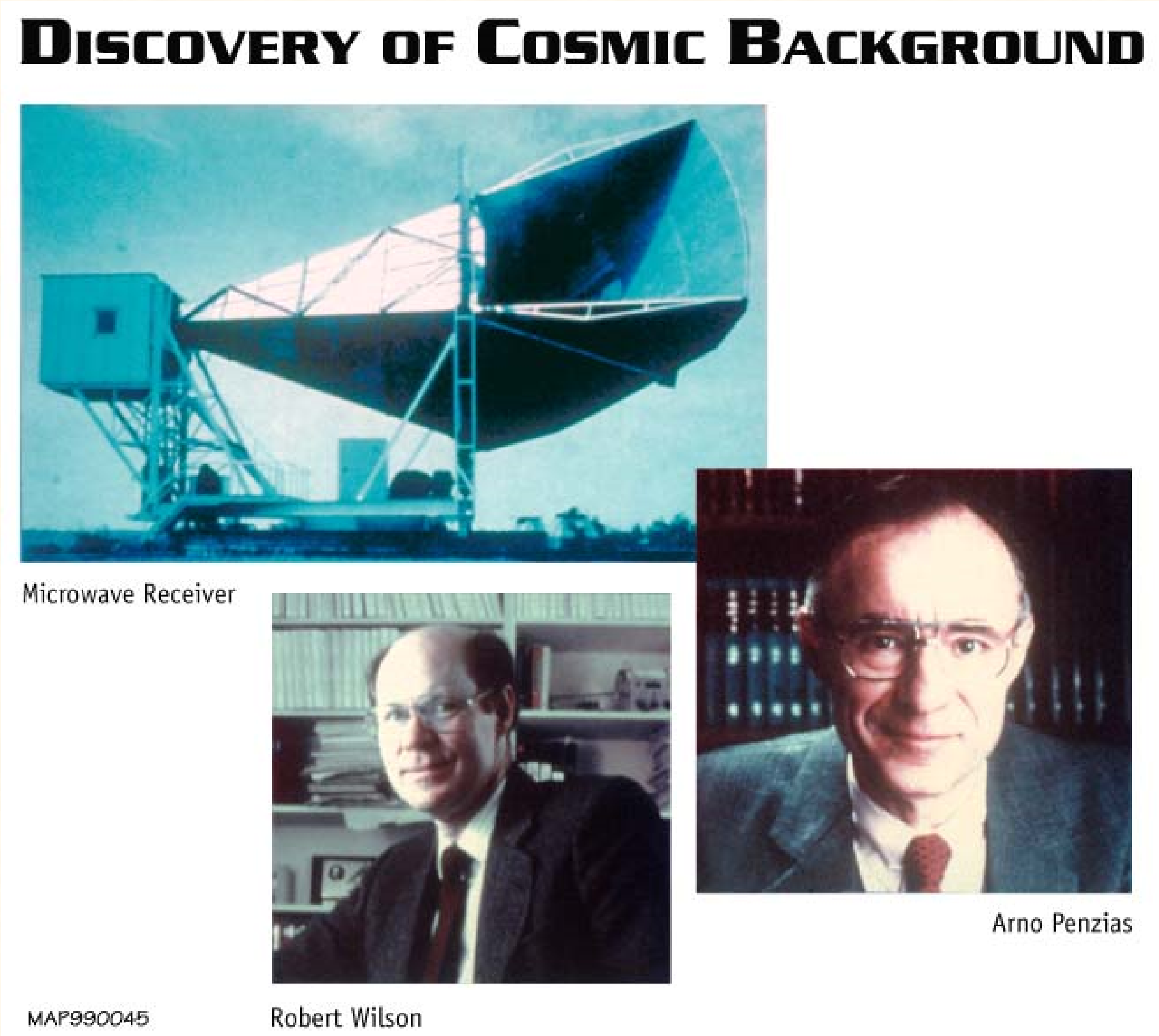

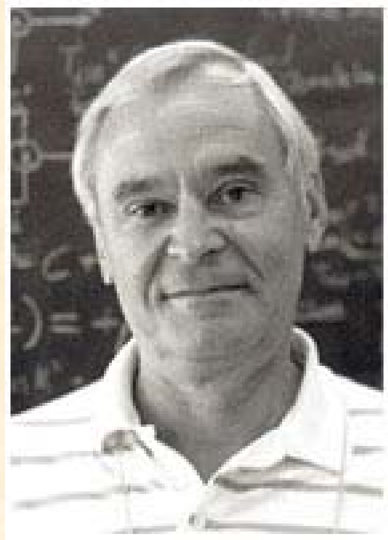

Dave Wilkinson

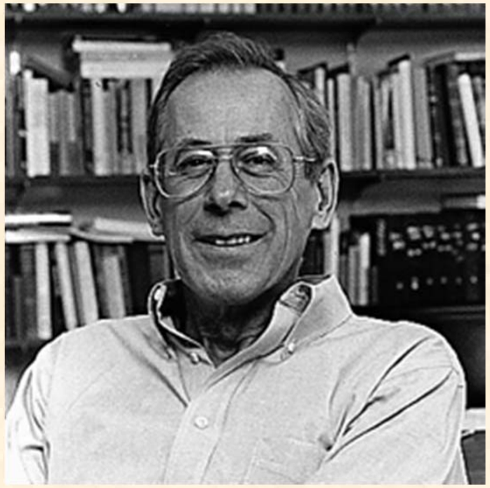

James Peebles

Carbon Bond : hybridized orbitals

- Carbon : atomic number 6, $1s^2$ [$2s^2$ $2px^1 2py^1$]

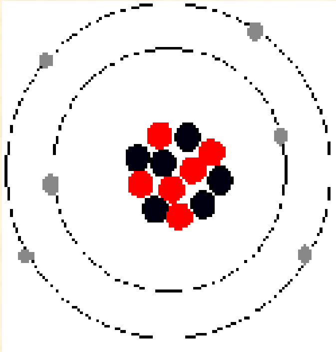

Molecular orbital :

$$\psi_j = \sum_i C_{ij} X_i$$

X_i : atomic orbitals

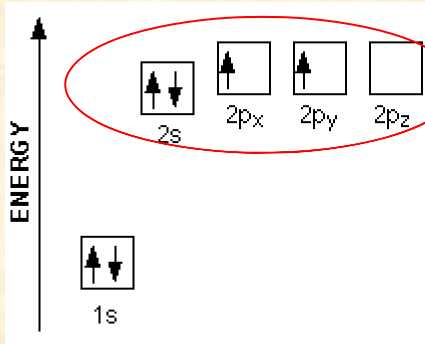

	Orbitals used for bond	Shape & bond angle	Examples:	
Sp	s, px	Digonal 180°	C_2H_2 Acetylene	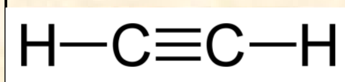
Sp^2	s, px, py	Trigonal 120°	Graphite, C_2H_4 Ethylene	
sp^3	s, px, py, pz	Tetrahedra 109°28’	Diamond, CH_4 Methane	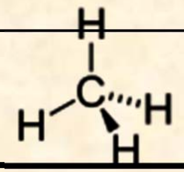

Allotropic forms in solid carbon

- **Many stable and known forms at R.T.**

Examples: diamond, graphite, amorphous carbon, fullerene, carbon nanotube and nanobud…etc

- **Two main structures :** one with sp^3 hybrid bonds (diamond) and the other with sp^2 hybrid bonds (graphite, fullerene, nanotube and nanobud)

- Dramatic different properties between diamond and graphite

	Diamond	**Graphite**
Electric	Insulator	Conductive
Hardness	10 (Mohs scale)	1-2
Appearance	Transparent	Opaque (black)
Value	Expensive	cheap

Structure of C_{60}

- European Football like molecule containing 60 carbons
  - 12 pentagonal and 20 hexagonal faces
  - Double bond length 1.4 Å and single bond 1.46 Å
- Named after architect R. Buckminster Fuller (1895-1983)

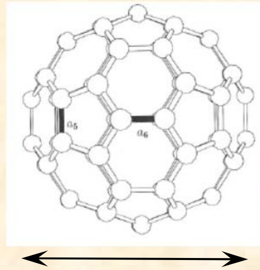

7.1 Å

Geodesic dome

- Geometrically-allowed fullerene C_{20+h*2}

12 pentagonal faces + arbitrary number of hexagonal faces (h)

- Smallest Fullerene C_{20}
- Smallest isolated (stable) Fullerene C_{60}

Euler's theorem for polyhedral:

$$f + v = e + 2, \quad f : \#\text{of faces}, v : \#\text{of vertices}$$
$$e : \#\text{of edges}$$

Discovery of Fullerene C_{60}

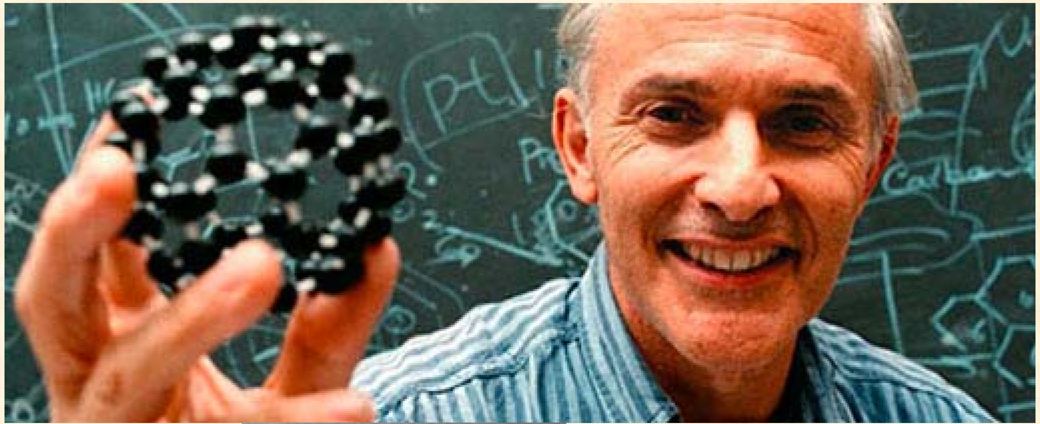

“An idea from outer space”
5.6 eV optical extinction

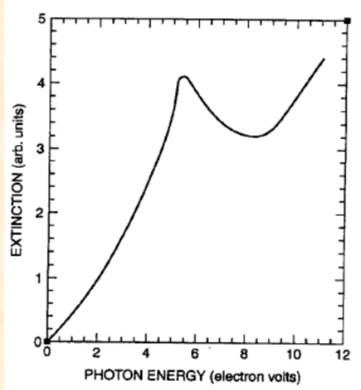

Harold Kroto
Univ. of Sussex
at Brighton UK

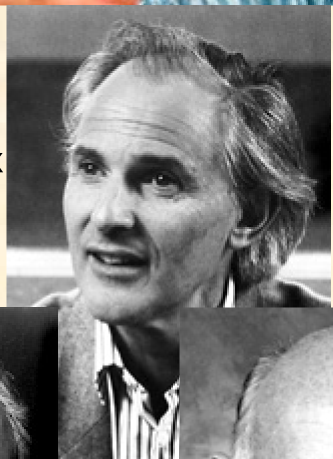

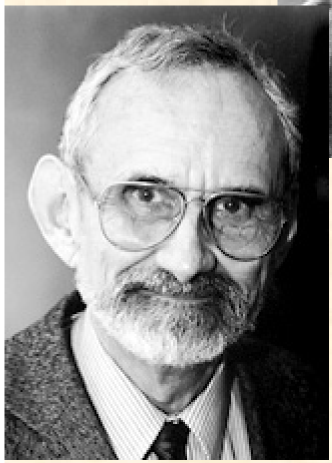

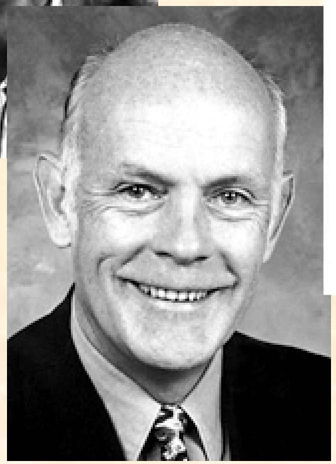

Robert Kurl, and Richard Smalley, Rice Univ. at Houston

Nobel Prize laureates in Chemistry 1996

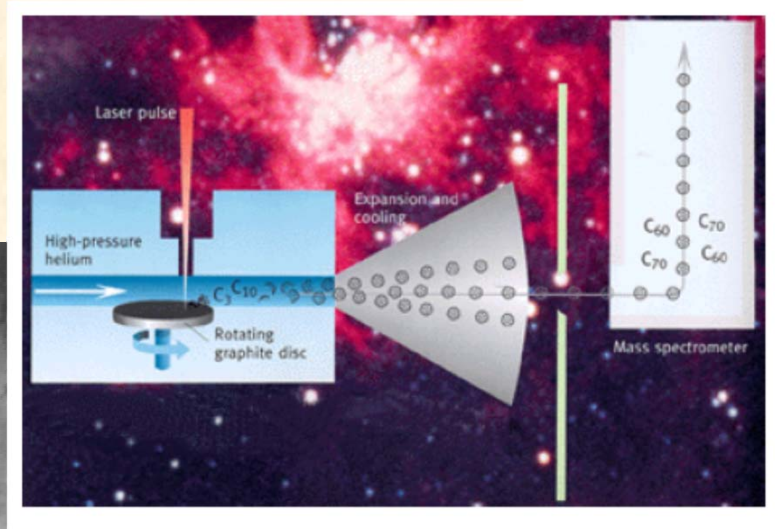

C60 and C70 clusters:

- Highly stable
- react weakly with gases

A molecule with
great symmetry as a sphere

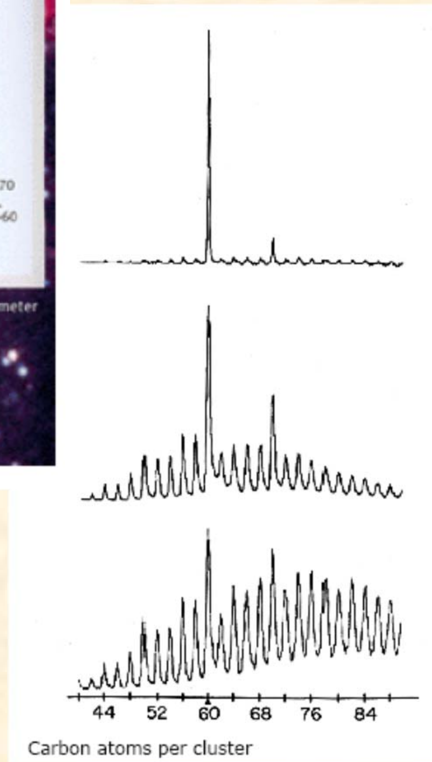

Development of Fullerene

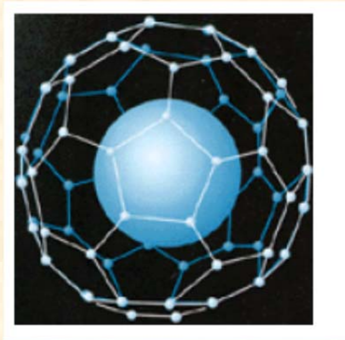

- Carbon ball with a metal core
- Mass production of Fullerene by astrophysicists D. R. Huffmann and W. Krätschmer
- Carbon nanotube – special electric and mechanical properties
- New superconducting crystals M_3C_{60}

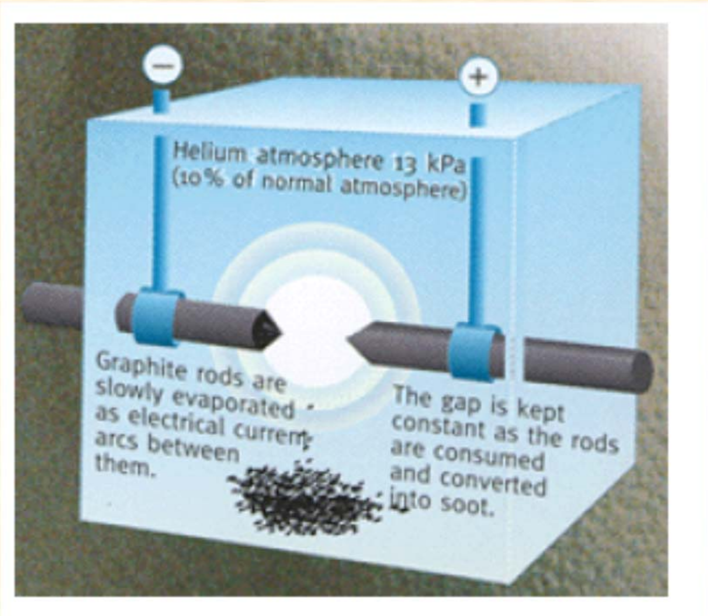

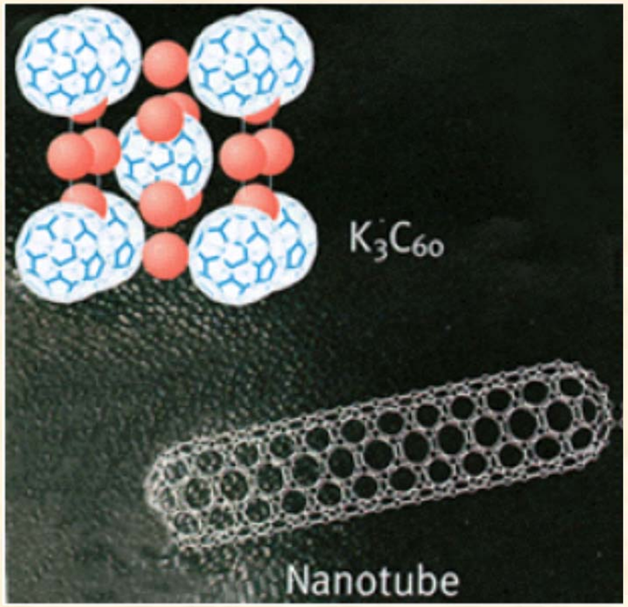

Adsorption of free-radicals(自由基) using Water-Soluble Fullerene C_{60}

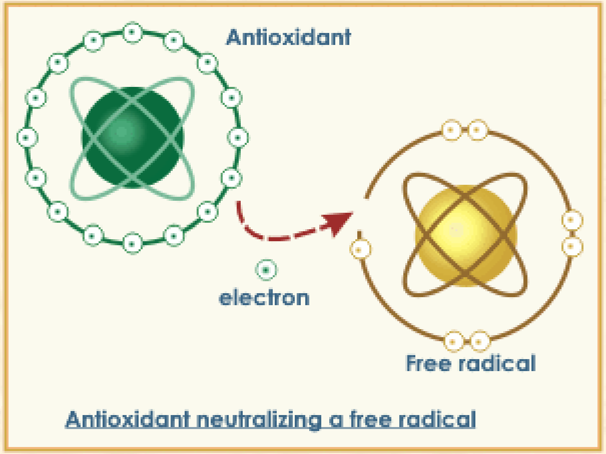

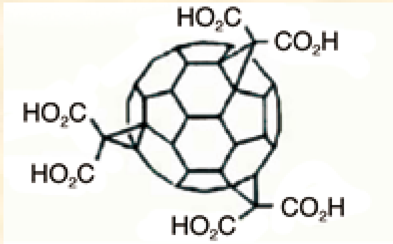

Water-soluble C_{60}

Free-radicals refer to atoms or molecules containing unpaired electrons at the surface. They are highly reactive and can cause damage to the cell or tissue by removing their electrons.

C_{60} can effectively bond to the free-radicals and has been used as an ingredient in anti-oxidant medicine.

Effect of size and dimensionality on electronic property

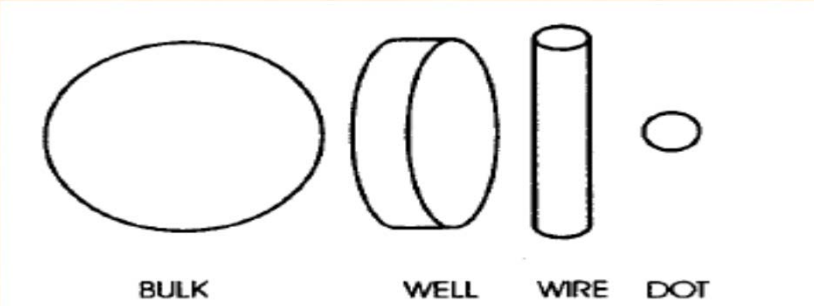

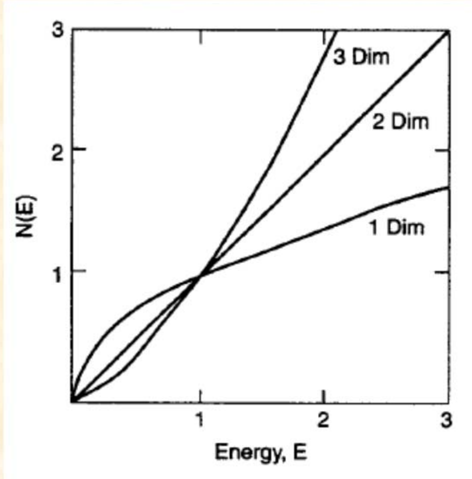

Table 9.4. Number of electrons N and density of states $D(E) = dN(E)/dE$ as a function of the energy E for conduction electrons delocalized in one, two, and three spatial dimensions[a]

Number of Electrons N	Density of States $D(E)$	Delocalization Dimensions
$N = K_1E^{1/2}$	$D(E) = \frac{1}{2}K_1E^{-1/2}$	1
$N = K_2E$	$D(E) = K_2$	2
$N = K_3E^{3/2}$	$D(E) = \frac{3}{2}K_3E^{1/2}$	3

[a]The values of the constants K_1, K_2, and K_3 are given in Table A.2 (of Appendix A).

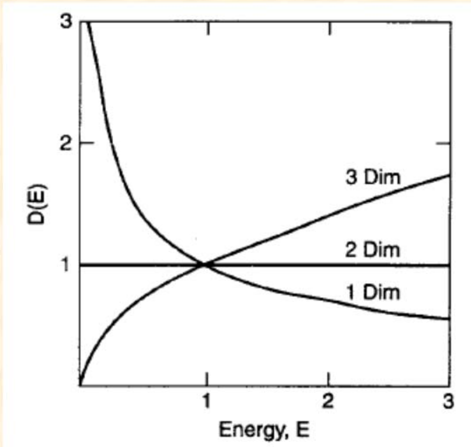

0-D quantum dot : an artificial atom

- quasi-0D system : d < ℓ_{mfp}

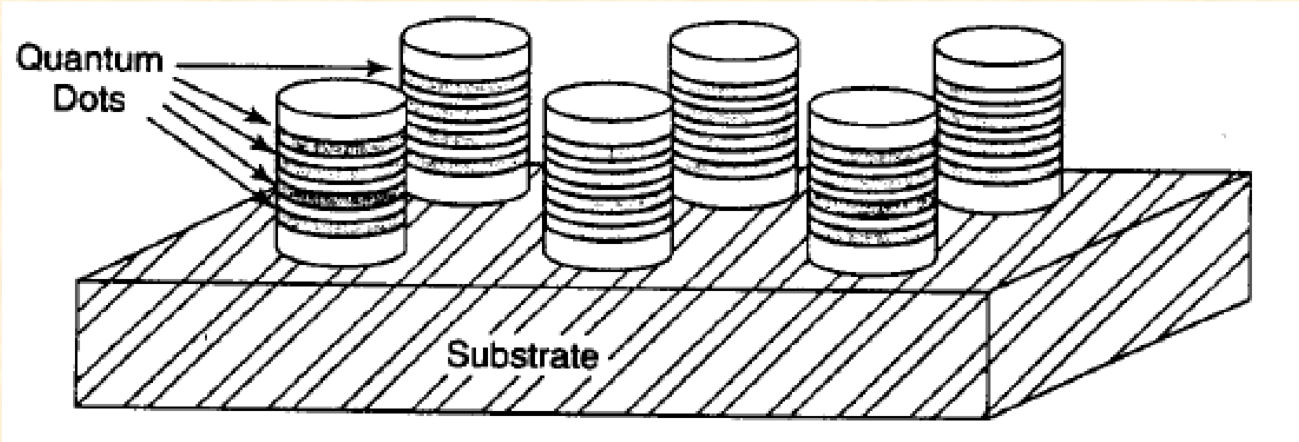

- Discrete energy level resembles the atomic level of a free atom
  - ex : 3-D infinite rectangular square well

$$E_n = \left(\frac{\pi^2\hbar^2}{2ma}\right)(n_x^2 + n_y^2 + n_z^2) = E_0 n^2$$

Quantum number = 0,1,2…

6 degeneracy (including spin) at ground state level E_o

Drude model (3-D): $\boxed{\ell_{mfp}(\rho, n) = \frac{(3\pi^2)^{1/3}\hbar}{e^2\rho \cdot n^{2/3}}}$

- For a metal: n ~ 10^{23} cm^{-3} and ρ = 10^{-8} Ohm-m ℓ_{mfp}~ 59 nm
- For a semiconductor with n ~ 10^{16} cm^{-3} and ρ = 10^{-5} Ohm-m, ℓ_{mfp}~ 2,700 nm

Molecular orbital levels of a "free" C_{60}

- Shell model in a free fullerene : symmetry-based model
- 60 π-electrons filling the molecular level

LUMO

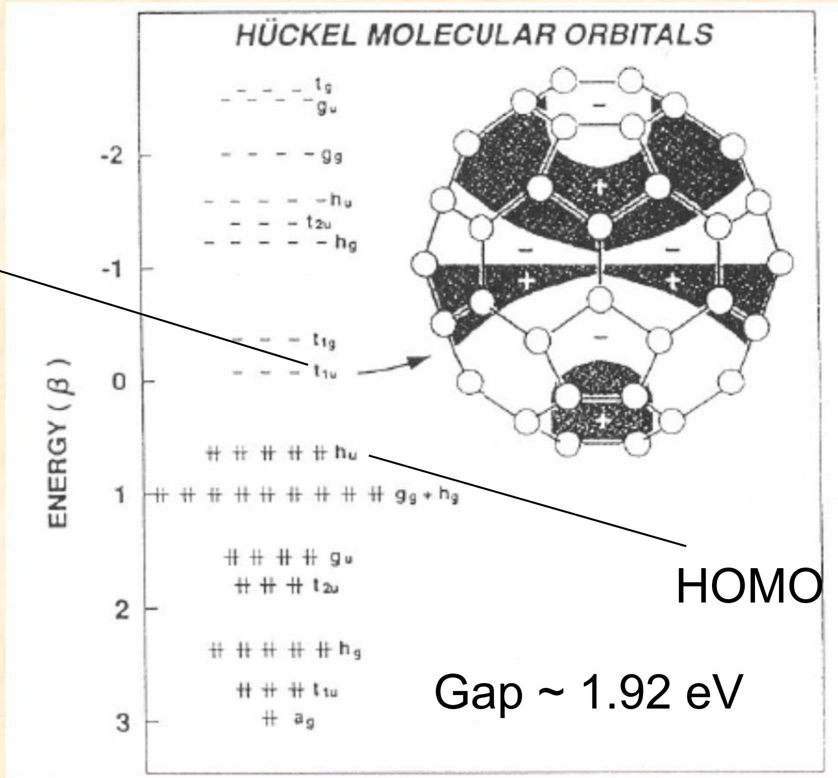

HOMO

Gap ~ 1.92 eV

π energy states (in eV) of the C_{60} phenomenological Hamiltonian model.

ℓ	Symmetry	Model[a]	Ab initio[b]
0	a_g	−7.41	−7.41
1	f_{1u}	−6.87	−6.87
2	h_g	−5.87	−5.82
3	f_{2u}	−4.40	−4.52
	g_u	−4.13	−3.99
4	h_g	−2.21	−2.44
	g_g	−2.12	−2.37
5	h_u	−0.20	−1.27
	f_{1u}	0.88	0.62
	f_{2u}	1.82	2.71
6	f_{1g}	3.38	1.59
	h_g	3.43	2.78
	g_g	4.92	4.60
⋮	⋮	⋮	⋮

- Free C60 molecule should be a good insulator

Band structure of solid C_{60}

- Molecular crystal : BCC stacking structure

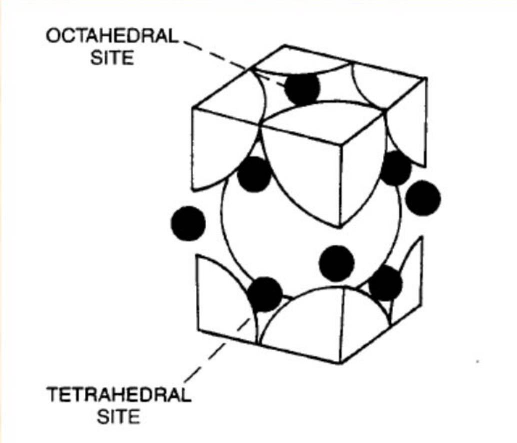

- Grown by slow evaporation from benzene solution

  filled with C60 molecules

- Band calculation :

  LDA + Gaussian orbital basis set

- Useful information :

  - Insulator with direct band gap ~ 1.5 eV band width ~ 0.4 eV

  - charge density map suggest weak coupling b/w fullerene molecule

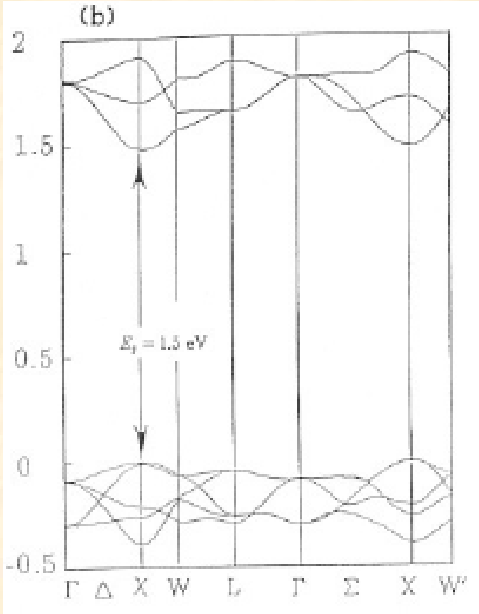

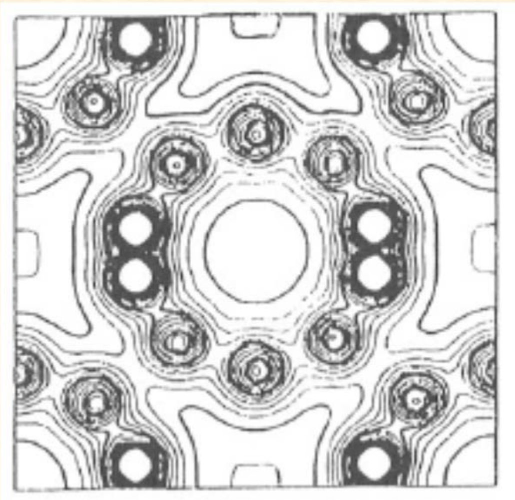

Symmetry consideration and Merohedral disorder in C_{60}

• Two standard orientations of fullerene molecule

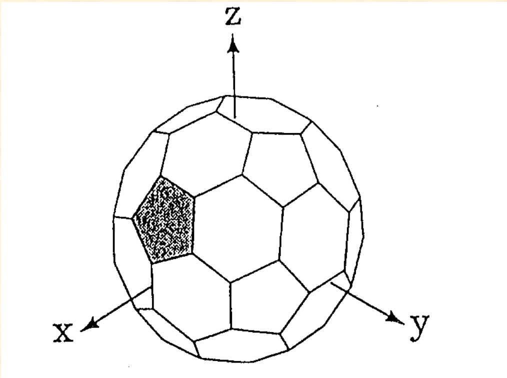

Two fold sym. axis

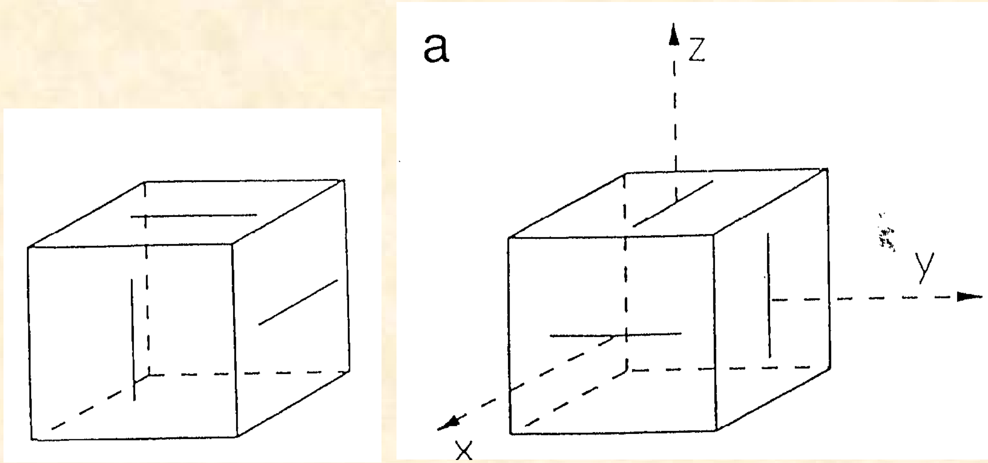

Two standard orientations

• Merohedral disorder : random choice b/w one of the two possible standard orientations (lack of four fold symmetry point)

➢ relative orientation b/w adjacent C_{60} can affect its physical properties.

Doping Buckyball solid : M_xC_{60}

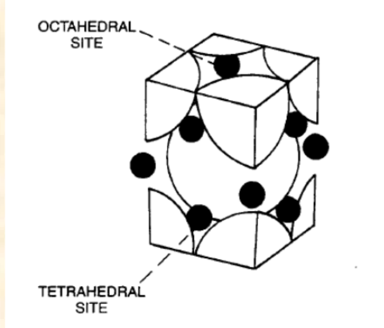

- Electrons transfer from alkali metal element M
- Two competing process due to doping effect:
  - decrease of C_{60} wave func. overlap
  - increase of the D.O.S
- Best conductivity occurs at x ~ 3 (half filled band)

-available sites (octahedral and tetrahedral) all filled

- undoped fullerene ρ_{300K}~ 10^8 Ωcm
- Single crystal K_3C_{60} ρ_{300K} ~ 5 mΩcm
- Strongly correlated electronics system
  - $k_F\ell$ <1 , one electron model may fail
  - from photo emission, large Hubbard U (1-2 eV)

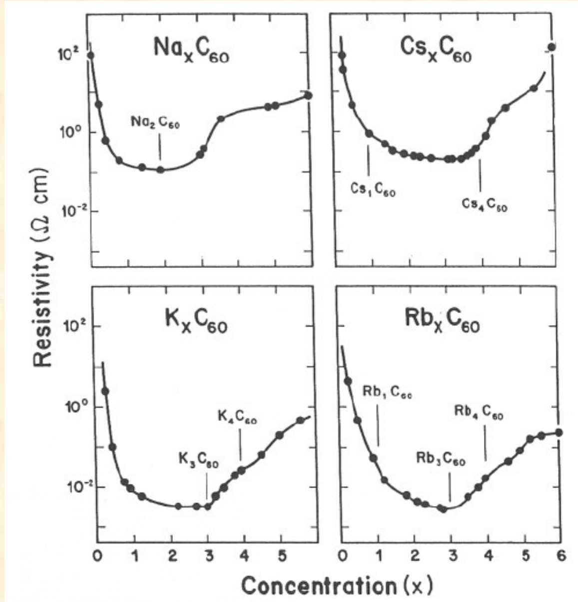

Drude model (3-D): $\boxed{k_F\ell_{mfp}(\rho,n) = \frac{(3\pi^2)^{2/3}\hbar}{e^2\rho\cdot n^{1/3}} \sim 0.5 < 1 \text{ for } K_3C_{60}}$

Superconductivity in M_3C_{60}

- Discovered in K_3C_{60} by Hebard (Bell lab, 1991) T_c ~ 19.8 K
- Highest Tc ~ 33K in Cs_2RbC_{60}
- The larger the radius of the dopant alkali atom the higher the T_c

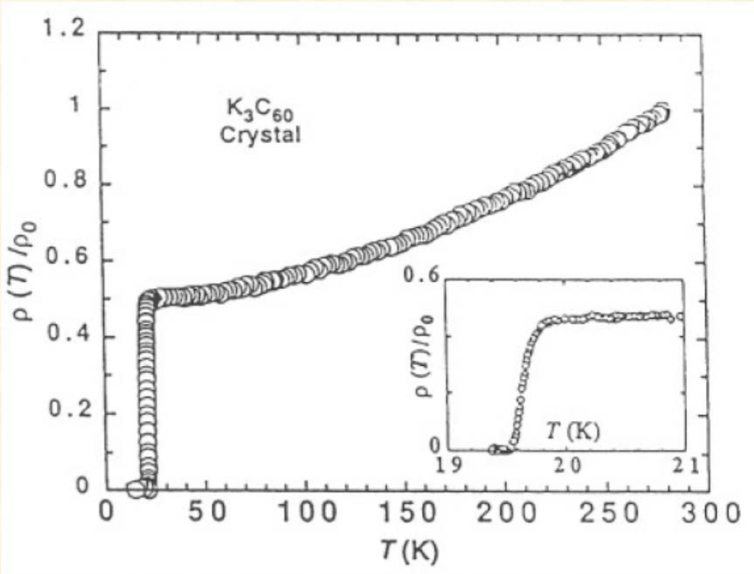

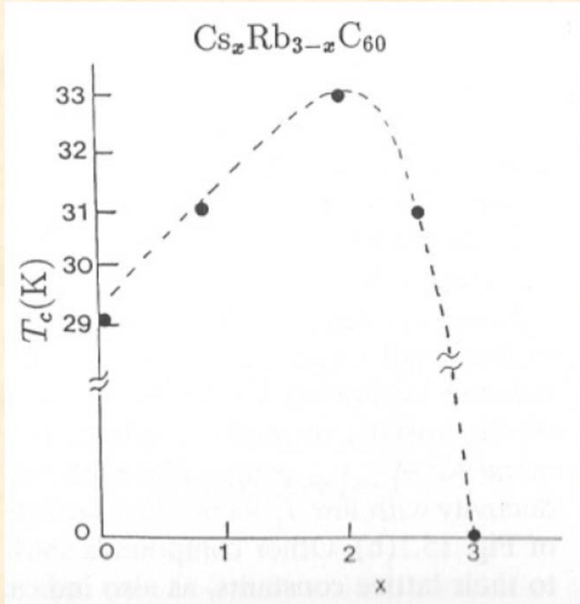

K_xC_{60}

X=0 ←——— 3 ———→ 6

insulator superconductor insulator

Strongly correlated electronic nature

Bardeen-Cooper-Schrieffer Theory

- In weak-coupling limit (λ <<1)

$$k_B T_c = 1.13\hbar\omega_D \exp[-1/\lambda],\ \lambda \equiv N(E_F)V$$

$$\lambda : \text{dimentionless e - phonon coupling parameter}$$

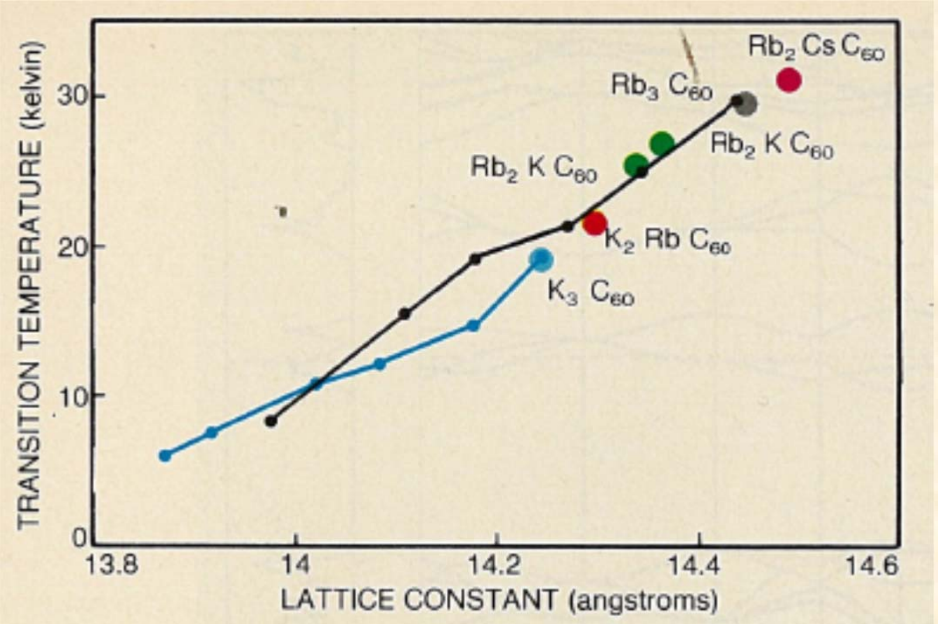

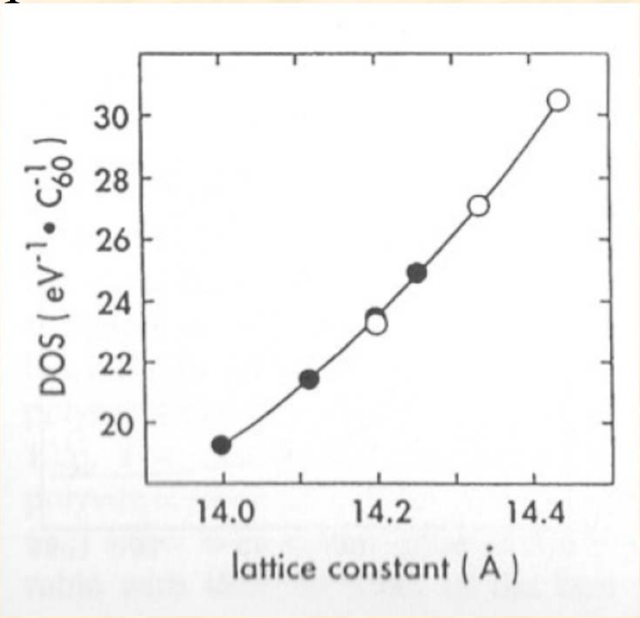

- Increase in lattice spacing reduced overlap of molecular orbital

⇨ reduced band width and increased D.O.S. $N(E_F)$

$$N(E_F) = \frac{3}{2}\frac{n}{E_F}$$

n fixed , lattice spacing ↑ k_F ↓ and $N(E_F)$ ↑

Other properties in K_3C_{60}

- Hall coefficient : $R_H = 1/ne$
  - ✓Sign change at 200K
  - ✓Both electron and hole like pockets

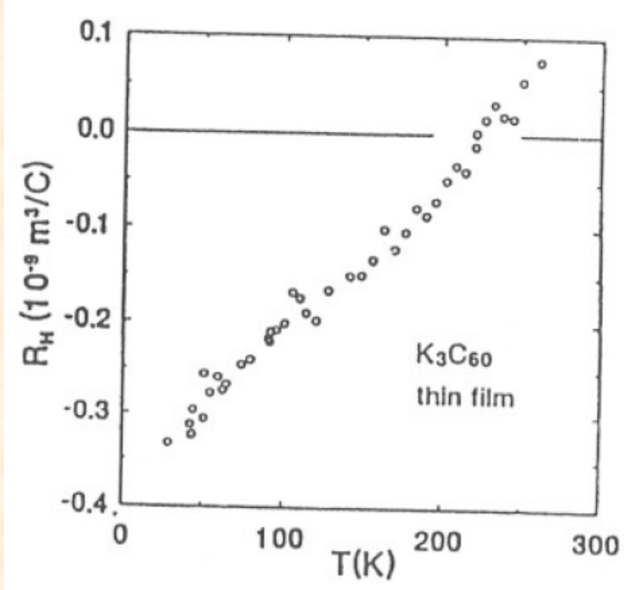

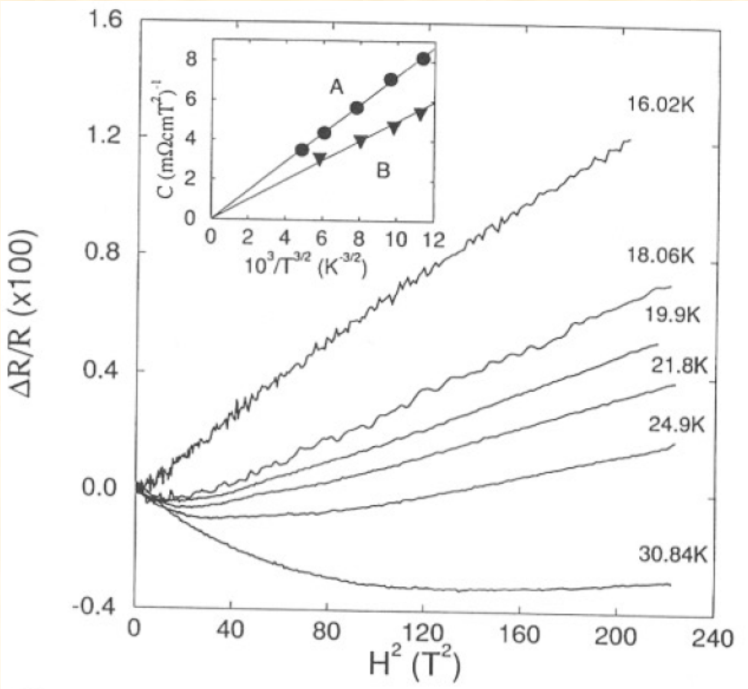

•Transverse magnetoresistance :

$$\frac{\Delta\rho}{\rho_0} = \frac{\Delta\rho_C}{\rho_0} + \frac{\Delta\rho_{L,I}}{\rho_0}$$

Classical orbital contribution : positive and quadratic in H

Weak localization and e-e interaction:

Negative, H^2 at low H and $H^{1/2}$ in high H

Weak localization in disordered system

• Appeared In disordered + time reversal symmetric system

• Negative MR : Strongly suppressed by applying magnetic field

• Merohedral disorder and also missing alkali ion at the tetrahedral and octahedral sites

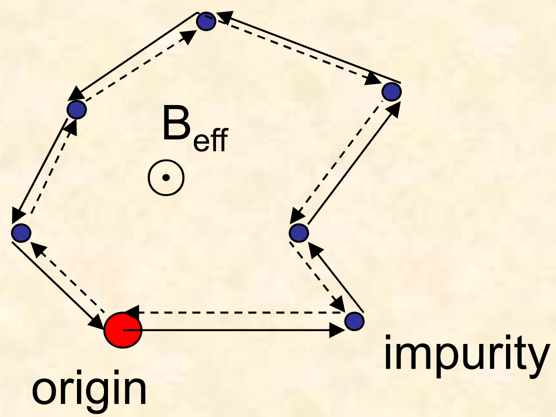

Constructive $|2A|^2$ ⇨ localization

$$\int B \cdot dA = \oint A \cdot d\ell : \text{additional phase change}$$

PartI: Concluding Remarks

- Fullerene structure : C_{20+h*2}
- An example of strongly correlated electronic system

  Insulator – undoped C_{60}

  Metallic – Alkali-doped C_{60}

  Superconductivity – A_3C_{60} (A=K, Rb,CsK,RbCs)
- T_c increase linearly with lattice constant : BCS theory prediction
- Reduced Hall coefficient and sign change at 200K : both electron and hole pocket
- Weak localization effect associated with Merohedral disorder and missing alkali ions.
- D.O.S. at Fermi Level in K_3C_{60}:

  Pauli susceptibility : 28 states/eV-C60(spin fluctuation enhancement

  Thermopower S : 11 states/eV-C60

  Specific heat : 12 states/eV-C60

Carbon nanostructures

Wei-Li Lee, IoP, Academia Sinica

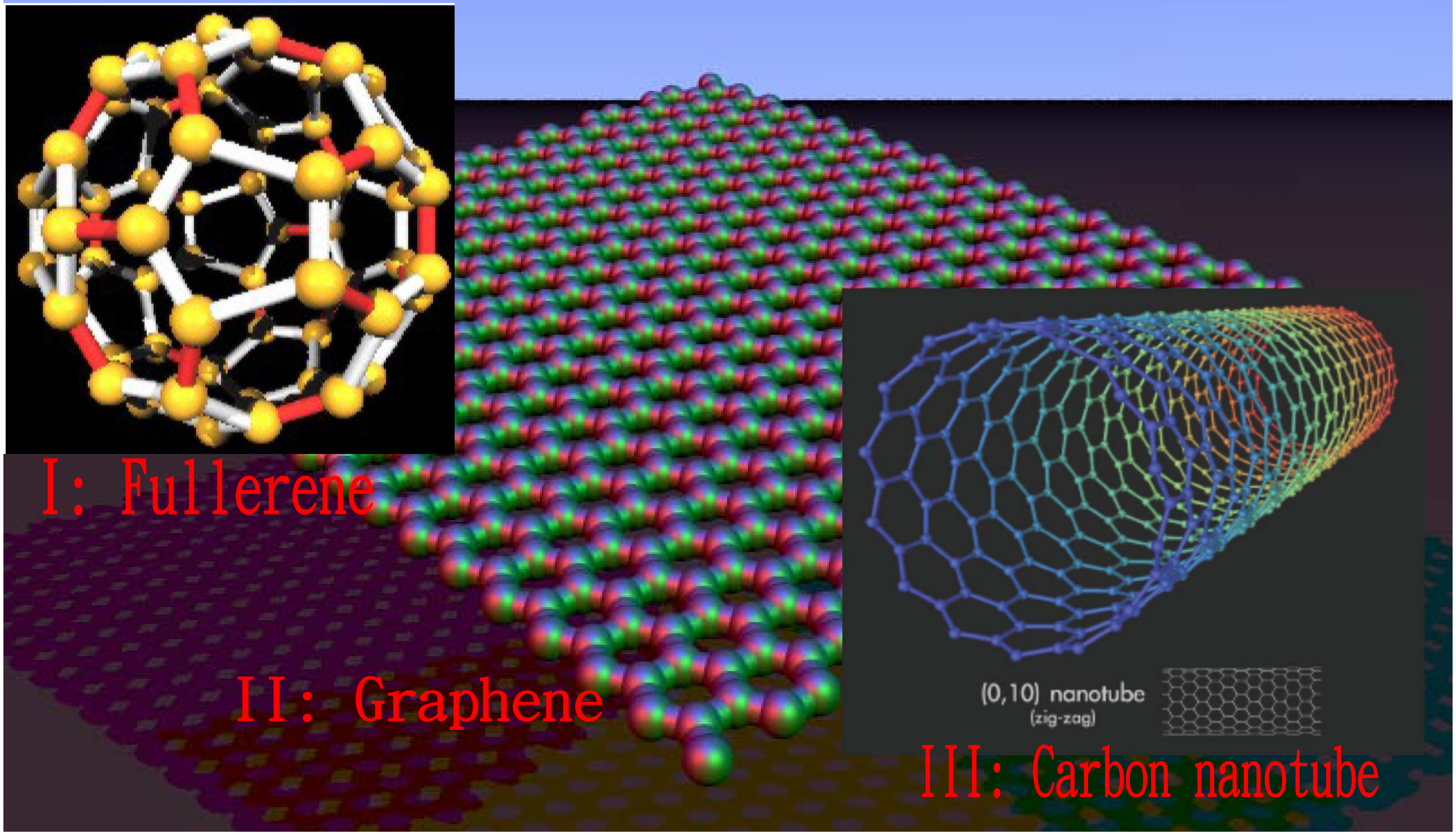

Part - 1

Basics of graphene

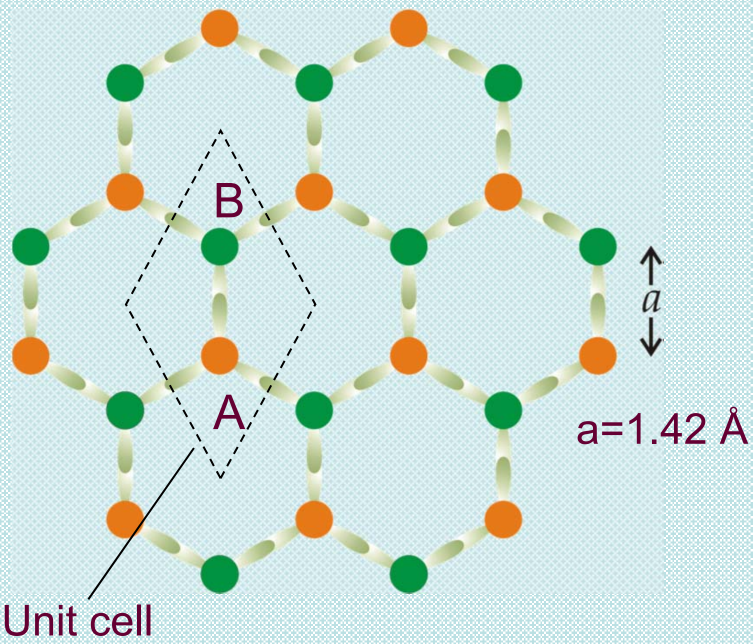

Honeycomb structure

- **Condensed-matter systems usually described accurately by the Schrödinger equation.**

$$i\hbar\frac{\partial}{\partial t}\psi(\vec{r},t)=\left(\frac{\hat{P}^2}{2m}+\hat{V}(\vec{r})\right)\psi(\vec{r},t)=E\psi(\vec{r},t)$$

- **Electron transport in graphene is governed by Dirac's (relativistic) equation.**

$$i\hbar\frac{\partial}{\partial t}\psi(\vec{r},t)=\left(\alpha_k p_k c+\beta mc^2\right)\psi(\vec{r},t)=\pm E\psi(\vec{r},t)$$

- **Charge carriers in graphene mimic relativistic particles with zero rest mass and effective speed of light $v_F \approx 10^6$m/s.**

- **Variety of unusual phenomena associated with massless Dirac fermions.**

Lattice structure

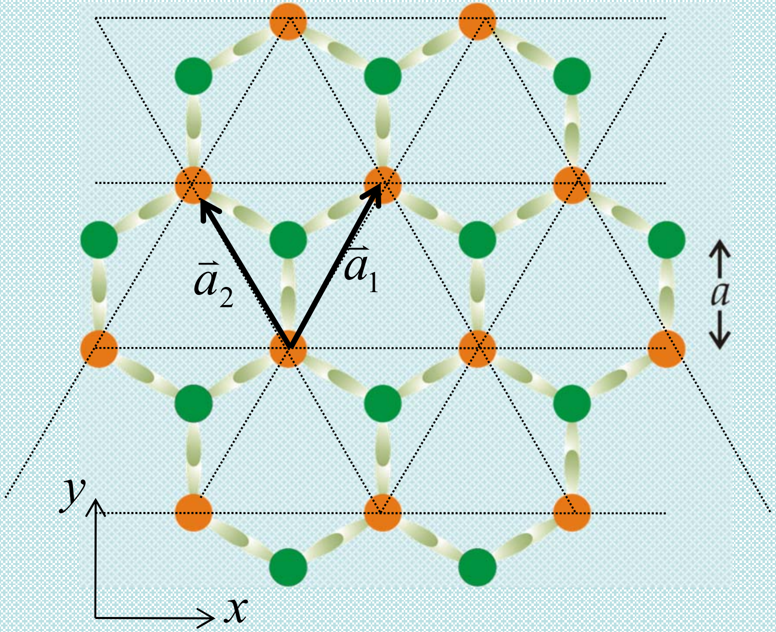

Triangular Bravais Lattice
with basis of 2 carbon atoms

- **Triangular Bravais lattice :**

$$\vec{a}_1 = a\sqrt{3}\left(\frac{1}{2},\frac{\sqrt{3}}{2}\right),\quad \vec{a}_2 = a\sqrt{3}\left(-\frac{1}{2},\frac{\sqrt{3}}{2}\right)$$

- **Reciprocal Lattice :**

$$\vec{b}_1 = \frac{2\pi}{3a}(\sqrt{3},1),\quad \vec{b}_2 = \frac{2\pi}{3a}(-\sqrt{3},1)$$

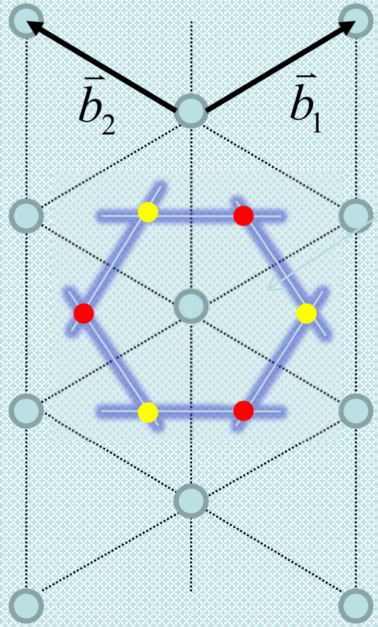

First Brillouin Zone
with 6 vertices
(Dirac points)

$$\vec{a}_i \cdot \vec{b}_j = 2\pi\delta_{ij}$$

Electronic Structure : Tight Binding Model

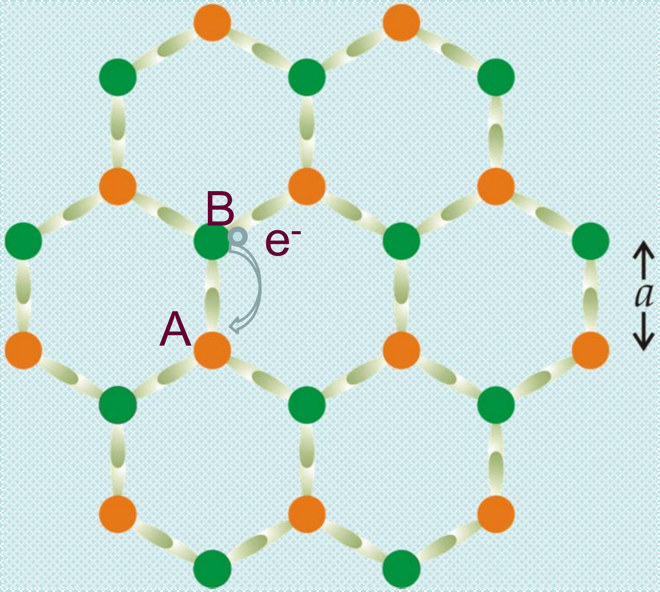

t : nearest neighbour hopping amplitude

- **Hamiltonian :**

$$H_{\text{int}} = -t \sum_{<i,j>,\sigma} \left[a^{+}{}_{i\sigma} b_{j\sigma} + H.C. \right]$$

$$-t' \sum_{<<i,j>>,\sigma} \left[(a^{+}{}_{i\sigma} a_{j\sigma} + b^{+}{}_{i\sigma} b_{j\sigma}) + H.C. \right] + H_{imp.}$$

- **Eigen energy E_k (neglect t' and H_{imp}):** $E_k =$

$$\pm t \left[1 + 4\cos(\frac{\sqrt{3}a}{2} k_x)\cos(\frac{3a}{2} k_y) + 4\cos^2(\frac{\sqrt{3}a}{2} k_x) \right]^{1/2}$$

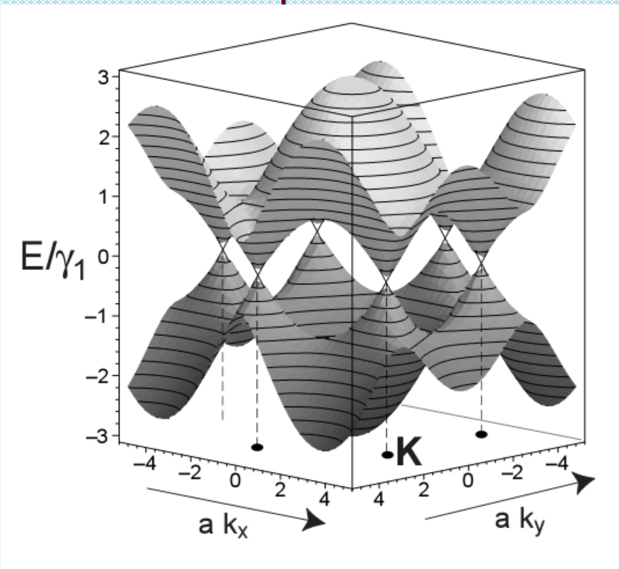

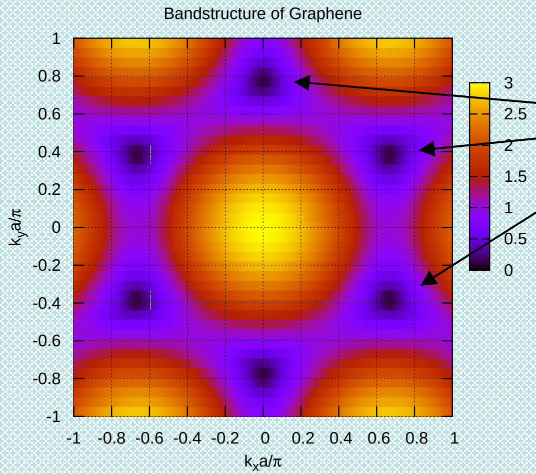

$E(\vec{q} = \vec{K}) = 0$

Dirac points

In a perfect graphene sheet μ crosses the Dirac points

Dispersion relation near Dirac point

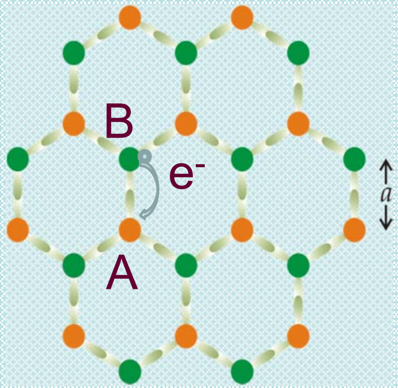

- Low energy Hamiltonian : expand around the Dirac point

  K→K1+k (K1 is one of the 6 Dirac points or vertices)

- Dirac's (relativistic) equation with zero mass

$$\mathrm{H} = \hbar \upsilon_{\mathrm{F}} \vec{\sigma} \cdot \vec{k} = \hbar \upsilon_{\mathrm{F}} \begin{pmatrix} 0 & k_x - ik_y \\ k_x + ik_y & 0 \end{pmatrix}, \quad \mathrm{H} \begin{pmatrix} \psi_{\mathrm{A}} \\ \psi_{\mathrm{B}} \end{pmatrix} = E \begin{pmatrix} \psi_{\mathrm{A}} \\ \psi_{\mathrm{B}} \end{pmatrix}$$

"Pseudospin" state

Pauli "spin" matrices

$$E(\vec{k}) = \pm \upsilon_F \hbar \left| \vec{k} \right|, \ \ \upsilon_F \approx 10^6 ms^{-1}$$

Massless quasiparticle !

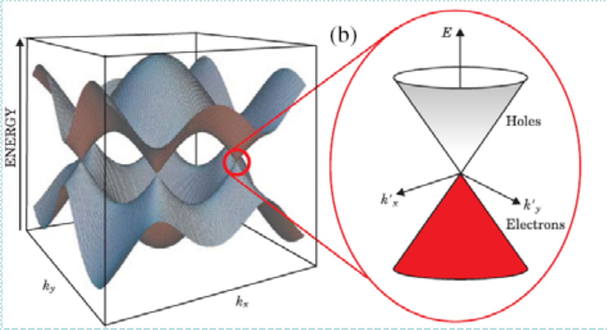

- Well-defined chirality: $\sigma \cdot$p = +1 or -1:

  Positive for electron and negative for hole (positron)

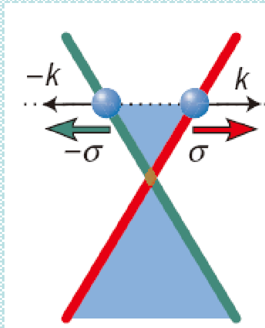

*J. Gonzalez, F. Guinea, M.A.H. Vozmediano, PRB **59,** R2474 (1999)*

Electron-electron interactions

- How effective the screening of interactions in graphene?

In normal metal (Thomas-Fermi theroy),

$$\text{Potential} \sim \frac{1}{\text{r}} e^{-k_0 r} \quad \text{(Yukawa potential)}$$

In graphene, DOS(E_F)=0 $\Rightarrow$ *Interactions imperfectly screened*

- *Marginal* Fermi Liquid behavior

At T=0 K, the quasiparticle lifetime at low energies scales as

$$\tau_E \sim (E - E_F)^{-1}$$

Confirmed experimentally (ARPES): *S. Xu et al., PRL **76**, 483 (1996)*

[Usual Fermi Liquid scales as $\tau_E \sim (E-E_F)^{-2}$]

Preparation of Single-Atomic Layer Graphite – Mission Impossible？

Andre Geim
51
Univ. Manchester

Konstantin Novoselov
36
Univ. Manchester

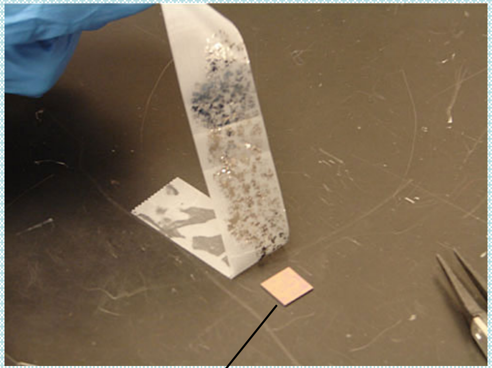

290 nm SiO_2/ Si(100)

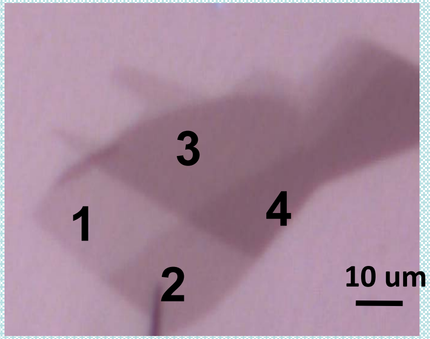

Seeing a single-atomic layer graphene！

Graphite

Tape

Optical Micro.

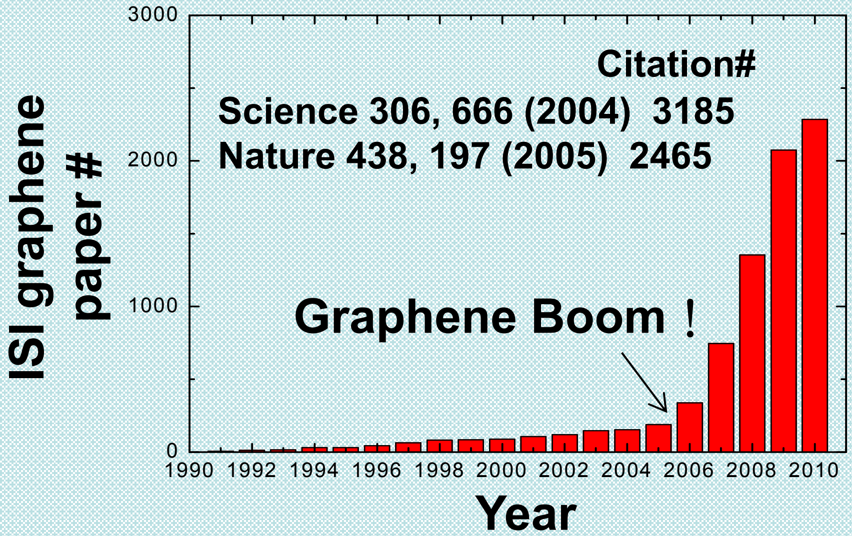

Geim and Novoselov: 2010 Nobel Prize in Physics

{ a perfect 2D crystal does exist
High tech. in not the only route

Superior Material Properties in Graphene ：

Practical application in the future

- Extremely light weight，density~0.77 mg/m^2。
- Tensile strength 100 times higher than steel。
- Nearly Transparent，light adsorption ~ 2.3%。
- Conductivity 1.6 times higher than copper。
- Fast electron traveling speed ~ c/300。
- At RT，thermal conductivity 10 times higher than copper。

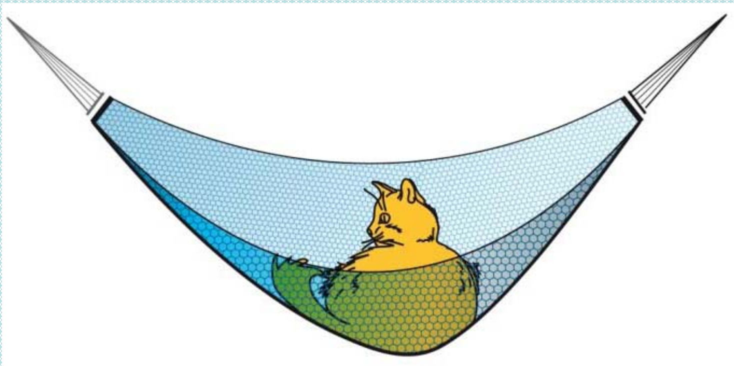

A hanger made by 1m^2 graphene(~0.77mg and invisible) : hold up to 4kg without breaking。

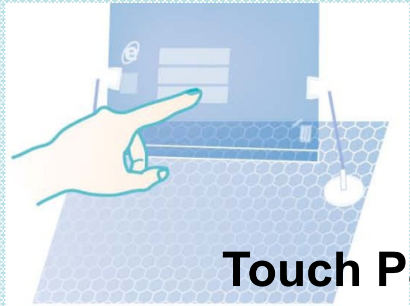

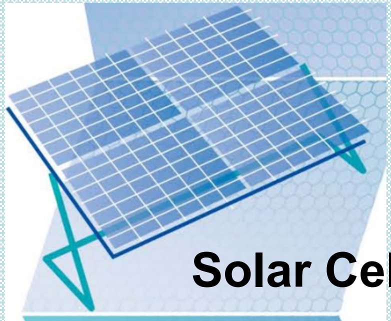

Future Applications of Graphene
Graphene can be used as flexible and stretchable transparent electrodes in the future.

Fabrication of large area graphene

Chemical Vapor Deposition
SiC high Temp. anneal
} Succeeded in producing graphene roll with 70 cm in width

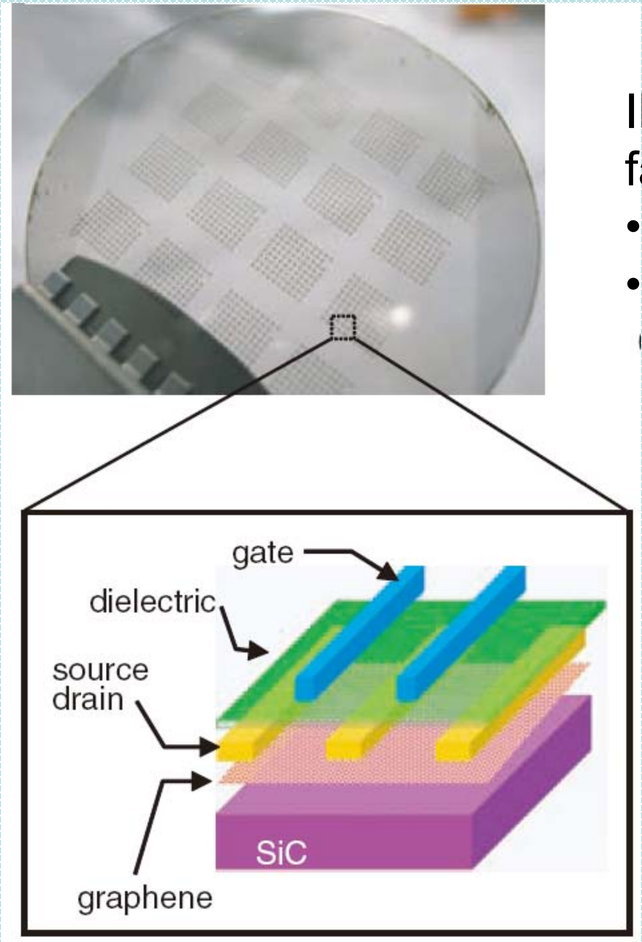

IBM team demonstrated wafer-sized fabrication of graphene transistor array

- Cut-off freq. for current gain:100 GHz.
- Cut-off freq. for power gain:10 GHz.

Few-layer graphene has great potential in replacing the silicon based electronics.

Angle-resolved photoemission spectroscopy (ARPES)

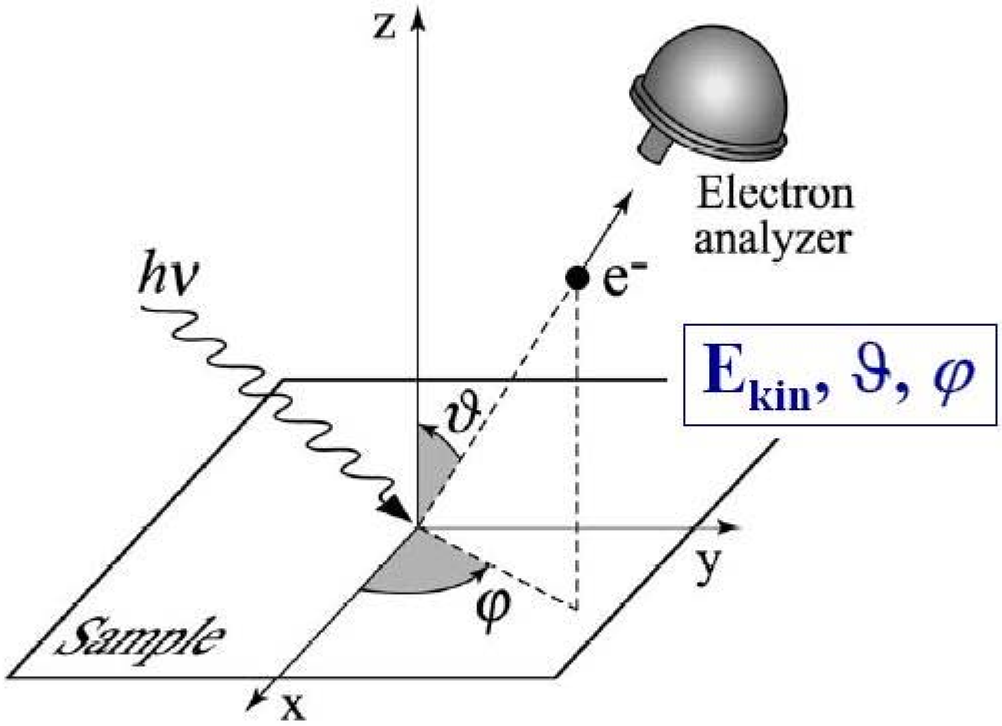

$$\mathbf{K} = \mathbf{p}/\hbar = \sqrt{2m\boldsymbol{E}_{kin}}/\hbar$$

$$K_x = \frac{1}{\hbar}\sqrt{2mE_{kin}}\sin\vartheta\cos\varphi$$

$$K_y = \frac{1}{\hbar}\sqrt{2mE_{kin}}\sin\vartheta\sin\varphi$$

$$K_z = \frac{1}{\hbar}\sqrt{2mE_{kin}}\cos\vartheta$$

- **E_{kin}, K can be measured in UHV**
- **Conservation law : $E_{kin}=h\nu - \varphi - E_B$**
  $k_f-k_i=k_\nu$
- **E_B and k in solid can be determined**
  ⇨ direct probe for dispersion relation in solids

Angle-resolved photoemission spectroscopy (ARPES)

- State-of-art apparatus :
  2meV energy resolution and 0.2 degree angular resolution

• Surface sensitive : only surface electrons carry inherent information without suffering complicated scattering

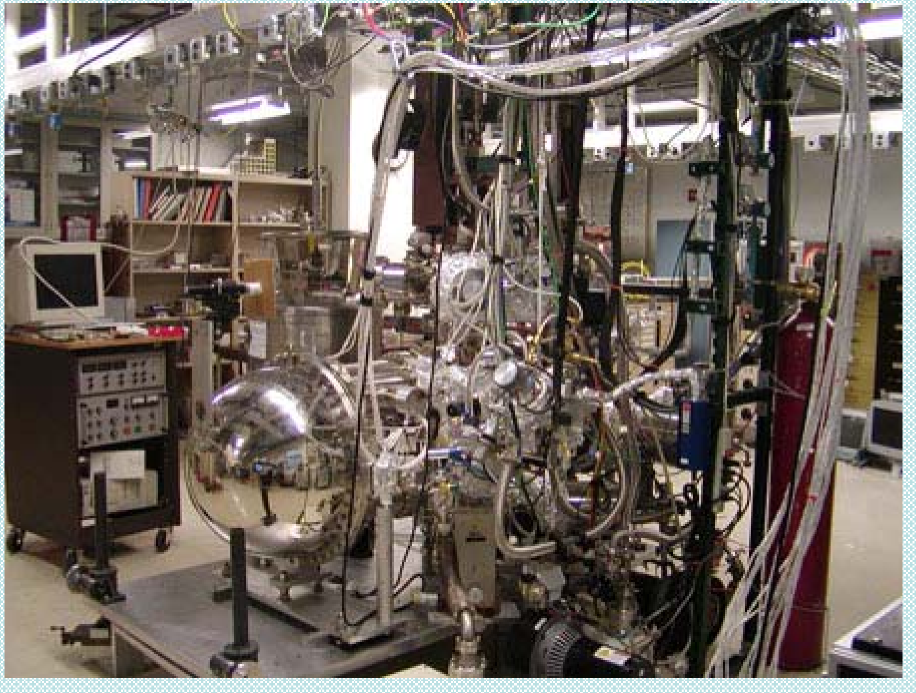

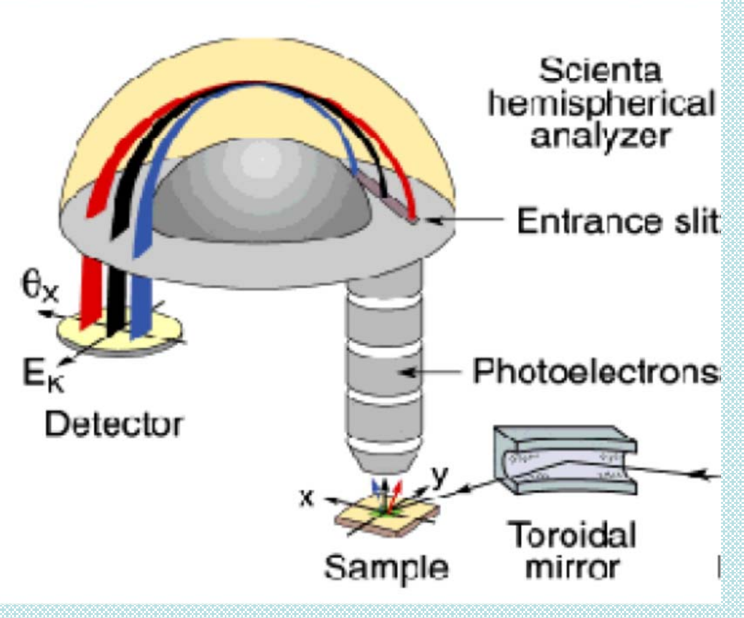

ARPES at Shen's group at Stanford Univ.

Direct observation of Dirac Fermions

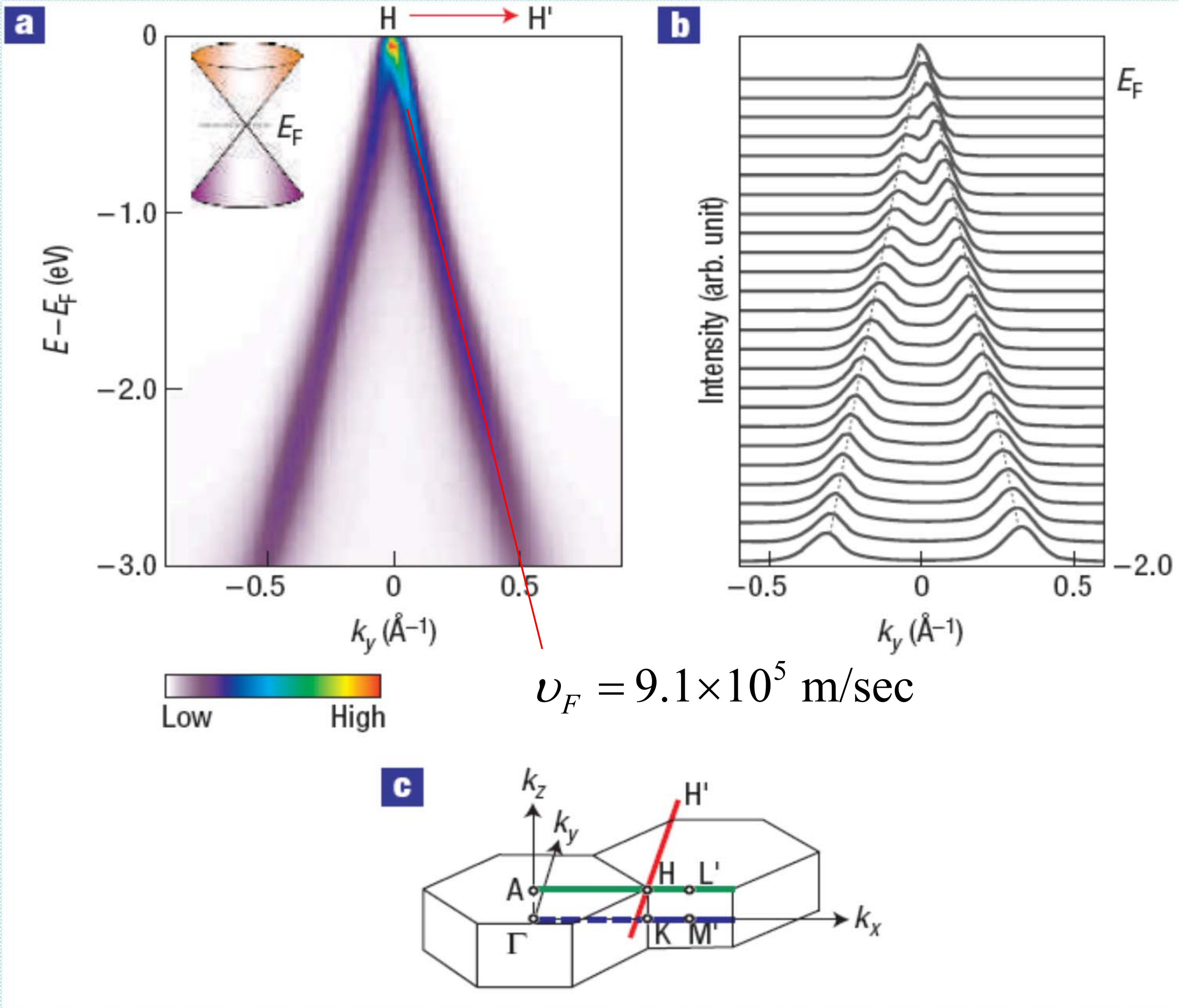

$$\upsilon_F = 9.1\times10^5 \text{ m/sec}$$

M. I. Katnelson, K. S. Novoselov, and A. K. Geim, cond-mat/0604323

Relativistic Physics in Condensed Matter System-

Klein Paradox in Graphene

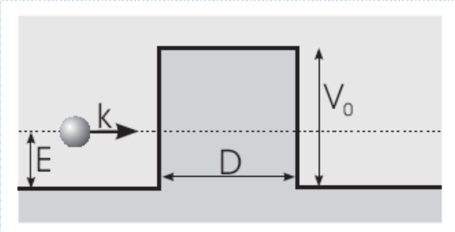

Klein paradox: unimpeded penetration of relativistic particles through high and wide potential barriers - 1930

Monolayer **Bilayer**

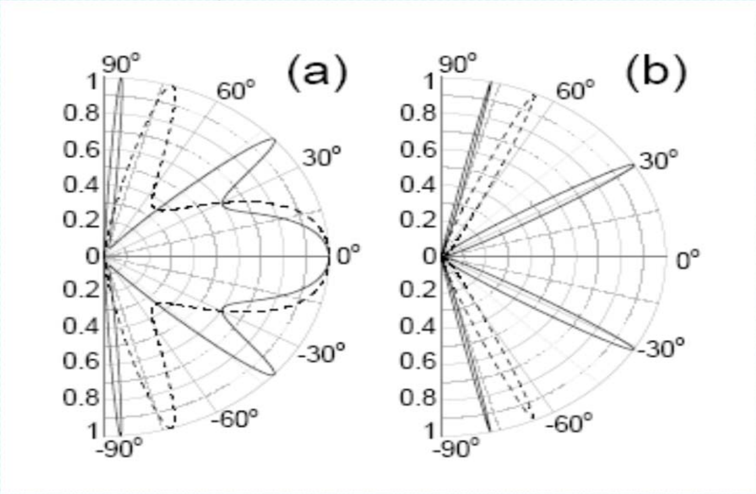

Barrier *always* transparent for angles close to normal incidence !!

Massive fermions are reflected close to normal incidence!

Impurity scattering in the bulk of graphene is strongly suppressed !!!

Fabry-Pérot (FP) Interference in p-n-p Heterojunctions

- Shytov, et al., PRL 08'

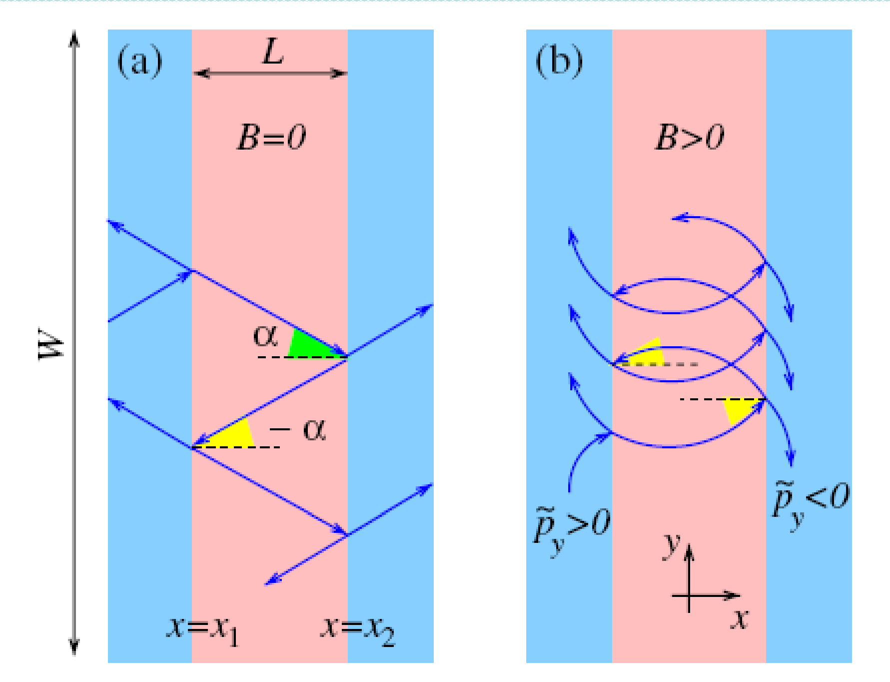

p-n-p junctions

Interference due to e^- bouncing b/w p-n interfaces

- **FP interference :**

$$\Delta\theta = 2\theta_{WKB} + \Delta\theta_1 + \Delta\theta_2,$$

$$\theta_{WKB} \equiv \int_1^2 p_x(x')dx',$$

$\Delta\theta_{1(2)}$: Klein Backreflection phase change.

- **Conductance oscillation in the p-n-p junctions**

$$G_{osc} \sim \cos(\Delta\theta)$$

- **($\Delta\theta_1$+ $\Delta\theta_2$) do not cancel at finite field.**

- **For a perfect Transmission (T = 1) at normal incident (α=0) suggested by Klein paradox, the back-reflection phase should undergo a π-shift at α=0 !**

Quantum Interference in Graphene p-n Heterojunctions

- Young, et al., Nat. Phys. 09'

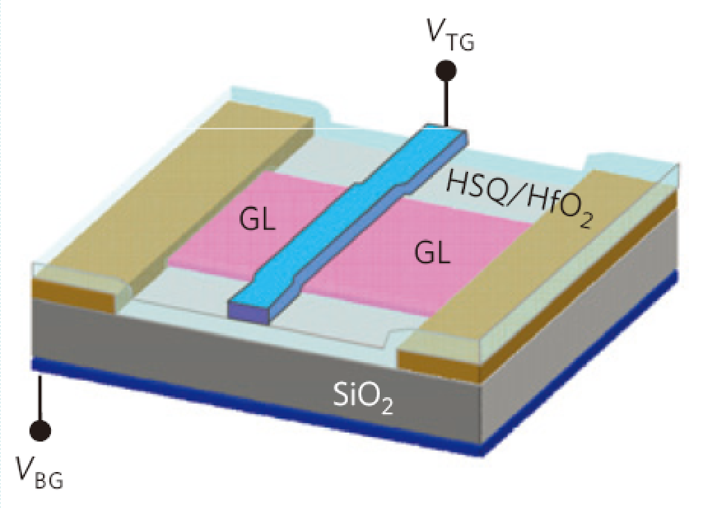

- Tuning α across 0 by B field
- Phase shift at field B ~ 400mT
- Perfect transmission at normal incident → Klein Paradox !

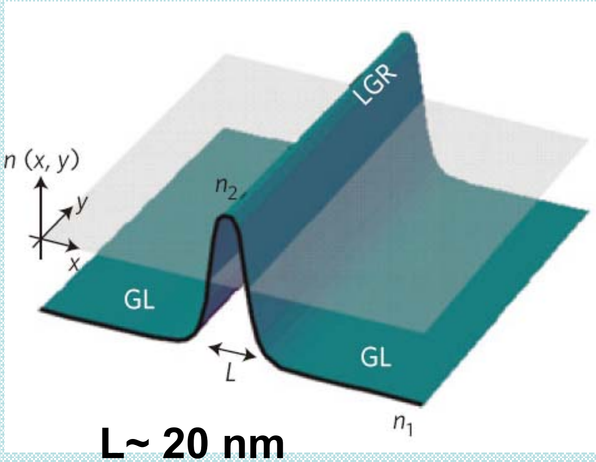

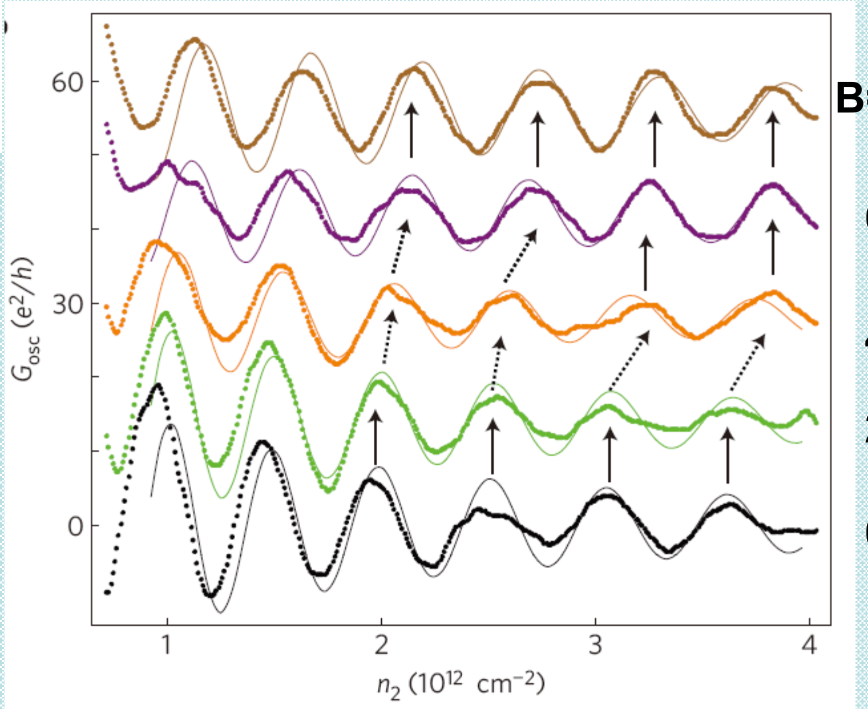

B=800 mT

600 mT

400 mT

200 mT

0 mT

L~ 20 nm

p-n junction : (n1*n2)<0

Transport in Graphene

Novoselov, et al., Science 04', Nature 05'

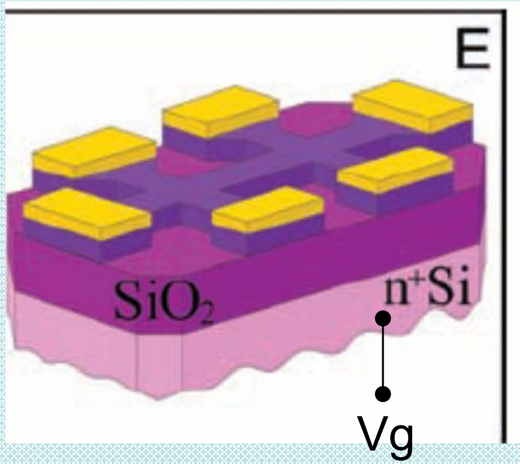

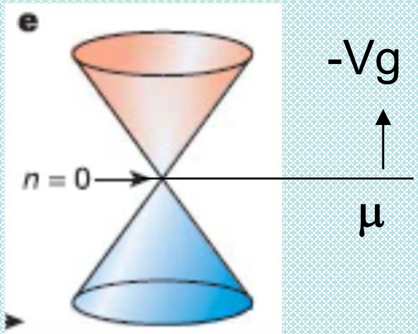

Electric field effect in graphene

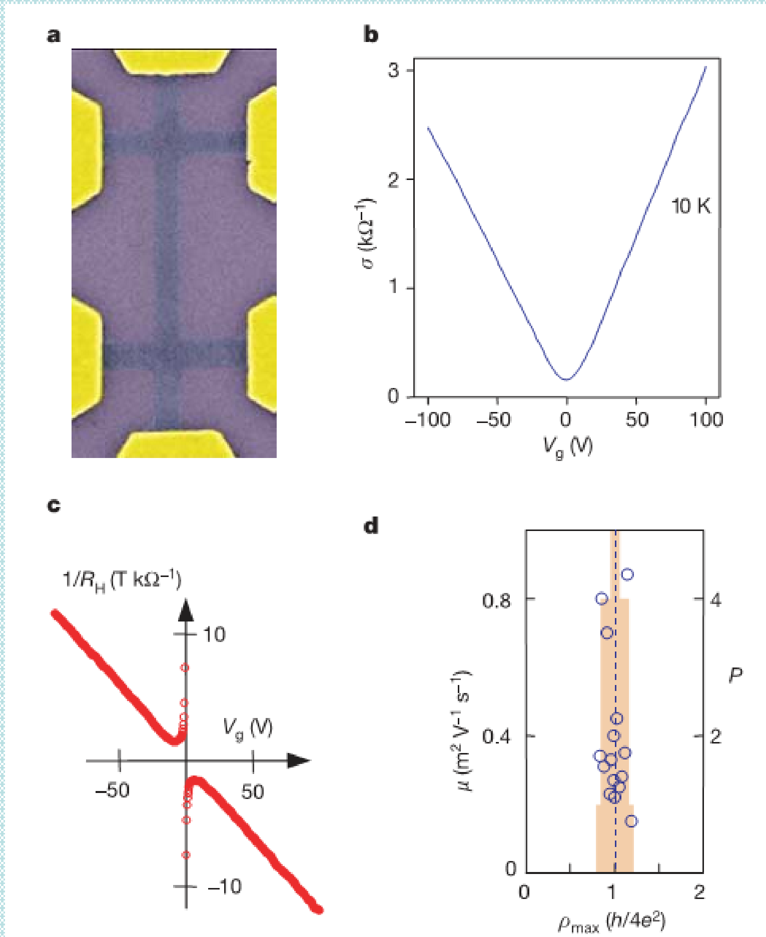

- **Chemical potential tuned by $V_g \sim n_c$**
- **Ambi-polar field effect**
- **Robust minimal conductivity ?**

$\sigma_{min} = 4e^2/h$, at Dirac point

Integer QHE in Graphene

Novoselov, et al., Nat. Phy. 06'

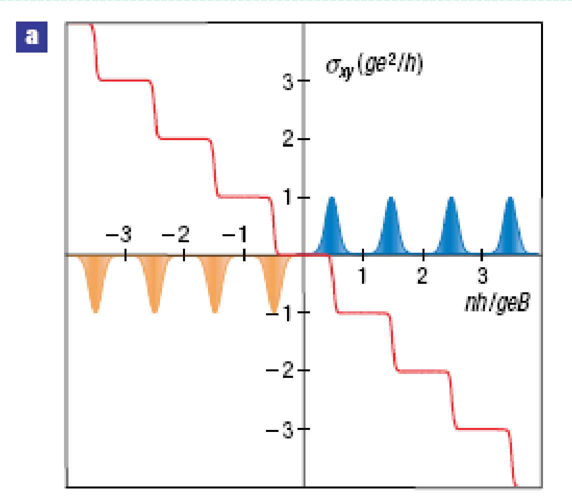

2-DEG
free-Fermion

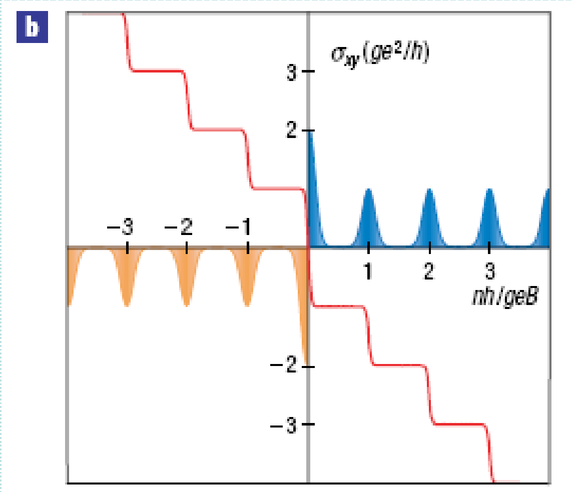

Bilayer graphene
Berry's phase 2π

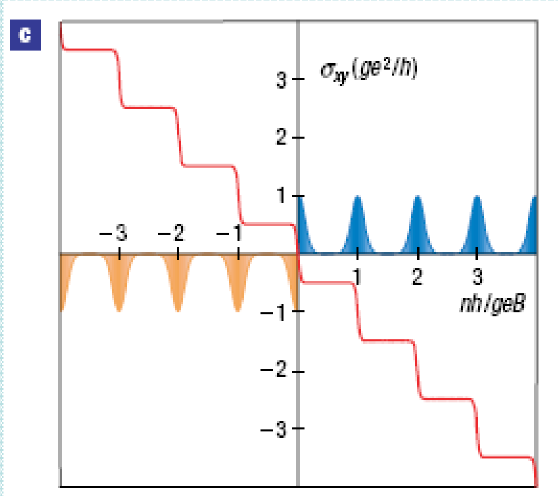

Single-layer graphene
Berry's Phase π

- For a given B, D.O.S. at each Landau level = gB/Φ_0
- Anomaly at lowest Landau level in graphene
- Internal field (Berry's phase) ⇨ non-zero QHE in zero external field*

* Haldane, et al., PRL 88'

Basic formalism of Berry's phase

Berry, PRSLA'84

Hamiltonian $H(\vec{R})$

$$H\left|n(\vec{R})\right\rangle = E_n\left|n(\vec{R})\right\rangle$$

Adiabatic change in $\vec{R}$,

$$\left|\psi(\mathrm{t})\right\rangle = e^{i\gamma_n}\left[e^{-i\int_0^t E_n dt'}\left|n(\vec{R})\right\rangle\right]$$

γ_n can be determined by requiring

$$H(\vec{R})\left|\psi(\mathrm{t})\right\rangle = i\hbar\frac{\partial}{\partial t}\left|\psi(\mathrm{t})\right\rangle$$

Along a closed path C in $\vec{\mathrm{R}}$ space

$$\boxed{\gamma_n(C) = \int_C X(\vec{R})\cdot d\vec{R}, \quad X(\vec{R}) \equiv \left\langle n(\vec{R})\middle| i\nabla_R \middle| n(\vec{R})\right\rangle}$$

Berry's phase

Berry's vector potential

" remarkable and rather mysterious results "

- Berry 1983

" ….. is essentially that of the holonomy which is becoming quite familiar to theoretical physicists "

- Simom 1983

Parallel transport of vector v on curved surface

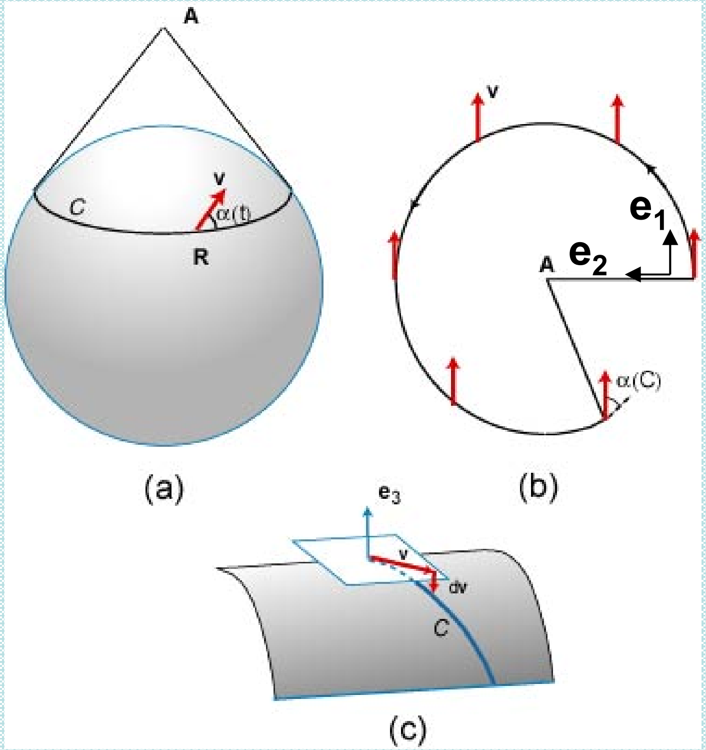

Constrain **v in local tangent plane;**
no rotation about e_3
$[e_1, e_2]$: local tangent plane

Parallel transport

$\boxed{\mathbf{e}_3 \times d\mathbf{v} = 0}$

v acquires geometric angle α relative to local $\mathbf{e}_1$

complex vectors $\hat{\boldsymbol{\psi}} = (\mathbf{v} + i\,\mathbf{w})/\sqrt{2}$ $\hat{\mathbf{n}} = (\mathbf{e}_1 + i\,\mathbf{e}_2)/\sqrt{2}$

angular rotation is a phase $\hat{\boldsymbol{\psi}} = \hat{\mathbf{n}}\,e^{i\alpha}$

$$\boxed{d\alpha = -\hat{\mathbf{n}}\cdot id\,\hat{\mathbf{n}}}$$

cf. $X(\vec{R}) \equiv \left\langle n(\vec{R}) \middle| i\nabla_R \middle| n(\vec{R}) \right\rangle$

Berry's phase and Geometry

Change Hamiltonian H (**R**) by evolving **R**(t) adiabatically
Constrain particle to remain in one state $|n(\mathbf{R})>$

Simon, PRL '83

Ong and Lee, cond-matt '05

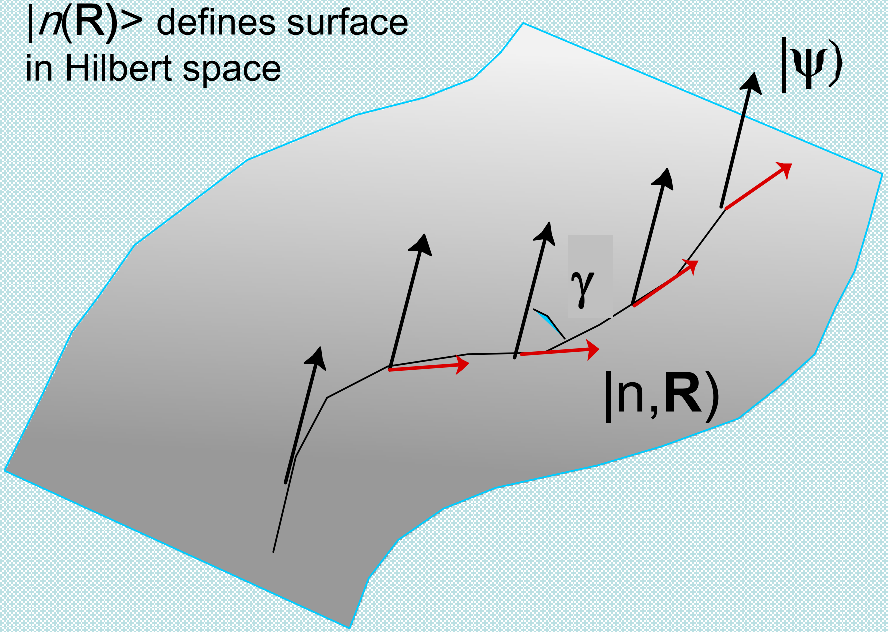

$$\left|\psi\right\rangle = \left|n(\mathrm{R})\right\rangle \mathrm{e}^{i\gamma}$$

wavefcn, *evolving on* surface |n **R**), acquires Berry phase γ

$$\gamma = \int d\,\mathrm{R}\cdot \mathrm{X}(\mathrm{R})$$

(holonomy)

$$\boxed{\mathrm{X}(\mathrm{R}) \equiv < n(\mathrm{R})\,|\,i\nabla_{\mathrm{R}}\,|\,n(\mathrm{R}) >}$$

⇨ **Berry vector potential**

$$\mathbf{\Omega}(\mathrm{R}) \equiv \nabla_{\mathrm{R}} \times \mathrm{X}(\mathrm{R})$$

⇨ **Berry curvature**

A particle with spin s in magnetic field

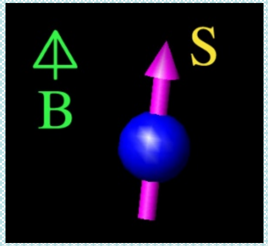

Hamiltonian

$$H(\vec{B}) = -g\mu_B \vec{s}\cdot\vec{B}, \text{ with eigenvalues } E_n = g\mu_B Bn \quad (n = -s, -s+1, ..+s)$$

$$H(\vec{B})\left|n(\vec{B})\right\rangle = E_n\left|n(\vec{B})\right\rangle,$$

Berry's curvature

$$\mathbf{\Omega}_n(\vec{B}) = \nabla_{\vec{B}} \times \left\langle n(\vec{B})\right| i\nabla_{\vec{B}}\left| n(\vec{B})\right\rangle = \mathrm{Im}\sum_{m\neq n}\frac{\left\langle n(\vec{B})\right|\nabla_{\vec{B}}H\left|m(\vec{B})\right\rangle \times \left\langle m(\vec{B})\right|\nabla_{\vec{B}}H\left|n(\vec{B})\right\rangle}{(E_n - E_m)^2}$$

With $\nabla_{\vec{B}}H = g\mu_B\vec{s}$,

$$\boxed{\mathbf{\Omega}_n(\vec{B}) = n\,\vec{B}/B^3}$$

Gauge field results from a monopole n at the origin of ***B*** space

Berry's phase with adiabatic variation of $\vec{B}$ around a loop C

$$\boxed{\gamma_n(C) = -\iint_C \mathbf{\Omega}_n(\vec{B})\cdot d\vec{S} = -n\,\Omega(C)}$$

Gauge flux through the loop *C*

Solid angle that *C subtends at origin*

Massless Dirac Fermion and π Berry's phase

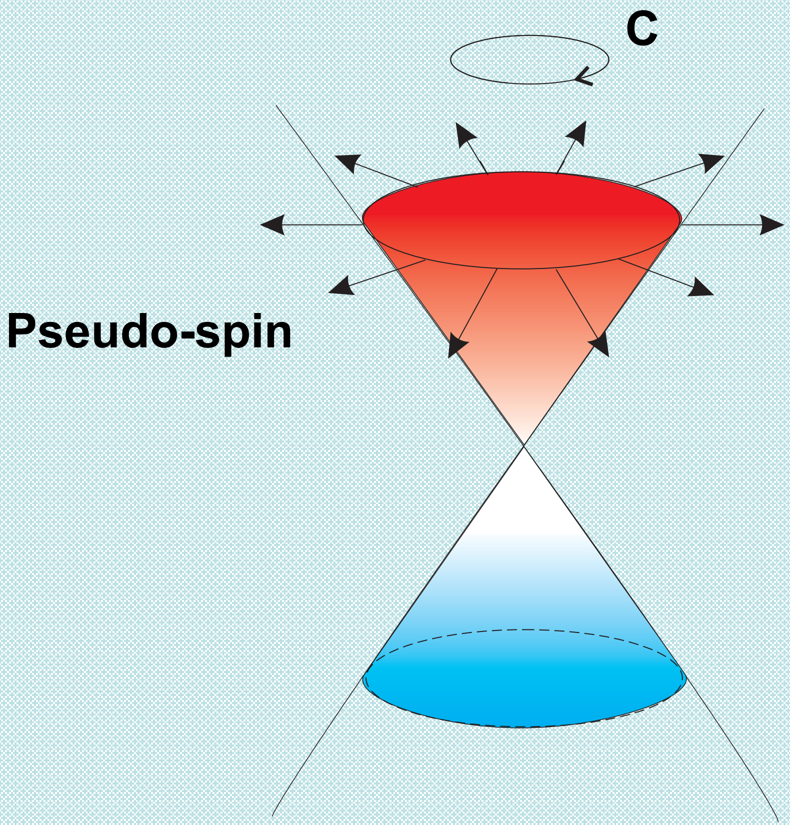

- Pseudospin eigenstate along $\vec{k}$
- Closed contour C in k space associated with cycltron path
- Berry's phase acquired along path C

$$\gamma(C) = -\iint_C \mathbf{\Omega}\cdot d\vec{S} = -\frac{1}{2}\Omega(C) = -\pi$$

Solid angle

Parallel transport of vector v on curved surface

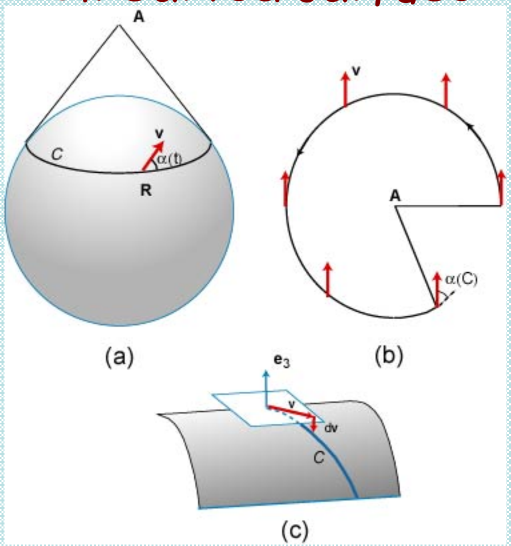

Quantum Hall Effect at Room Temperature !

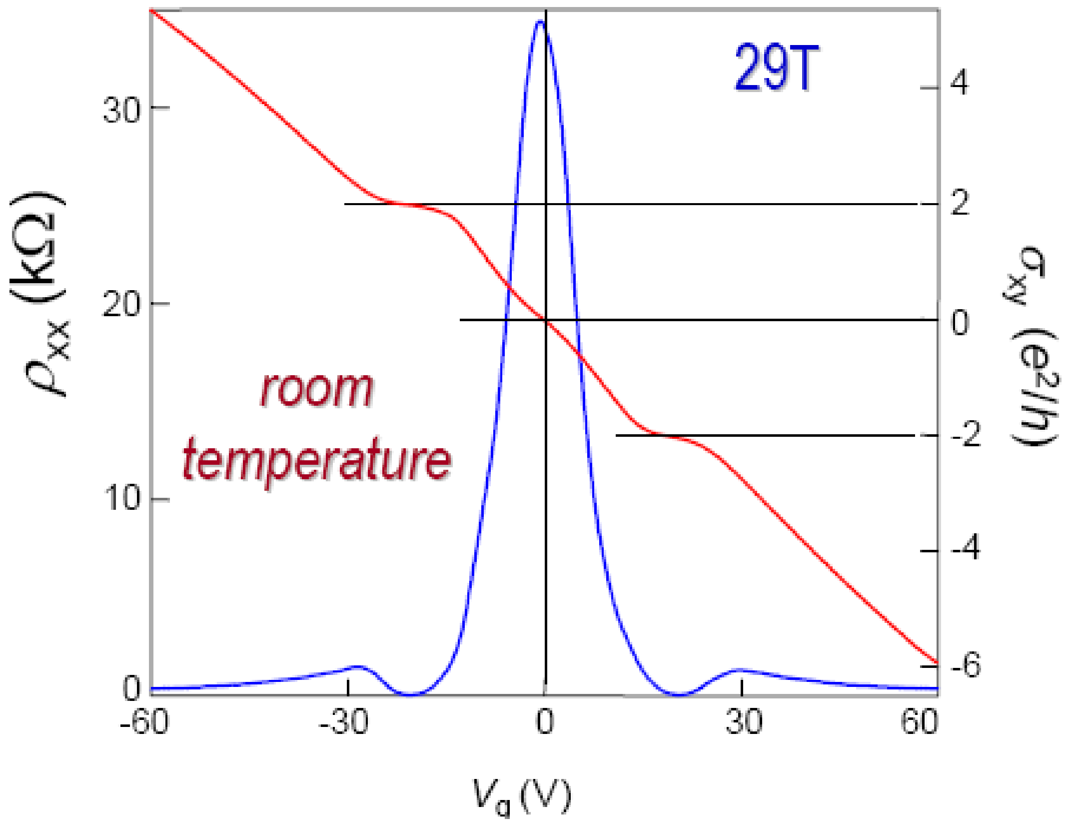

$$E_n = sign(n)(2n)^{1/2}\frac{\hbar\upsilon_F}{\ell_B}$$

For B = 29 Tesla, $E_1 - E_0 = 0.196\text{eV} = 2271\text{K}$!!

$$cf: \quad E_n = (n+\frac{1}{2})\hbar\omega_C,\ \Delta E = \hbar\omega_C = 3.36meV = 39K$$

Characterization of the thickness: Atomic Force Microscope

3 layers

4 layers

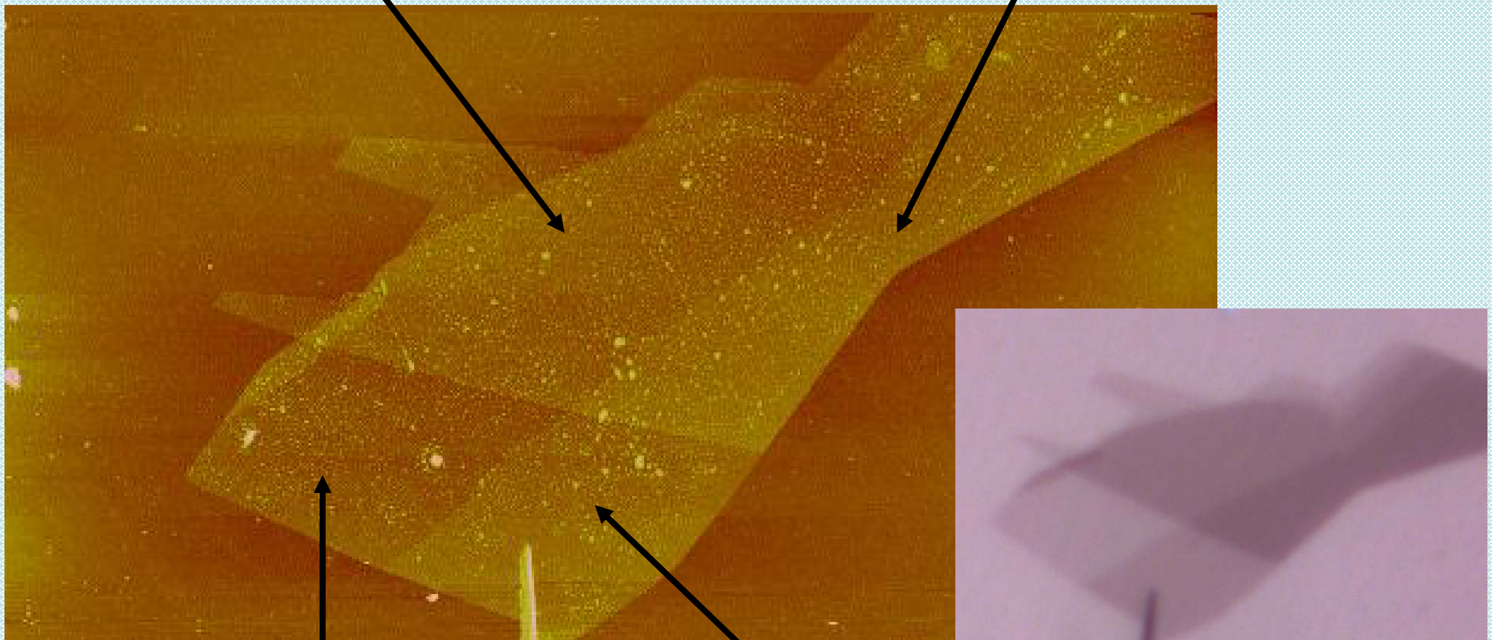

Graphene (single layer) ?

2 layers

Measured thickness ~ 0.8 nm > 0.34 nm

Characterization of thickness: Raman spectroscopy

Single and sharp 2D peak in
Single-layer graphene !!

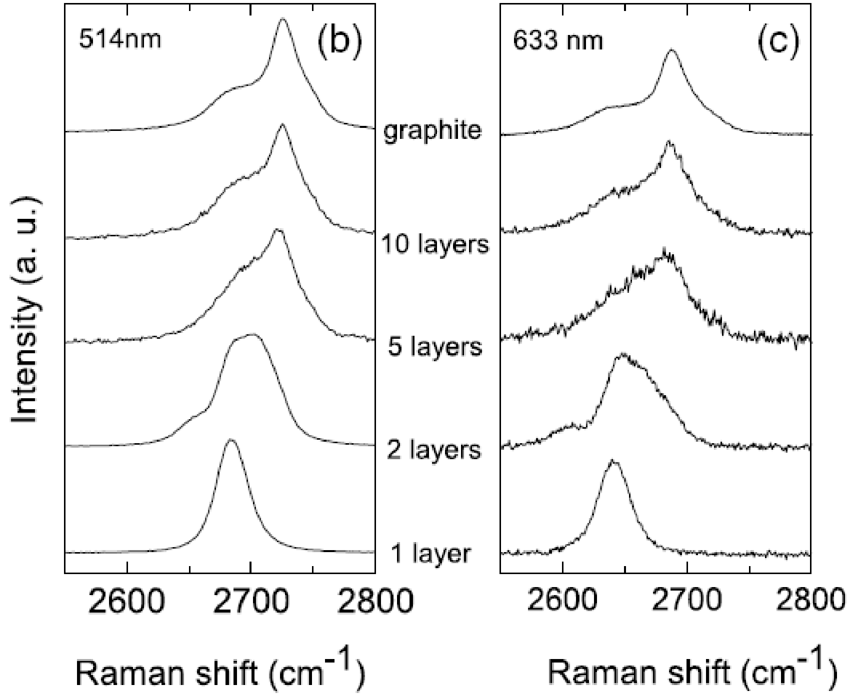

Double Resonant

Raman Process

- Ferrari, et al., PRL 06

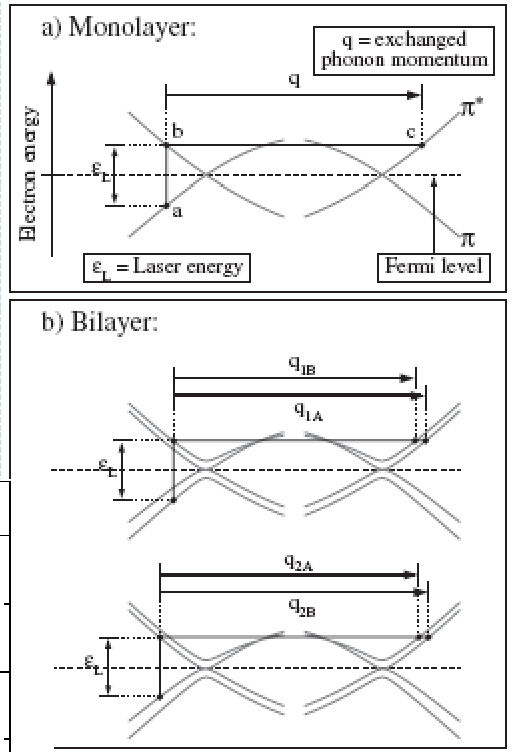

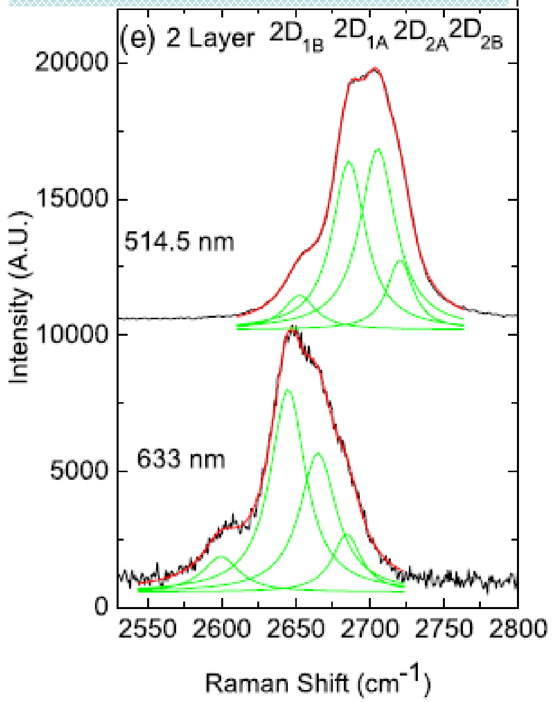

Large Area Graphene Fabrication- CVD on Cu

-- Li, et. al., Science 09'

Self-limiting growth of graphene on copper

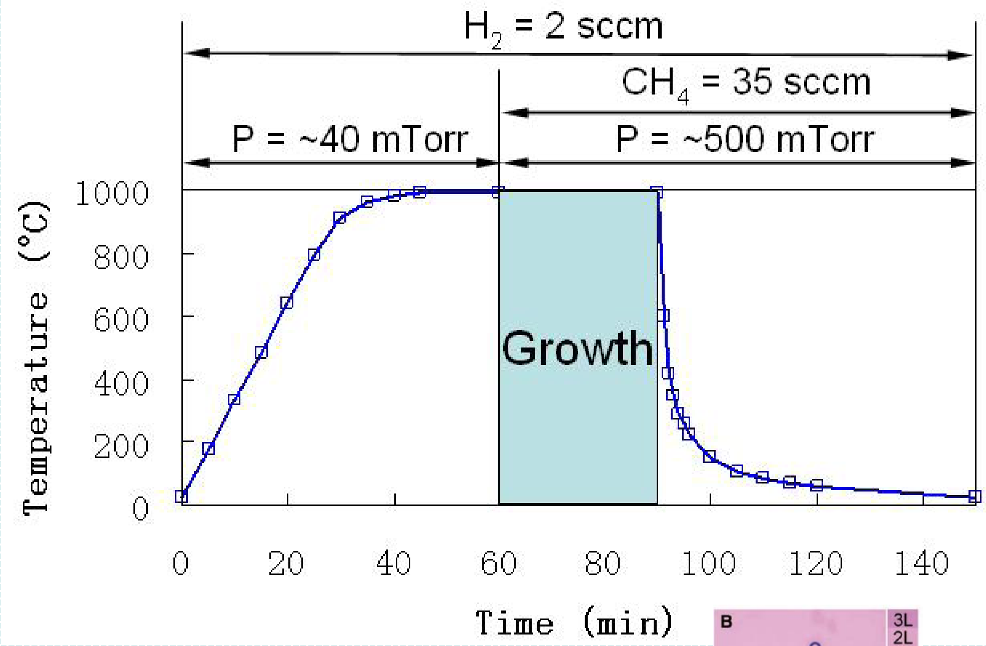

Bilayer graphene ~ 3-4%
Trilayer or thicker < 1%
Single atomic layer graphene >95%

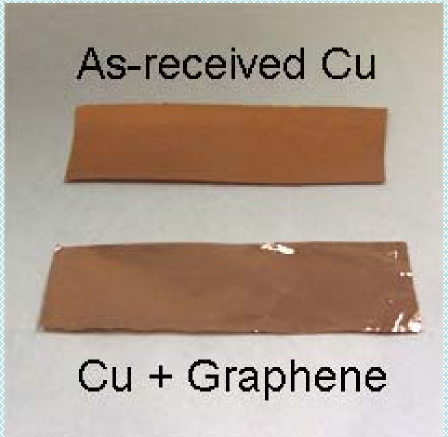

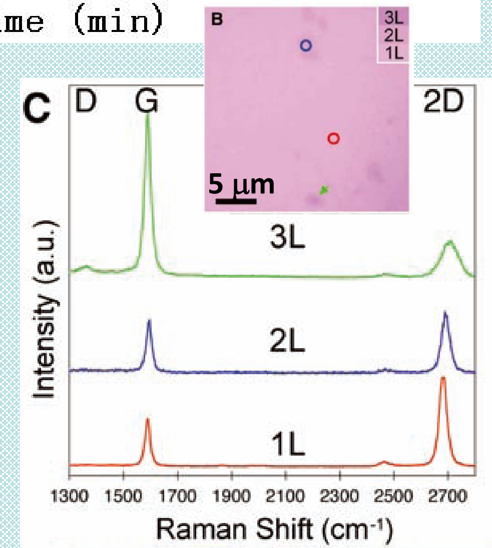

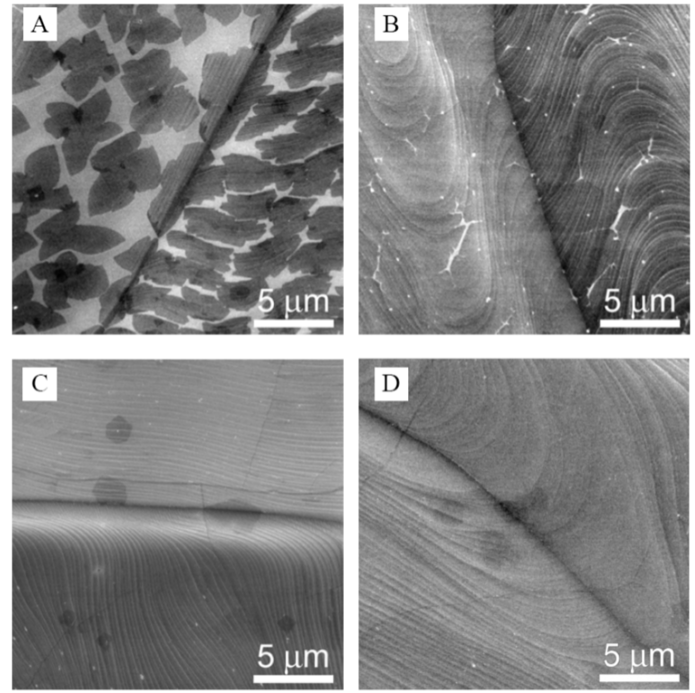

igure S3. SEM images of graphene on Cu with different growth times of (A) 1 min, (B) .5 min, (C) 10 min, and (D) 60 min, respectively.

Large Area Graphene Fabrication-CVD on Cu

-- Li, et. al., Science 09'

Self-limiting growth of graphene on copper

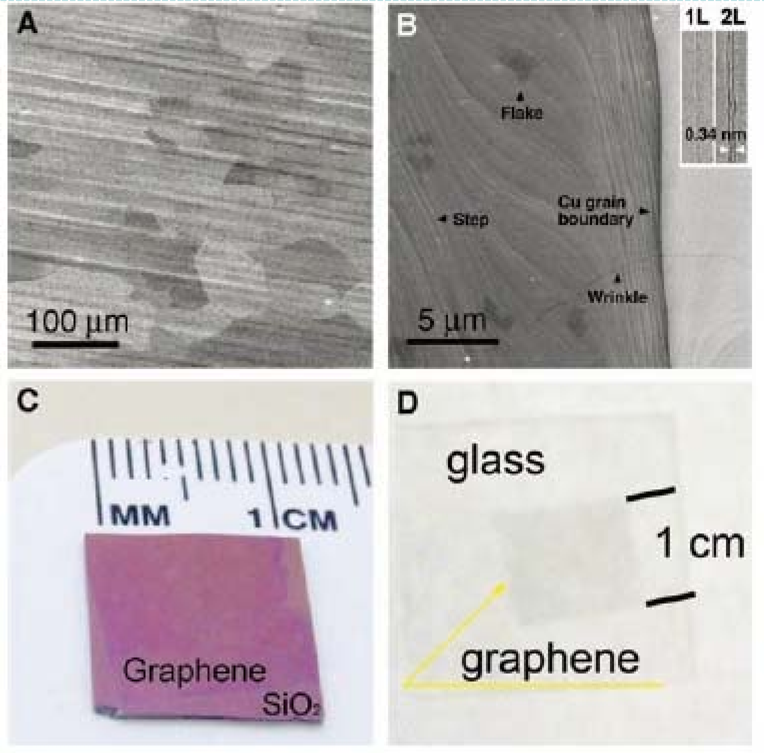

Mobility ~ 4000 cm^2/V-sec

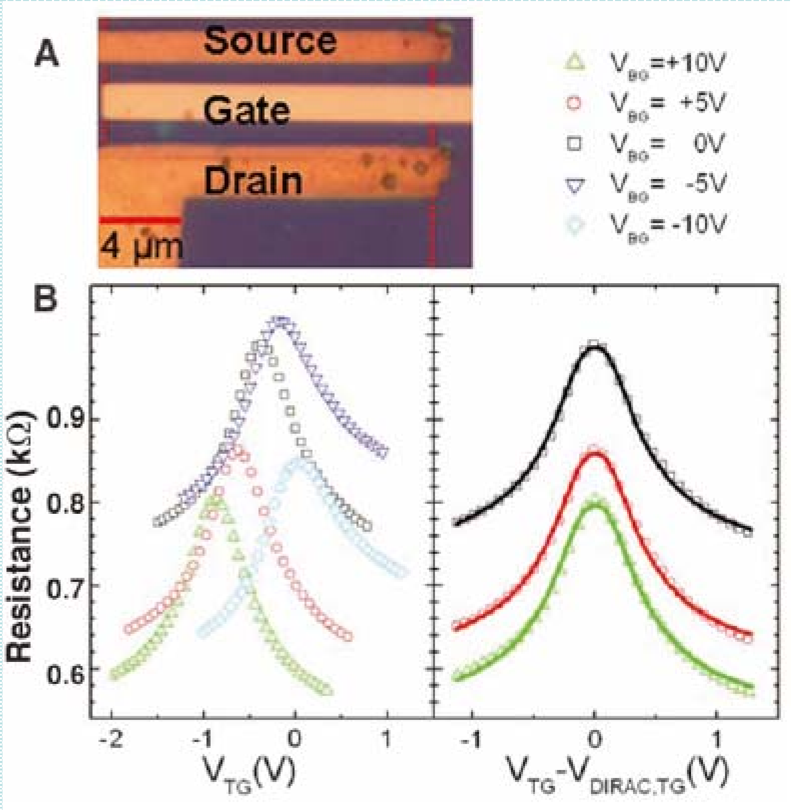

Large Area Graphene Fabrication- SiC

-- Berger, et. al., J. Phys. Chem. B 04′

Thermal decomposition at the surface of SiC(0001):

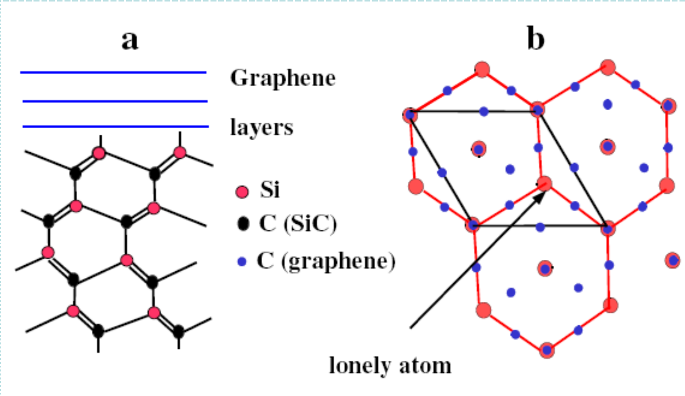

Sublimation of Si

+

graphitize the excess C

Thickness can be controlled by Temp.

4H-SiC (Si terminated)

6H-SiC (C terminated)

TABLE 1: Sample Properties[a]

Sample	C:Si	Thickness	R_{4K}	Mobility
A	10	3 ML	1.5 $k\Omega$	1100 cm^2/Vs
B	∞	>5	2.2	
C	9	3	22	
D	10	3	33	15
E	9	3	225	
F	7	2.5		

[a] Ratio of intensities in the C(271 eV) and Si(92 eV) AES peaks, calculated thickness in graphene monolayers, square resistance at 4 K, and mobility (where measured).

LEED image

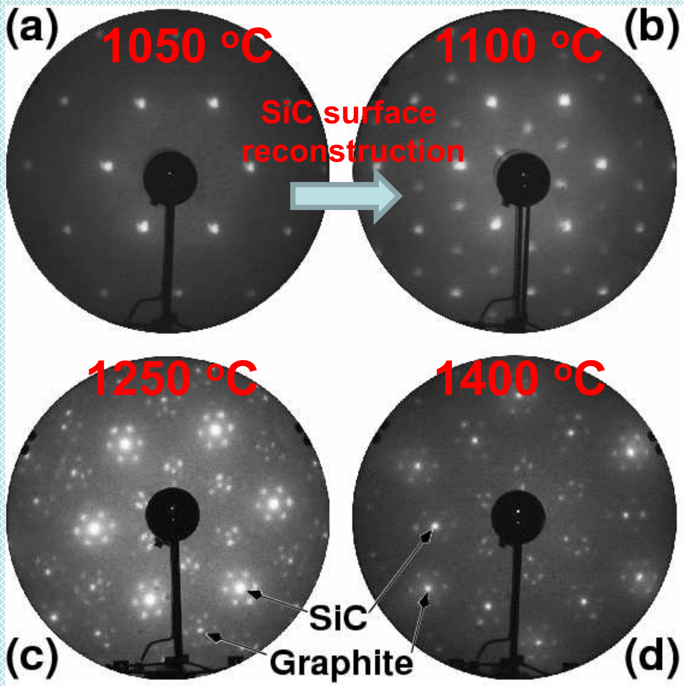

STM image

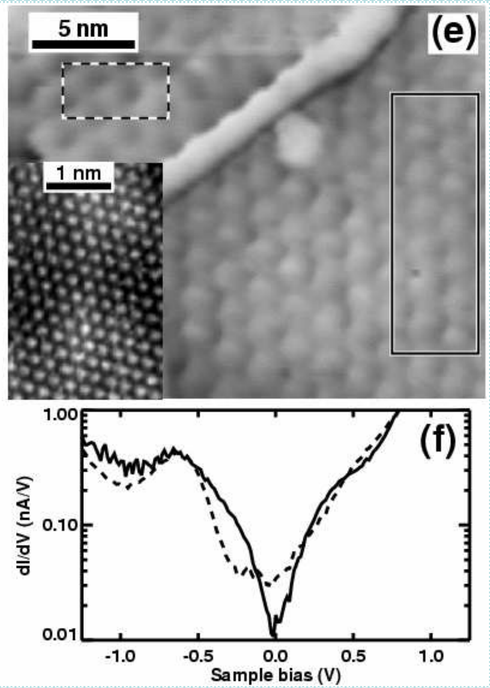

Large Area Graphene Fabrication- MBE

-- Park, et. al., Adv. Mater. 10′

Epitaxial Graphene using Molecular Beam Epitaxy

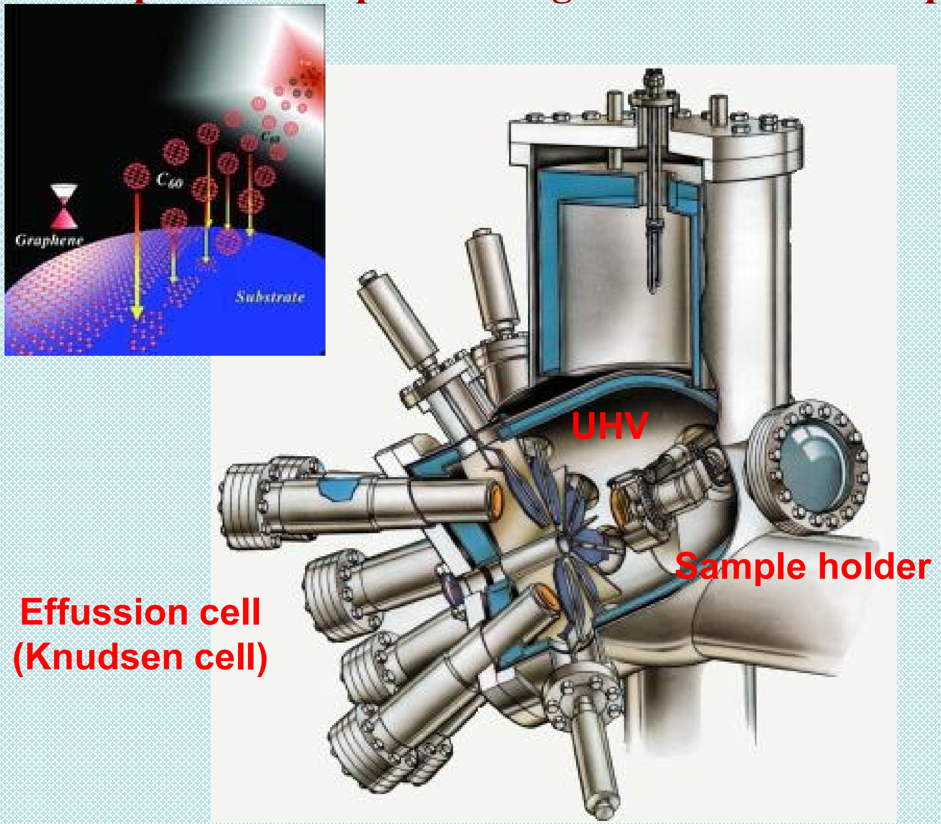

Raman Spectrum

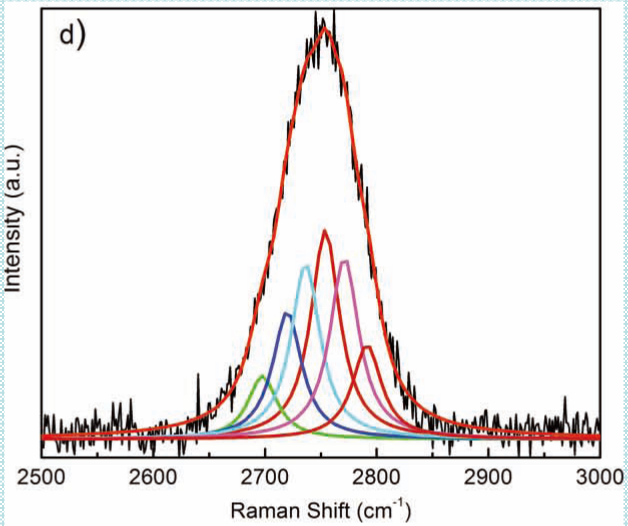

Trilayer graphene

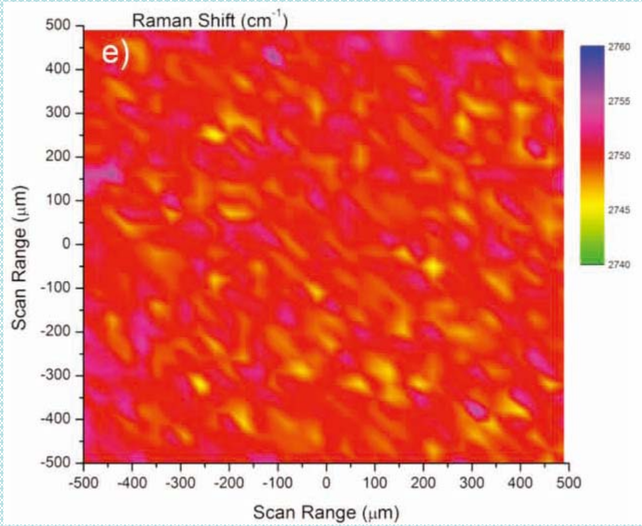

- C_{60} and graphite filament source
- Filament source at 1200°C
- Substrate temp. @ 1400°C
- Thickness control by carbon flux and substrate temp.

Can Graphene-based device replace current silicon based device ?

Comparison between graphene and semiconductor

	Semiconductor	Graphene
Electronic structure	Band gap > 1 eV	No-band gap (linear dispersion)
carrier	massive	massless (speed: c/300)
chirality	No	Yes
Dimensionality	Quasi-2D via electric field confinement (t~5-50 nm)	Ideal 2D (t ~ 0.34 nm)

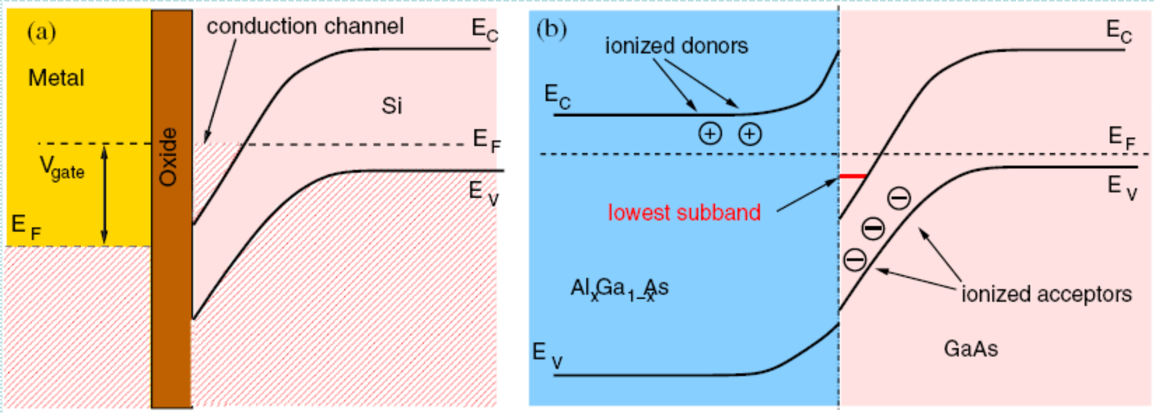

Quasi two-dimensional subband at interface

Graphene Nano-ribbon : Energy Gap Engineering

• **Gap opening due to quasi-1D confinement of the carriers**

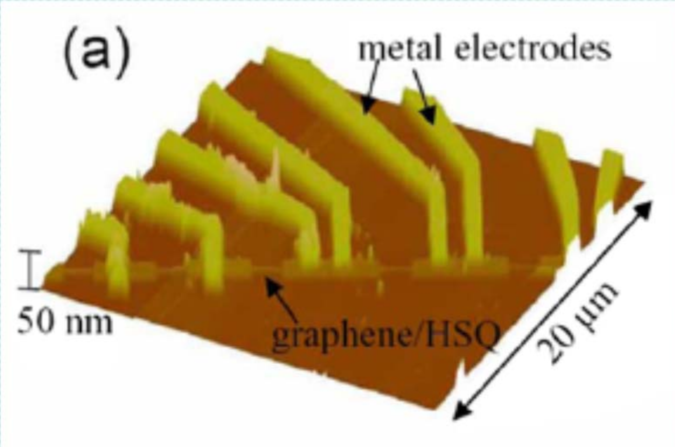

$$E_g = \frac{\alpha}{(W - W^*)}$$

$$\alpha \sim 0.2\,eV \cdot nm, W^* = 16nm$$

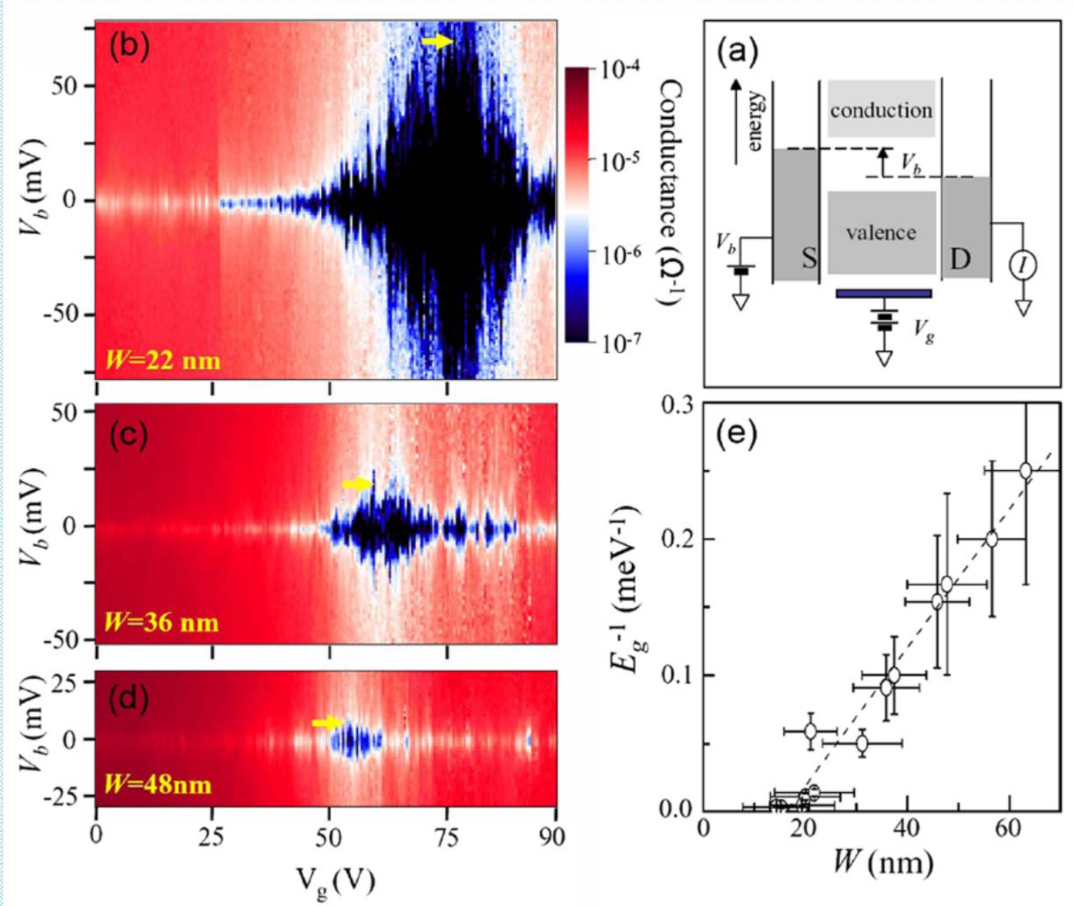

Field effect device: replacing current silicon-based device

- **Full-electric field tuning of band gap in bilayer graphene(BLG)**

-- Zhang *et al.*, Nature 09'

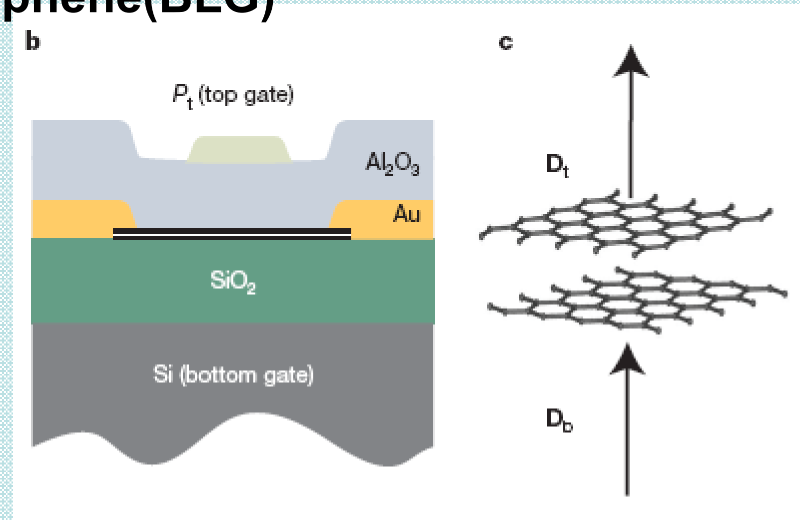

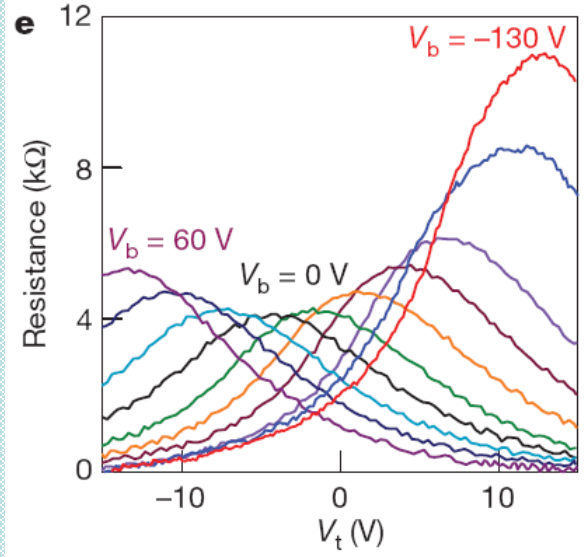

$$\vec{D} = [\varepsilon_b(V_{bg} - V_{bg0})/d_b - \varepsilon_t(V_{tg} - V_{tg0})/d_t]/2$$

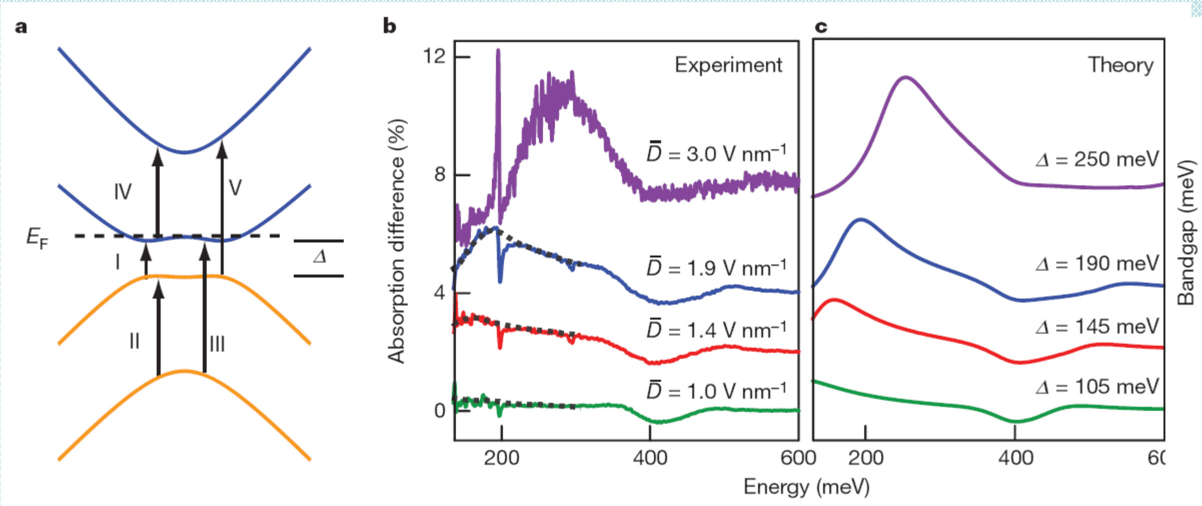

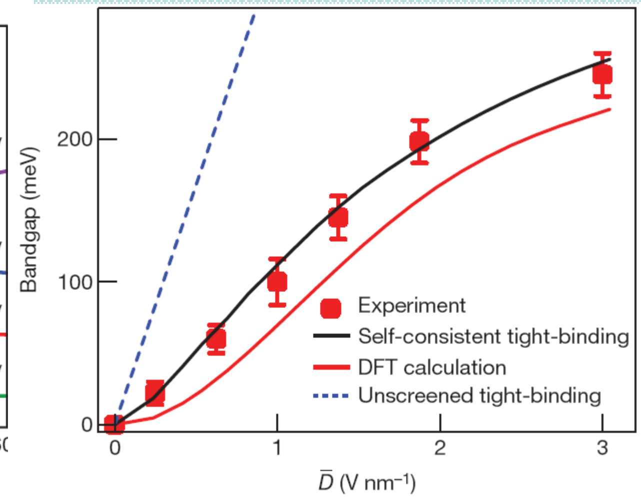

SQUID device

S/Graphene/S Josephson Junction

Heersche, et al., Nature 07'

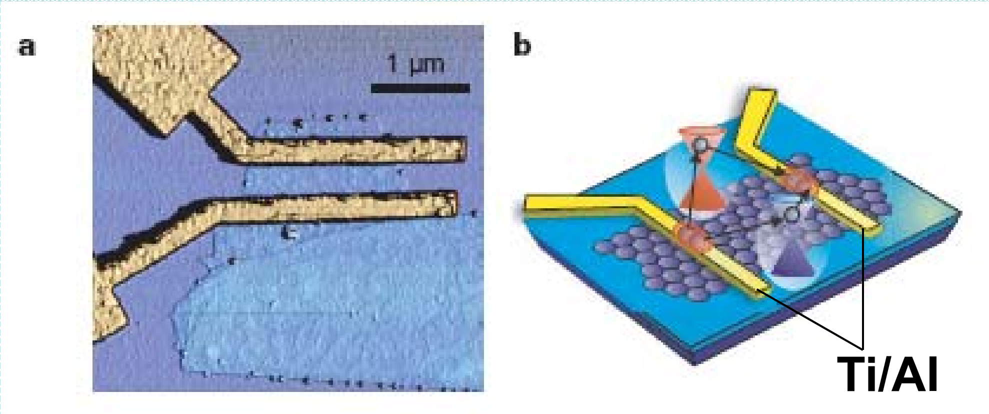

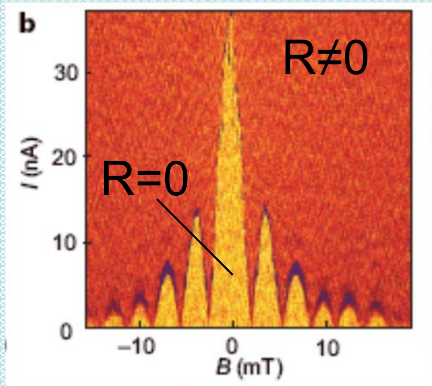

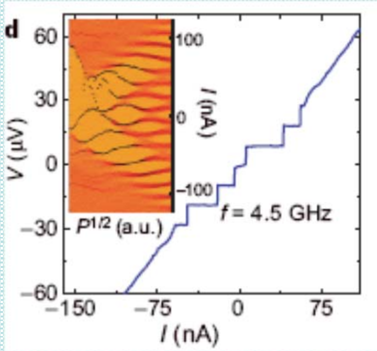

Shapiro steps

- **S electrodes spaced by graphene**
- **DC and AC Josephson effect**
- **Phase coherent transport at Dirac point**

DC Josephson :

$$I_C \propto \frac{\sin(\pi\Phi/\Phi_0)}{\pi\Phi/\Phi_0},\ \Phi = \text{total magnetic flux}$$

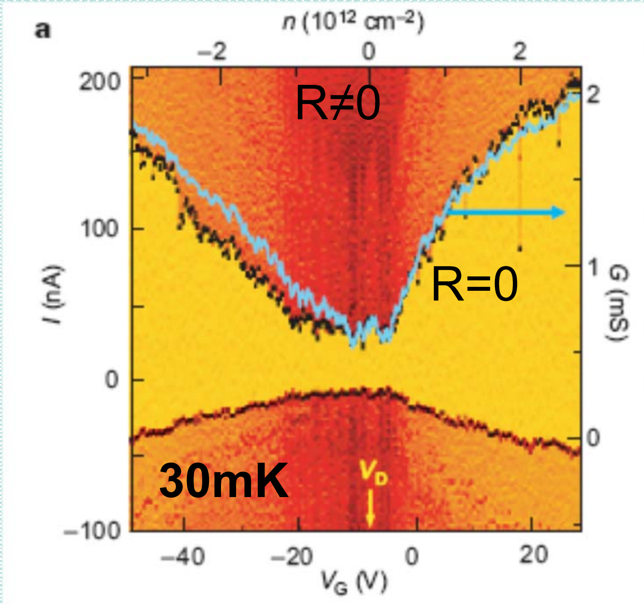

Spin electronics:

Spin transport and precession in graphene at room temperature

- Tombros et al., Nature 07'

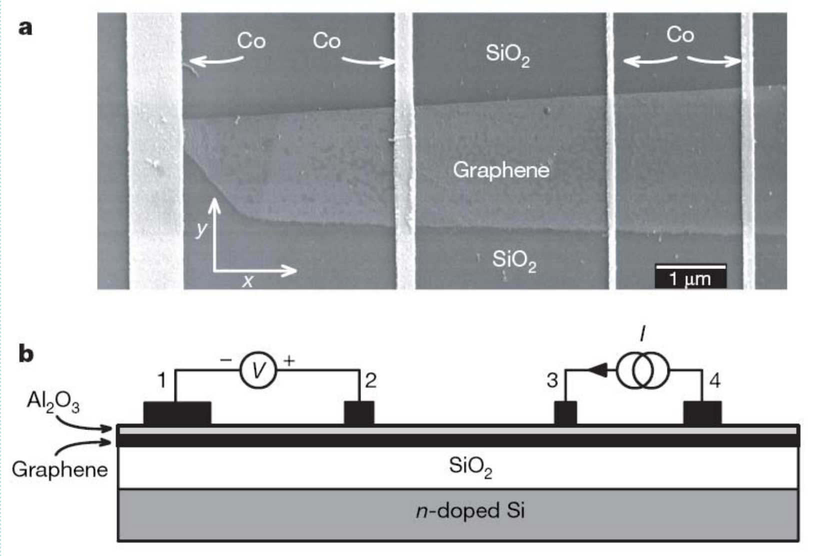

- **Large spin emf signal at R.T.**
- **Spin diffusion length λ_{sf}~ 1.5-2 μm**
- **Spin relaxation time τ_{sf} ~ 100ps**

$$R_{non-local} \propto \int_0^\infty P(t)\cos(\omega_L t)\exp(-t/\tau_{sf})dt$$

cf : λ_{sf}~ 0.5 μm

τ_{sf} ~ 10 ps in copper

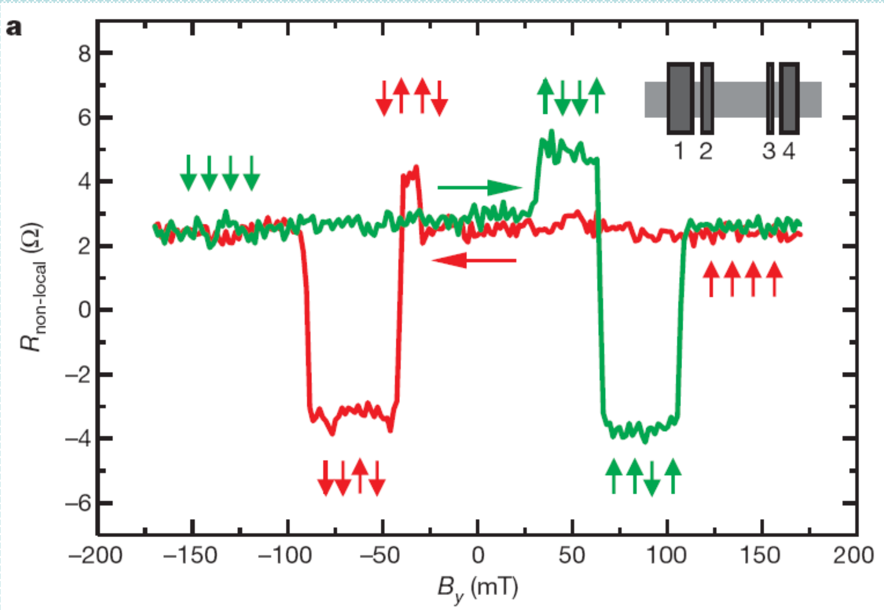

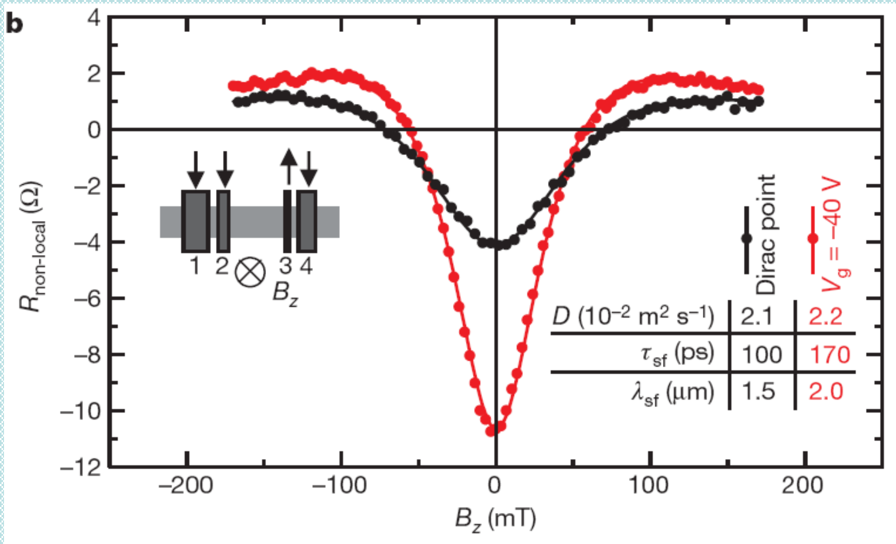

Optical application

- **Graphene photoluminescence(PL)**

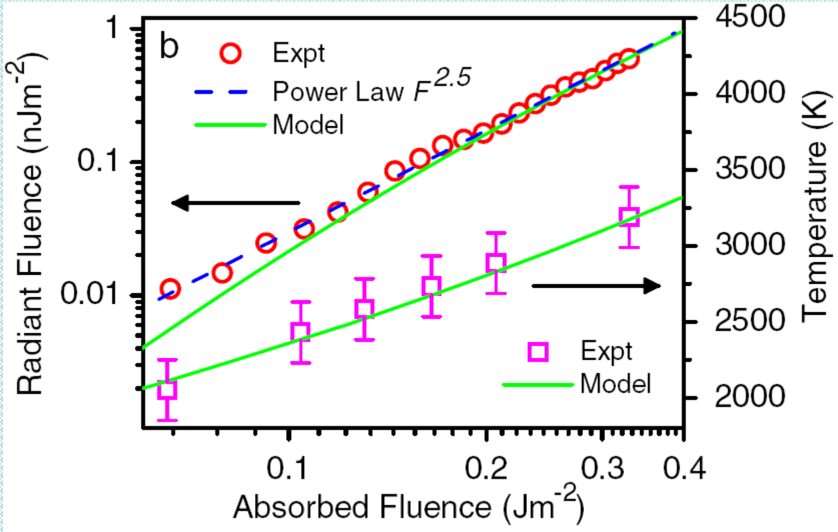

- **Ultrafast photon excitation ~ 30 fs: carriers with transient T > 2000K**

- **PL: thermal emission visible spectra range (1.7 – 3.5 eV) bigger than excitation laser ~ 1.5 eV**

- **PL in graphene oxide (GO) and gapped (bilayer) graphene:**

1L : single-layer graphene after O2 plasma treatment

PL intensity

Layer contrast

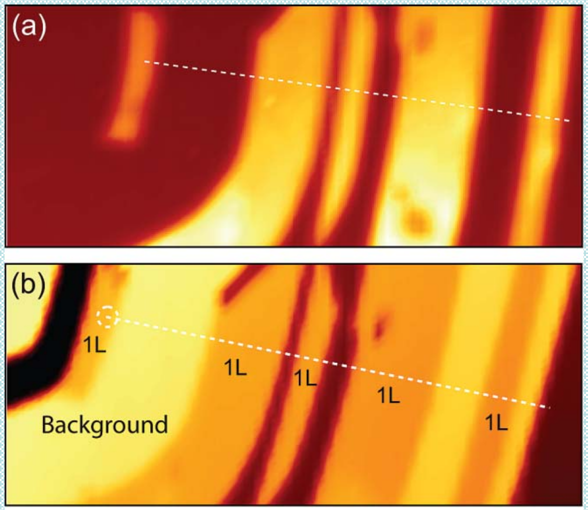

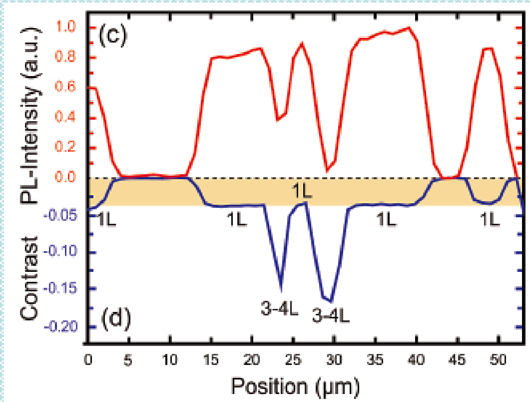

Figure 4. Correlation between PL and layer thickness. (a) PL image; (b) elastic scattering image[20] of the same sample area. (c,d) Corresponding cross sections taken along the dashed lines in (a,b). PL is only observed from treated SLG, marked 1L.

Graphene Nanophotonics

- F. Javier Garcia de Abajo, Science 13’

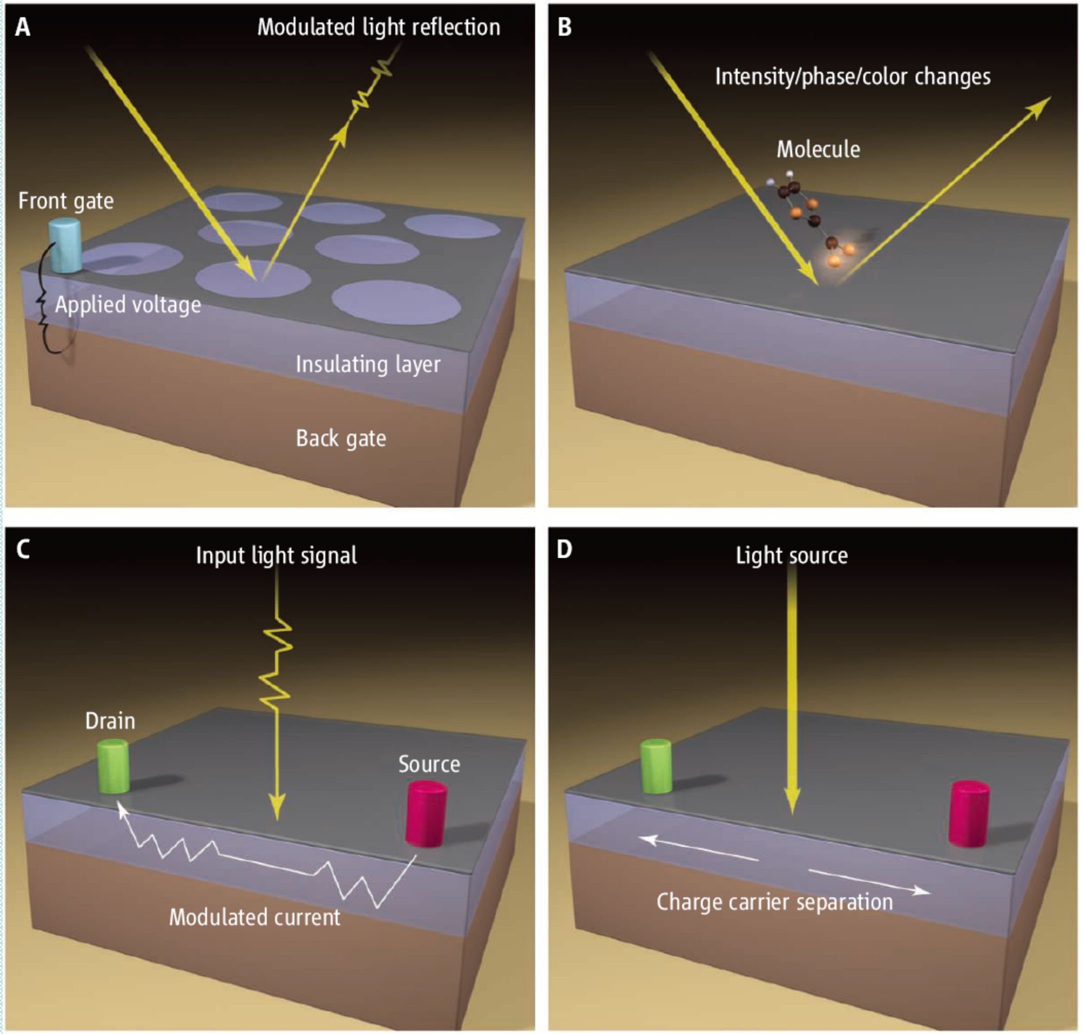

The graphene nanophotonics landscape. (**A**) Light modulation of the optical response of graphene is realized by applying voltages through electrical gates (*4–6*). (**B**) Molecular detection is accomplished through the modifications in the optical response associated with changes in the concentration of charge carriers (*9*). (**C**) Measurement of the electrical current modulated by photon absorption leads to efficient light detection (*11*, *12*). (**D**) Light harvesting occurs when the energy of absorbed photons is converted into charge carriers that are separated by doped gates to generate a net current.

RESEARCH FUNDING

Europe's €2 Billion Bet on the Future

This month, the European Union will pick two futuristic research proposals and shower them with up to €1 billion each. But will it be money well spent?

Science Magazine

E.U. Flagships: The Candidates at a Glance

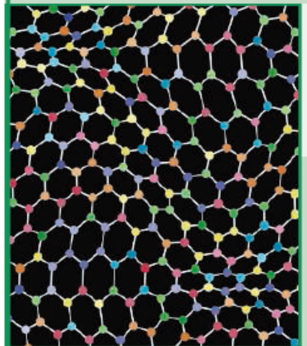

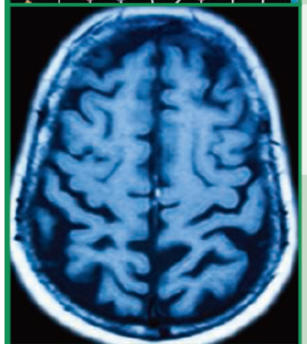

FuturICT. Proposes massive data mining to build a planetary scale simulator freely available for use. Promises "historic breakthroughs" in "revealing the hidden laws and processes underlying societies." 1

<< **Graphene.** Better batteries, lighter planes, and flexible electronics are some of graphene's promises. "Disruptive science" is hard to do piecemeal, proponents say; a Flagship grant would allow for coordination. 2

Guardian Angels. A network of energy-harvesting sensors that can monitor people's health status, scan the environment for dangers, and provide advice "to increase the happiness people experience." 3

<< **The Human Brain Project.** Supercomputers would simulate and help people understand the human brain. Key argument: Only a model can bring together everything we know about neuroscience. 4

IT Future of Medicine. Aims to use individual medical data to build a personalized computer model for 500 million Europeans. The approach is currently pioneered in cancer treatment. 5

<< **RoboCom.** Inspired by animals, its goal is to develop "robot companions" better able to respond to human needs. Engineering these machines would also help understand the design principles of biological bodies and brains. 6

A Long Game for Carbon-Based Materials

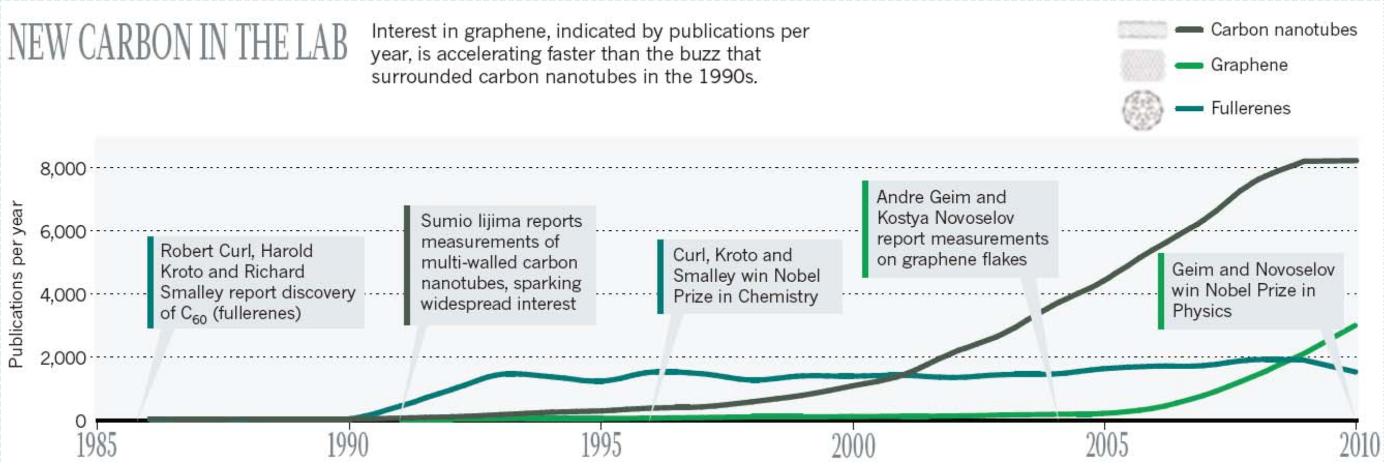

"Graphene will have its place, but it will just take longer than people think."

Cutting cost
+
higher quality

"It typically takes any technology some 20 years to emerge from the lab and be commercialized."

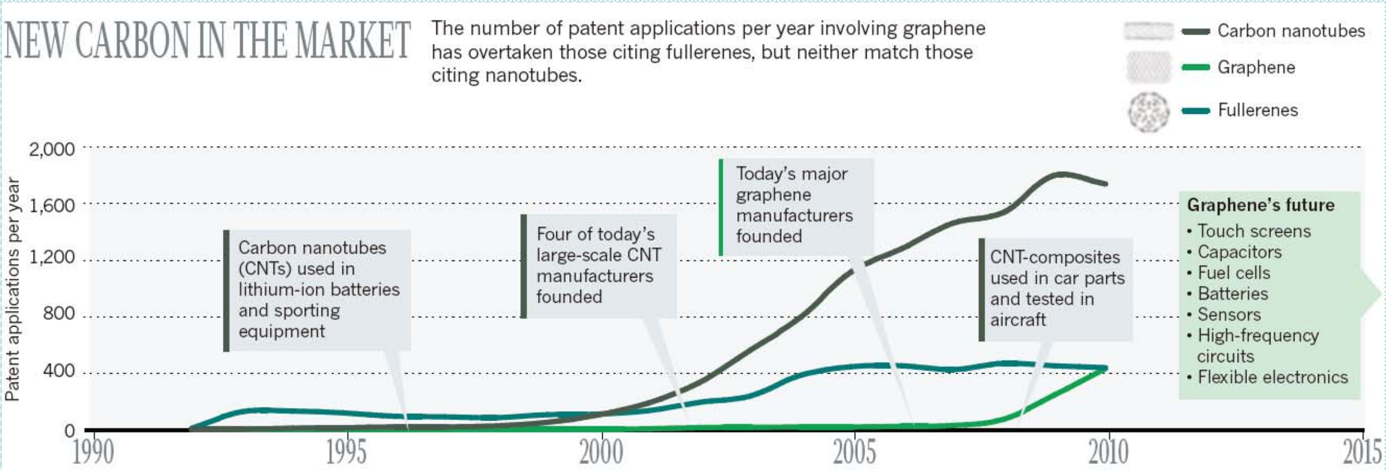

Graphene manufacturers

BGT BLUESTONE GLOBAL TECH
GRAPHENE INDUSTRIES
XG sciences
Vorbeck Materials — realizing graphene's possibilities
ANGSTRON MATERIALS
GRAPHENE SUPERMARKET
CVD
DGS
⋮

We are observing a revolution in electronics industry !
Commercial product made of graphene will have its debut in our time.

PartII: Concluding Remarks

- Massless Dirac Fermion and insensitive to impurity scattering
- Marginal Fermi-liquid behaviour
- Unavoidable defects and disorder in 2-D graphene
- Exhibit robust minimal conductivity and shifted IQHE
- Phase coherent transport at the Dirac point
- Appearance of band gap in graphene nanoribbon

Carbon nanostructures

Wei-Li Lee, IoP, Academia Sinica

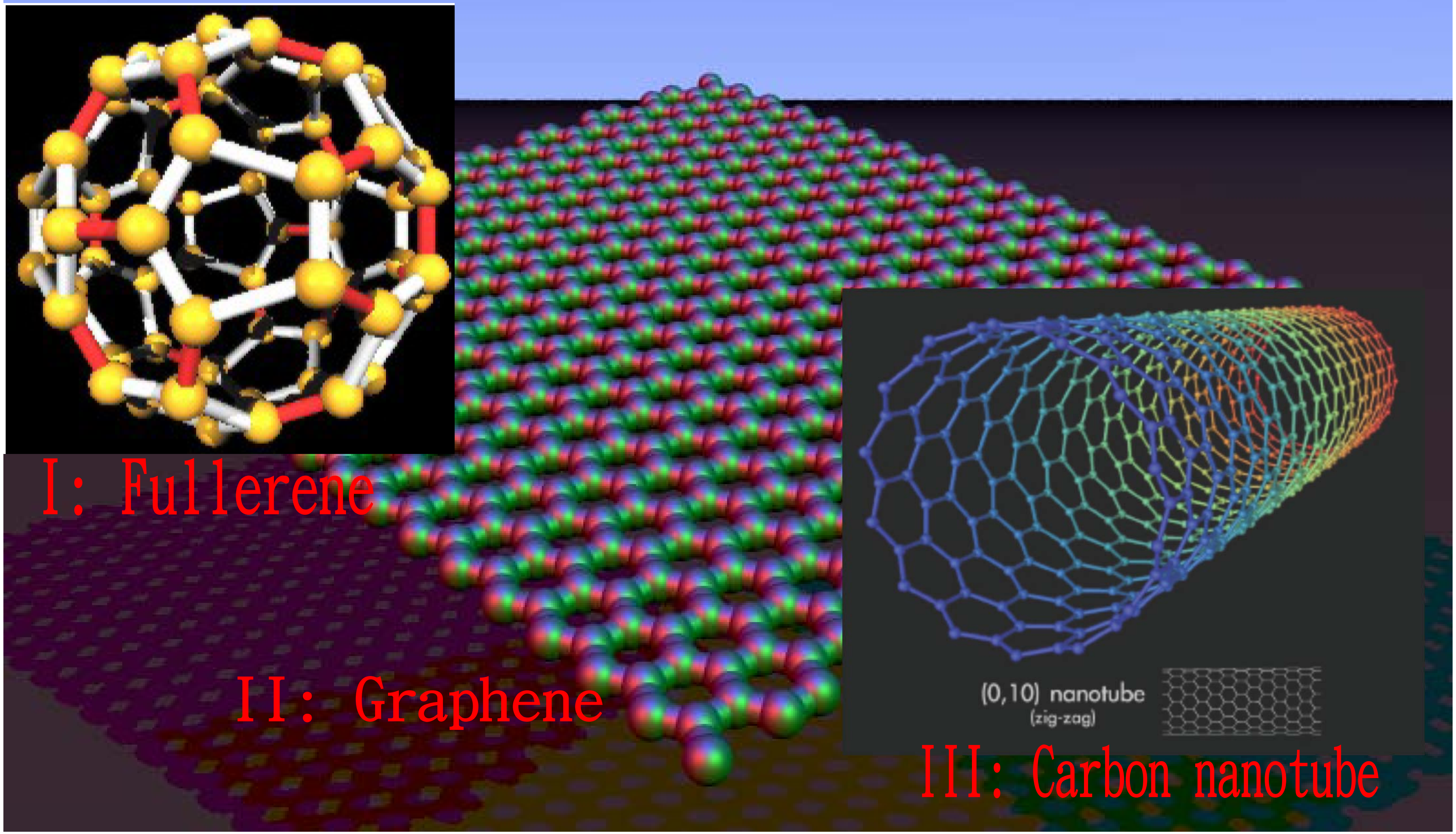

Part III

Carbon nanotube

Outline

- Structure of carbon nanotube
- Fabrication of carbon nanotube
- electronic property in carbon nanotube
- Applications of carbon nanotube

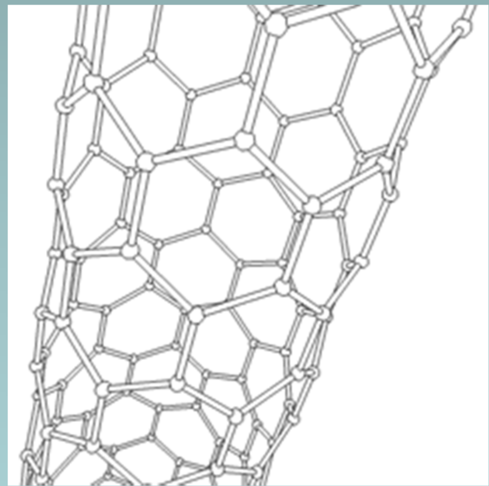

semiconducting

Zigzag (8,0) carbon nanotube

Structure of single wall carbon nanotube

Rolling of a 2-D graphene sheet

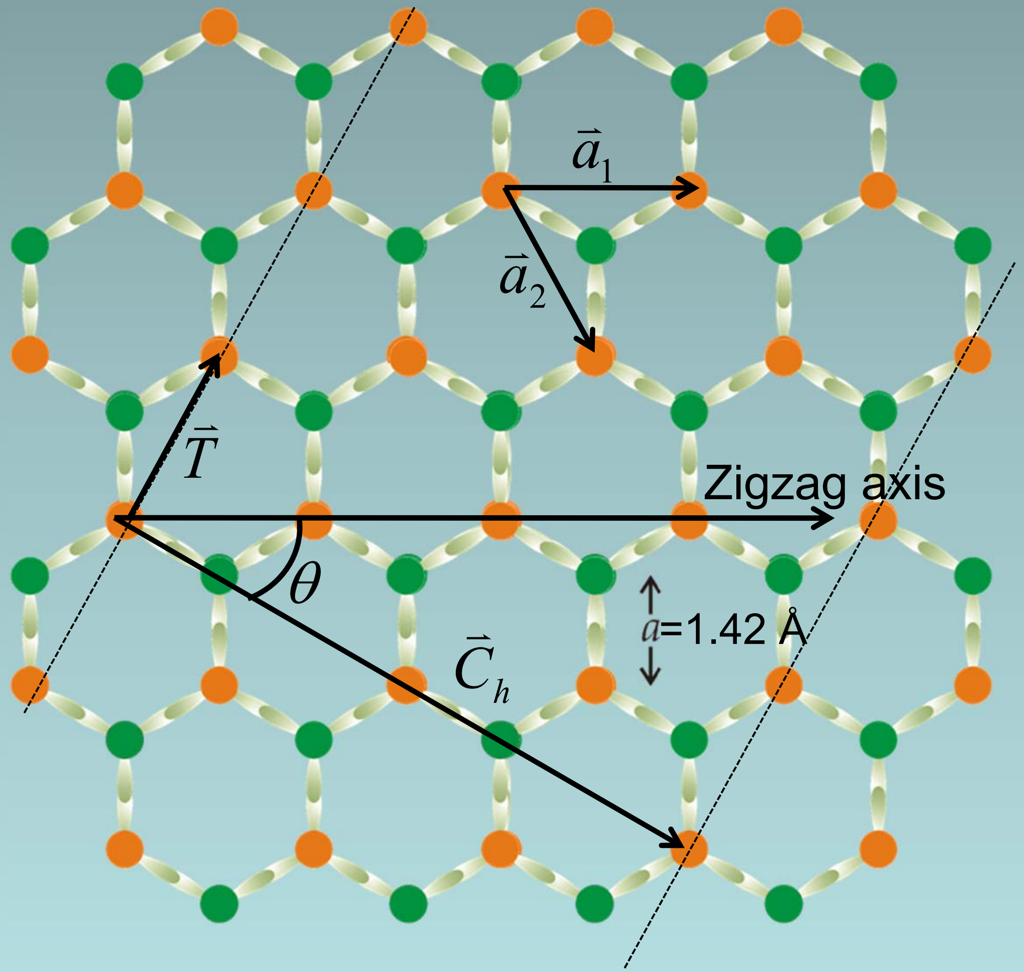

Chiral (Circumferential) vector

$$\vec{C}_h \equiv n\vec{a}_1 + m\vec{a}_2$$

Translational vector

$$\vec{T} \perp \vec{C}_h$$

Tube diameter d_t

$$d_t = \left|\vec{C}_h\right| / \pi$$

$$= \frac{a}{\pi}\sqrt{3(m^2 + mn + n^2)}$$

Angle $\theta = \tan^{-1}[\sqrt{3}m/(m+2n)]$

Rolling of a 2-D graphene sheet

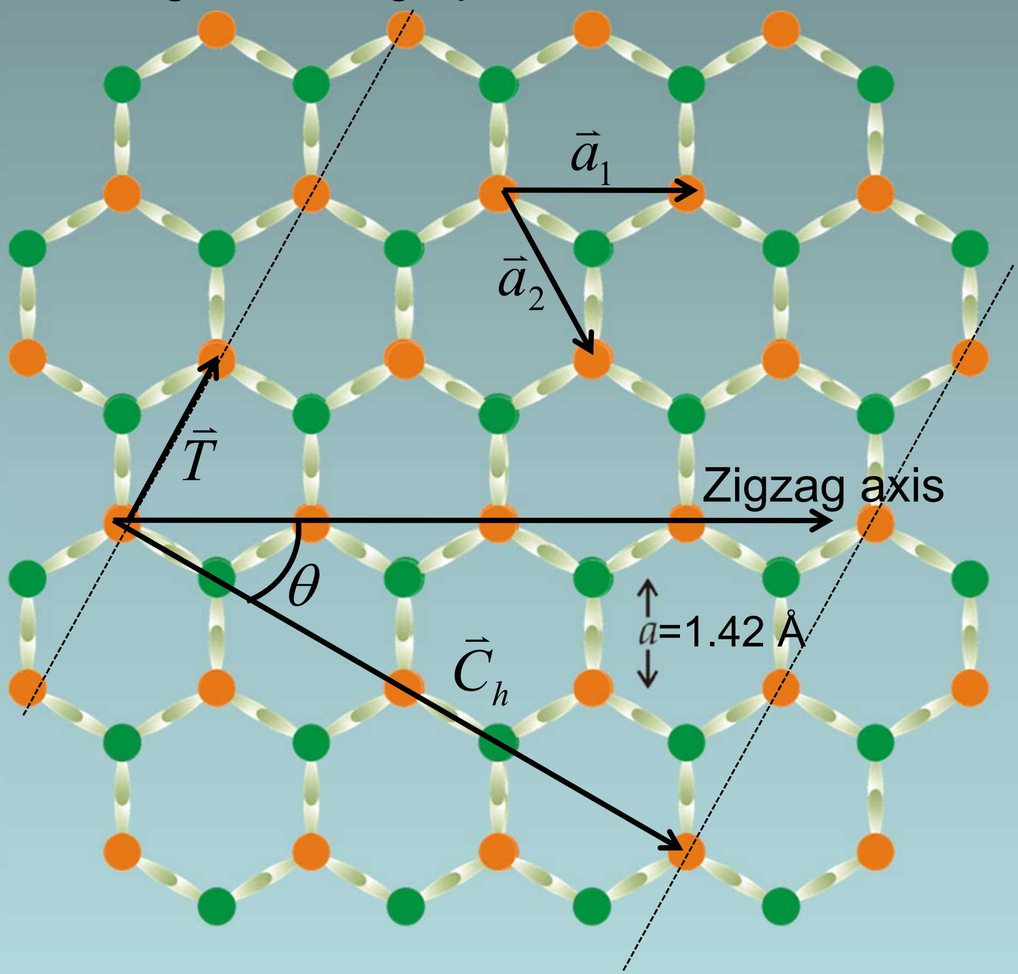

Label a carbon nanotube

$$(n, m),$$

$$where \quad \vec{C}_h \equiv n\vec{a}_1 + m\vec{a}_2$$

or

$$(d_t, \theta)$$

Tube diameter

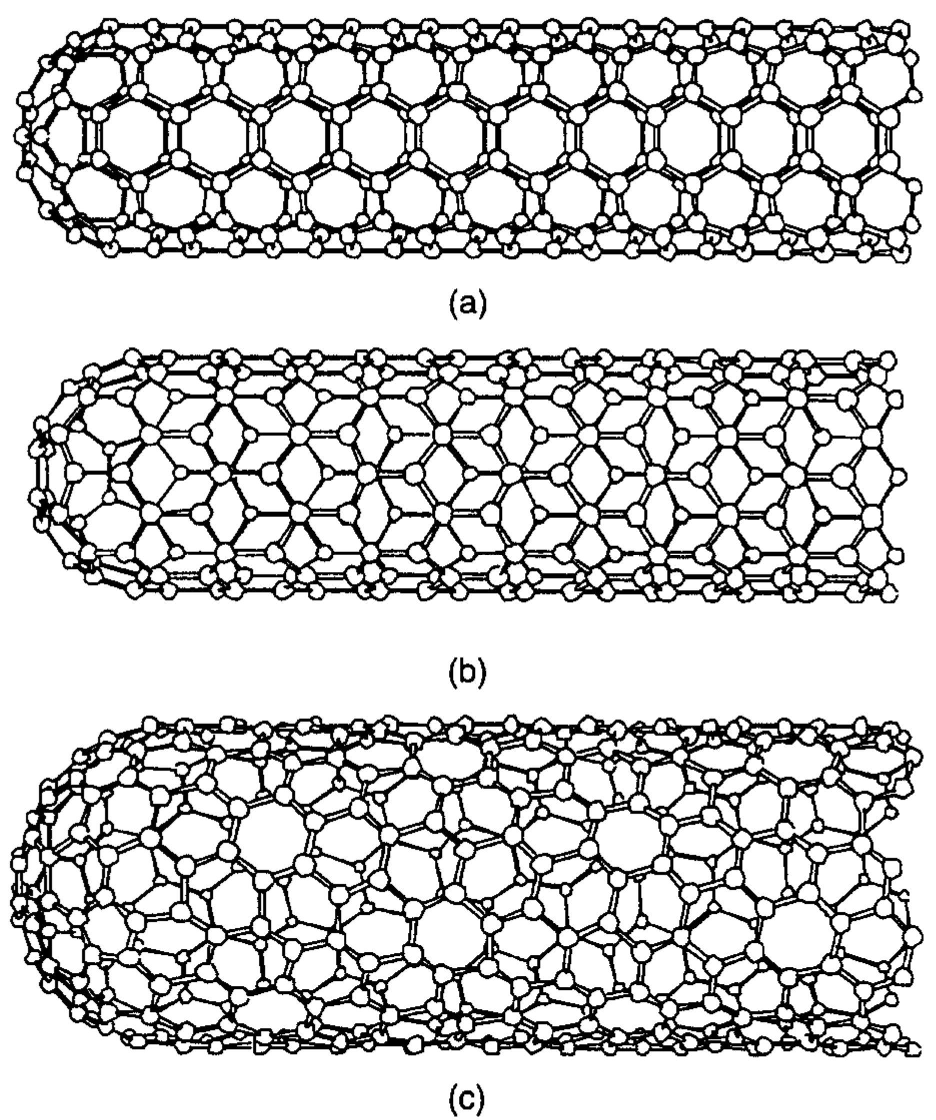

Armchair

$(5,5)$ (n,n)

Zigzag

$(9,0)$ $(n,0)$

Chiral

$(10,5)$ (n,m)

Electronic Band Structure in Materials

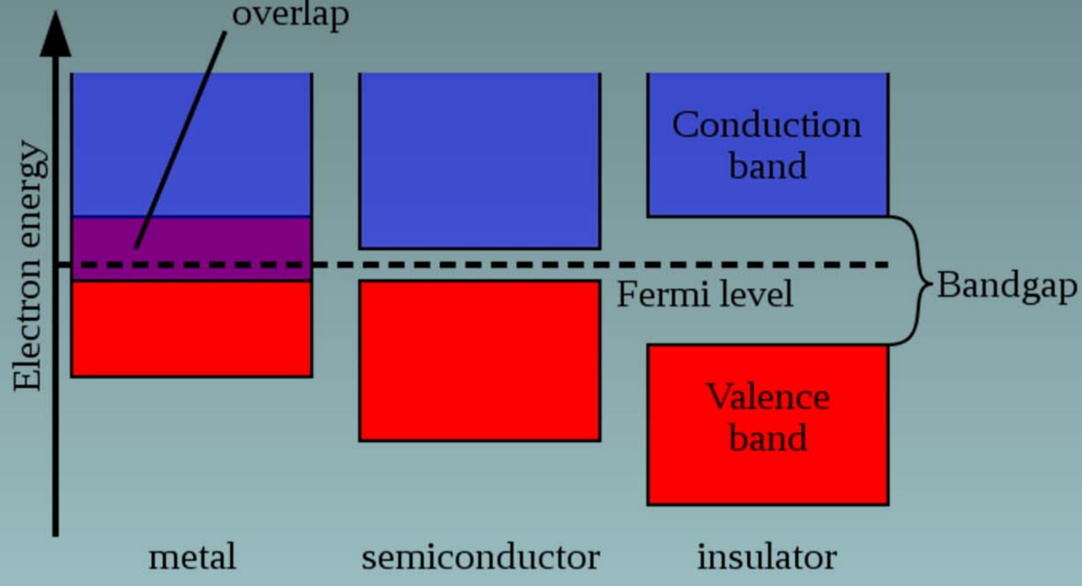

Armchair tubes are all metallic !!

Rule : metallic for n-m = 3 q
(q: an integer)

Why ?

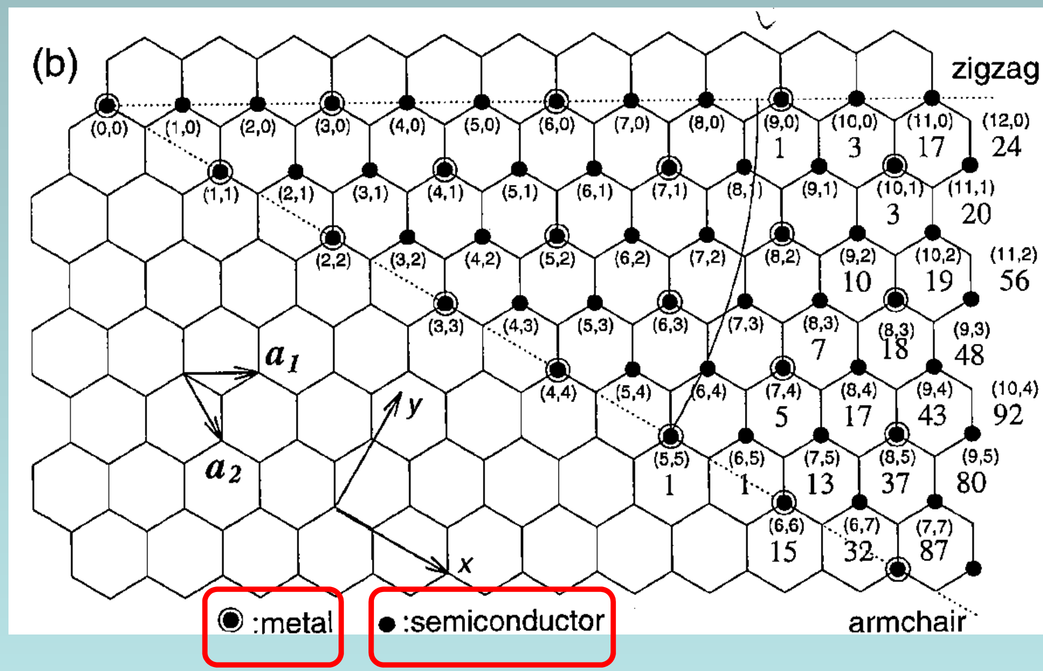

1-D Band structure for an armchair CNT (N_y,N_y):

2-D graphene sheet

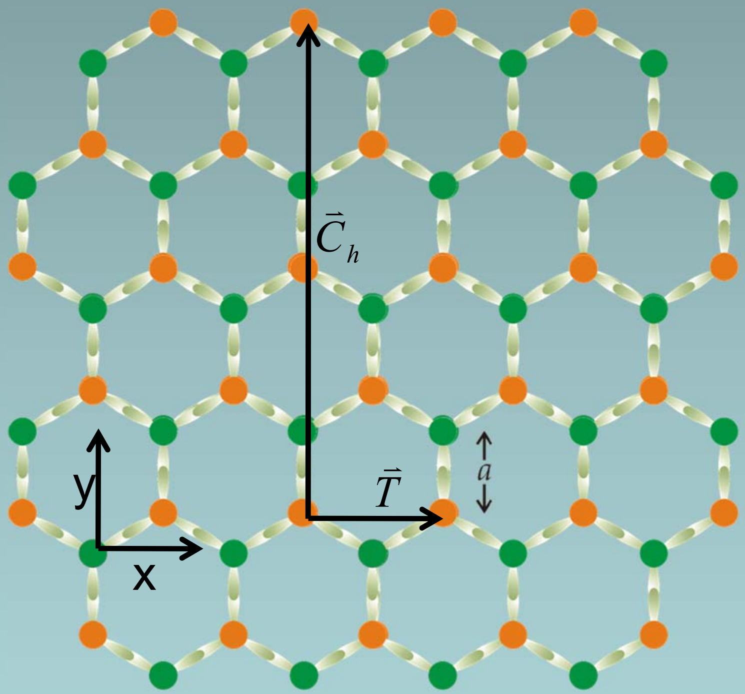

- Dispersion relation for 2D graphene :

$$E^{2D}(k_x, k_y) = \qquad \text{Eq(1)}$$

$$\pm t[1 + 4\cos(\frac{\sqrt{3}a}{2}k_x)\cos(\frac{3a}{2}k_y) + 4\cos^2(\frac{\sqrt{3}a}{2}k_x)]^{1/2}$$

Bohr-Sommerfeld quantization rule:

$$\int_{\substack{closed\\path}} p \cdot d\ell = qh \text{ , q is integer number}$$

- In 1D armchair CNT :

  k_y satisfy periodic boundary condition

$$\boxed{\because k_y 3aN_y = 2\pi q}$$

$$\therefore E^{1D}{}_{arm}(k_x = k)$$

$$= \sum_{q=1}^{N_y} \pm t[1 \pm 4\cos(\frac{\sqrt{3}a}{2}k)\cos(\frac{\pi q}{N_y}) + 4\cos^2(\frac{\sqrt{3}a}{2}k)]^{1/2}$$

$$-\frac{\pi}{2} \leq \frac{\sqrt{3}a}{2}k \leq \frac{\pi}{2}$$

Example : 1-D Band structure for a armchair CNT (5,5):

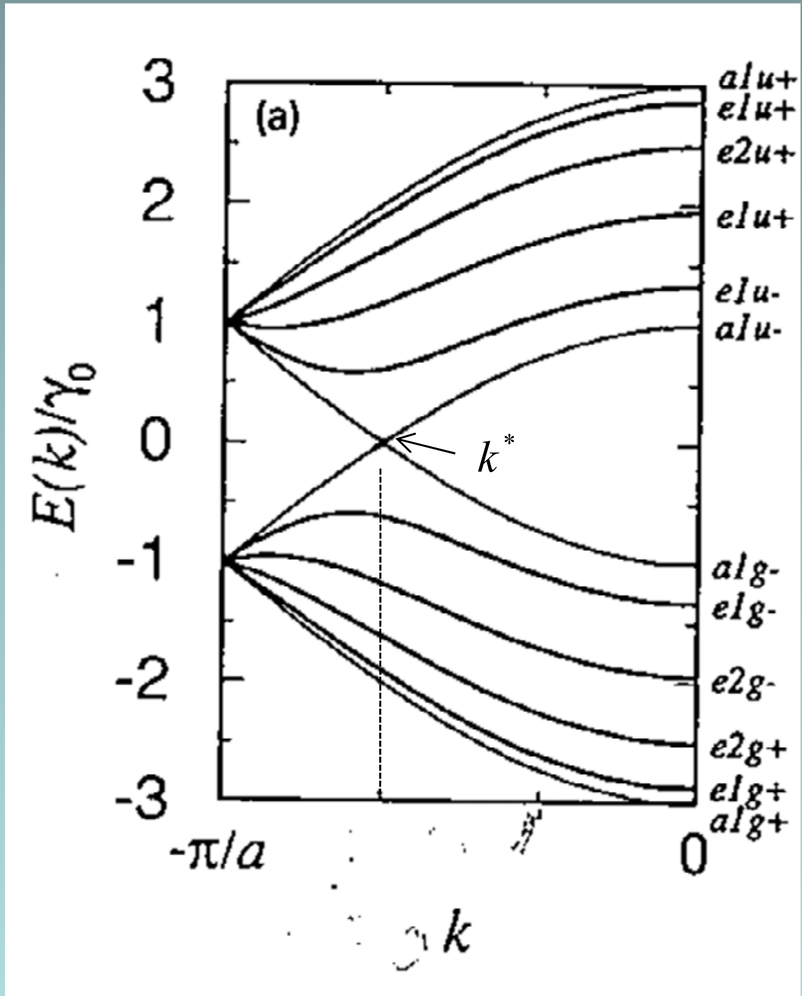

$$\therefore E^{1D}{}_{arm}(k_x = k, k_y = 2\pi q/15a)$$

$$= \sum_{q=1}^{5} \pm t[1 \pm 4\cos(\frac{\sqrt{3}a}{2}k)\cos(\frac{q\pi}{5}) + 4\cos^2(\frac{\sqrt{3}a}{2}k)]^{1/2}$$

$$-\frac{\pi}{2} \le \frac{\sqrt{3}a}{2}k \le \frac{\pi}{2}$$

- Conduction bands and valence bands each has
  - 4 doubly degenerate bands
  - 2 non-degenerate bands

- Band cross at k* : metallic conduction

$$\boxed{k^* = (\frac{2\pi}{3\sqrt{3}a}, \frac{2\pi}{3a})}$$

One of the Dirac point in 2-D band !!

1-D Band structure for a zigzag CNT (N_x,0):

2-D graphene sheet

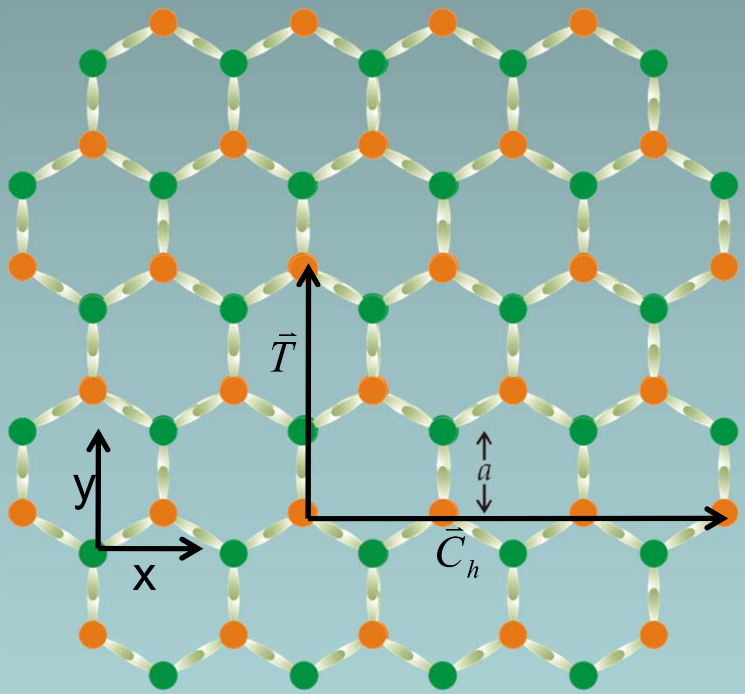

- In 1D zigzag CNT :

  k_x satisfy periodic boundary condition

$$\boxed{\because k_x \sqrt{3} a N_x = 2\pi q}$$

$$\therefore E^{1D}{}_{zigzag}(k_y = k)$$

$$= \sum_{q=1}^{N_x} \pm t[1 \pm 4\cos(\frac{3a}{2}k)\cos(\frac{q\pi}{N_x}) + 4\cos^2(\frac{q\pi}{N_x})]^{1/2}$$

$$-\frac{\pi}{2} \le \frac{3a}{2}k \le \frac{\pi}{2}$$

Example : 1-D Band structure for a zigzag CNT (9,0):

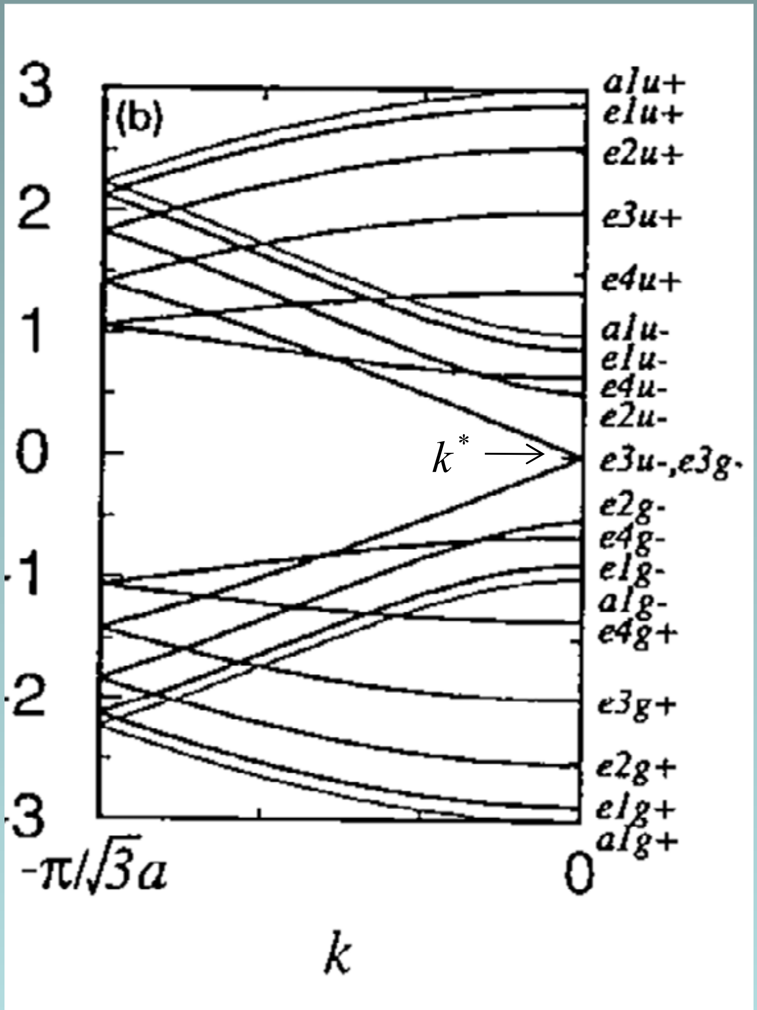

$$\therefore E^{1D}{}_{zigzag}(k_x = 2\pi q / 9\sqrt{3}a, k_y = k)$$

$$= \sum_{q=1}^{9} \pm t[1 \pm 4\cos(\frac{3a}{2}k)\cos(\frac{q\pi}{9}) + 4\cos^2(\frac{q\pi}{9})]^{1/2}$$

$$-\frac{\pi}{2} \le \frac{3a}{2}k \le \frac{\pi}{2}$$

- Conduction bands and valence bands each has
  8 doubly degenerate bands
  2 non-degenerate bands

- Band cross at k* : metallic conduction

$$\boxed{k^* = (\frac{4\pi}{3\sqrt{3}a}, 0)}$$

Another Dirac point in 2-D band !!

Example : 1-D Band structure for a zigzag CNT (10,0):

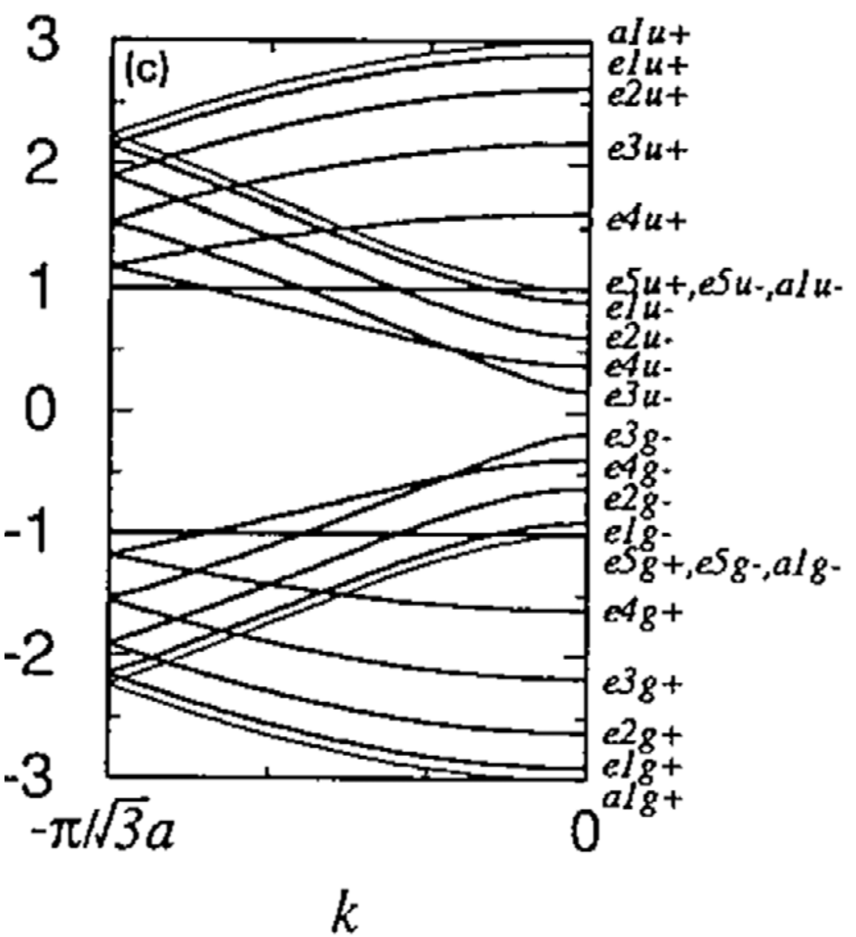

$$\therefore E^{1D}{}_{zigzag}(k_x = 2\pi q/10\sqrt{3}a, k_y = k)$$

$$= \sum_{q=1}^{10} \pm t[1 \pm 4\cos(\frac{3a}{2}k)\cos(\frac{q\pi}{10}) + 4\cos^2(\frac{q\pi}{10})]^{1/2}$$

$$-\frac{\pi}{2} \le \frac{3a}{2}k \le \frac{\pi}{2}$$

- Conduction bands and valence bands each has
  9 doubly degenerate bands
  2 non-degenerate bands

- No Band crossing : semiconducting transport !!

Slicing a 2-D graphene band

- alternative way of looking at 1-D Band in CNT

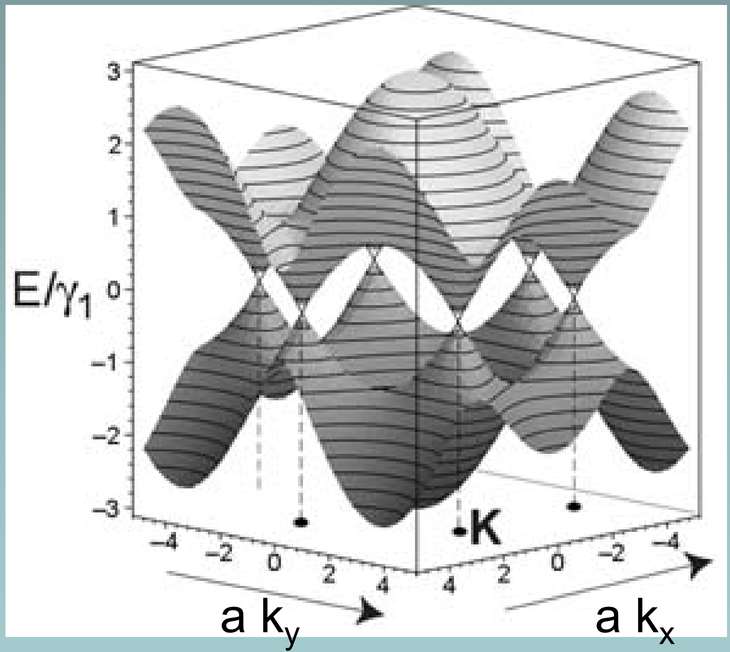

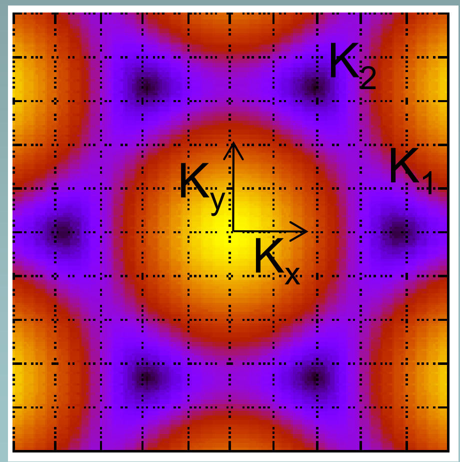

$E(\vec{q} = \vec{K}) = 0$

6 Dirac points

$$K_1 = \frac{4\pi}{3\sqrt{3}a}(1,0)$$

$$K_2 = \frac{4\pi}{3\sqrt{3}a}\left(\frac{1}{2}, \frac{\sqrt{3}}{2}\right)$$

- Whenever slicing through a Dirac point : metallic conduction otherwise : semiconducting transport behavior !

Armchair CNT (5,5):

$$\boxed{\because\ k_y = \frac{2\pi q}{15a}} \quad , -\frac{\pi}{\sqrt{3}a} \le k_x \le \frac{\pi}{\sqrt{3}a}$$

q=1,2…5

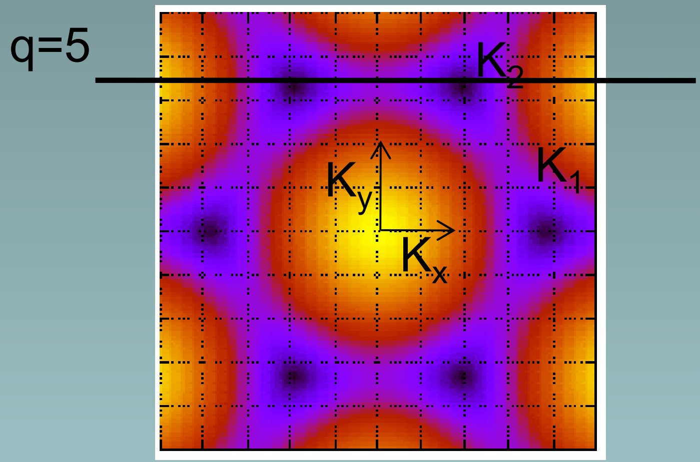

Slice through K_2 for q=5

$\Rightarrow$ Metallic conduction

$$\boxed{\begin{aligned} K_1 &= \frac{4\pi}{3\sqrt{3}a}(1,0) \\ K_2 &= \frac{4\pi}{3\sqrt{3}a}\left(\frac{1}{2},\frac{\sqrt{3}}{2}\right) \end{aligned}}$$

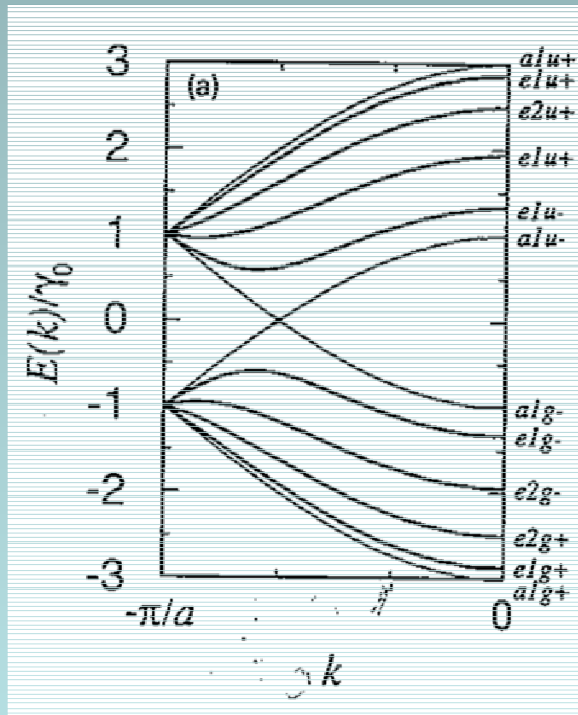

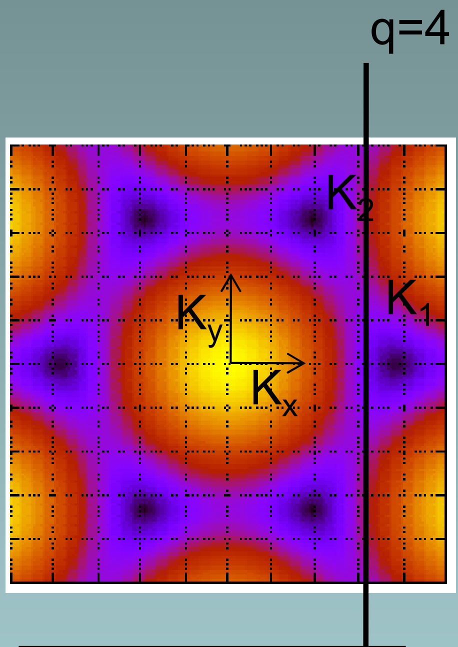

$$K_1 = \frac{4\pi}{3\sqrt{3}a}(1,0)$$

$$K_2 = \frac{4\pi}{3\sqrt{3}a}\left(\frac{1}{2},\frac{\sqrt{3}}{2}\right)$$

Zigzag CNT (10,0):

$$\boxed{\because k_x = \frac{\pi q}{5\sqrt{3}a}} \quad , -\frac{\pi}{3a} \le k_y \le \frac{\pi}{3a} \qquad q=1,2\ldots10$$

Does not Slice through any Dirac points

⇨ Semiconducting transport behavior

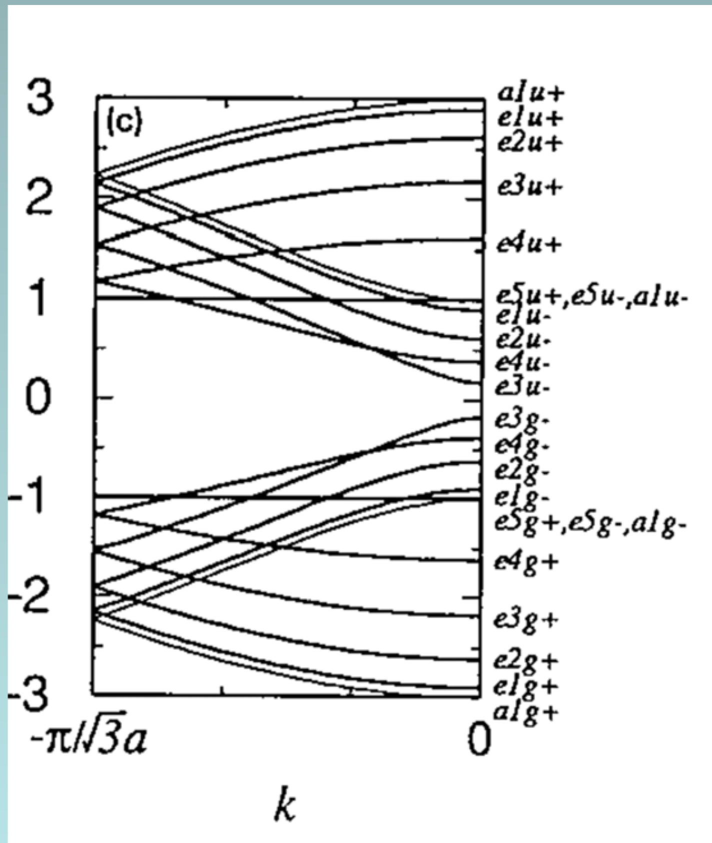

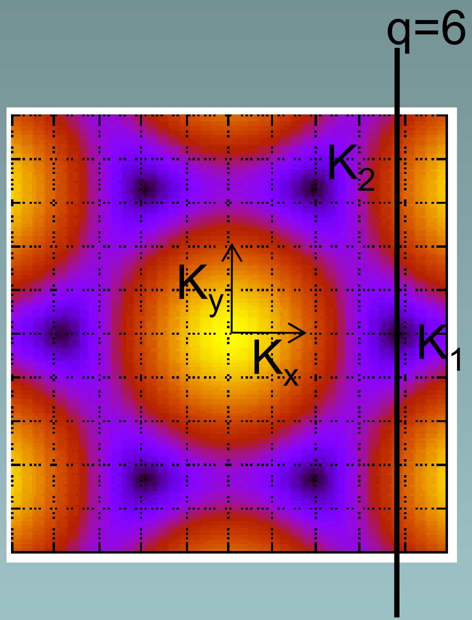

Zigzag CNT (9,0):

$$\boxed{\because k_x = \frac{2\pi q}{9\sqrt{3}a}} \quad ,-\frac{\pi}{3a} \le k_y \le \frac{\pi}{3a}$$

q=1,2…9

Slice through K_1 for q=6

⇒ Metallic conduction

$$\boxed{\begin{aligned} K_1 &= \frac{4\pi}{3\sqrt{3}a}(1,0) \\ K_2 &= \frac{4\pi}{3\sqrt{3}a}\left(\frac{1}{2},\frac{\sqrt{3}}{2}\right) \end{aligned}}$$

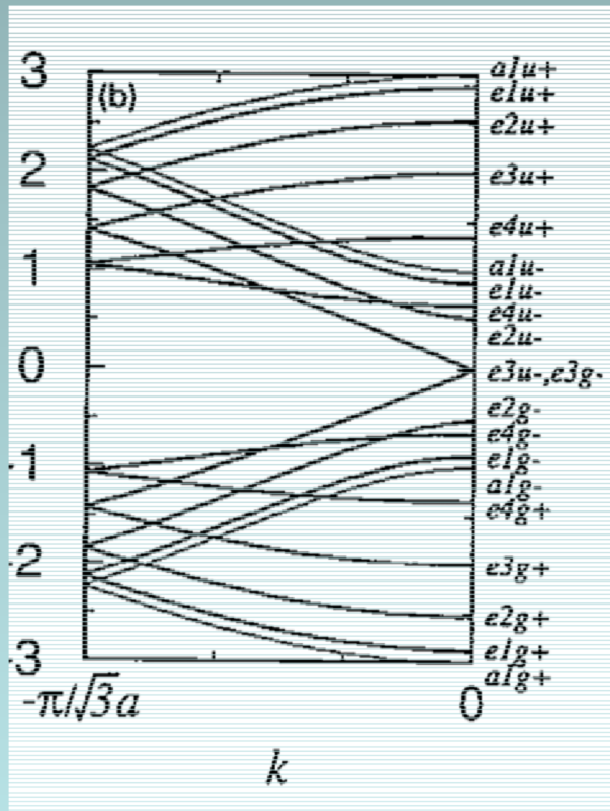

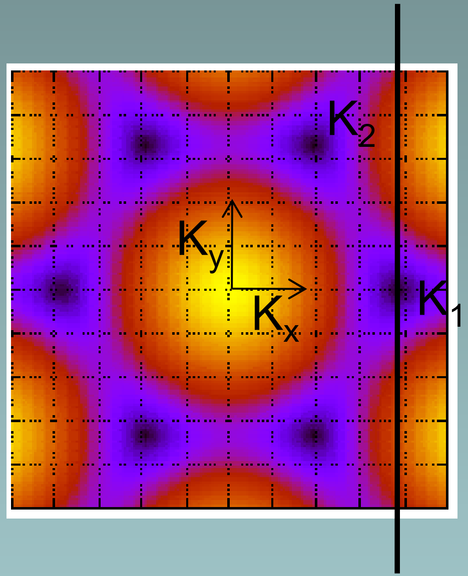

Zigzag CNT (N_x,0):

$$\because k_x = \frac{2\pi q}{N_x \sqrt{3} a}$$

q=1,2…N_x

- N_x : multiple of 3
  always Slice through K_1

⇨ 1/3 of Zigzag tube is metallic !!

$$K_1 = \frac{4\pi}{3\sqrt{3}a}(1,0)$$

$$K_2 = \frac{4\pi}{3\sqrt{3}a}\left(\frac{1}{2}, \frac{\sqrt{3}}{2}\right)$$

In general, metallic for n-m = multiple of 3
Magic number “3” in CNTs !!

Triangular lattice

Part III: Concluding remark

- Label for a CNT (n,m)
- Mass production of CNTs using plasma enhanced CVD
- 1-D band structure of CNTs : slicing 2-D band structure of graphene
- 1/3 of the CNTs with random (n,m) is metallic.
- Application : CNT FETs, chemical sensors,
  Fuel cell storage medium, mechanical reinforcement

Part IV

Topological insulator and the search for Majorana fermions in condensed matter system

Wei-Li Lee, IoP AS

- Brief Review
- Connection of curvature to transport phenomena
- Identification of topologically protected surface states
  - Transport, ARPES…etc.
- The challenge of the growth of single-crystals and epitaxial thin films
  - Se(Te) losses, highly sensitivity to air/moisture
- Doped topological insulator
  - Topological superconductor (SC), ferromagnetic topological insulator
- The pursuit for Majorana fermion in solid state system

Chern number and curvature

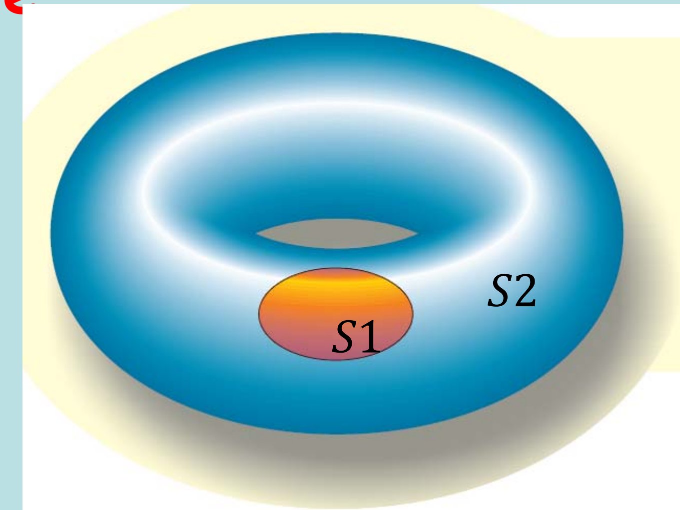

- Gauss-Bonnet (GB) formula:

$$\frac{1}{2\pi}\int_S KdA = 2\,(\,1 - g\,)$$

K : local curvature of a surface
g : # of handle

- Generalization of GB formula to geometry of eigenstates in parameter space

$$\frac{1}{2\pi}\int_S KdA = Chern\ number$$

$K = 2\,Im\langle\partial_\Phi\psi|\partial_\theta\psi\rangle$ local adiabatic curvature (Berry's curvature) with a Hamiltonian H(Φ,θ)

Considering a small loop

Berry's phase

$$\frac{1}{2\pi}\int_{S2} KdA + \frac{1}{2\pi}\int_{S1} KdA = \frac{1}{2\pi}\oint_{C_{out}} X\cdot d\ell + \frac{1}{2\pi}\oint_{C_{in}} X\cdot d\ell = \frac{2\pi\times(integer)}{2\pi}$$

$\boxed{\text{as S1} \rightarrow \text{0, Chern number is also an integer !}}$

Quantized Hall conductivity

- Hall effect Hamiltonian H(Φ,θ)

  Φ: *emf that drives the Hall current*

  Expectation value of Hall current

$$\langle\psi|I|\psi\rangle = \hbar c K \dot{\Phi}$$

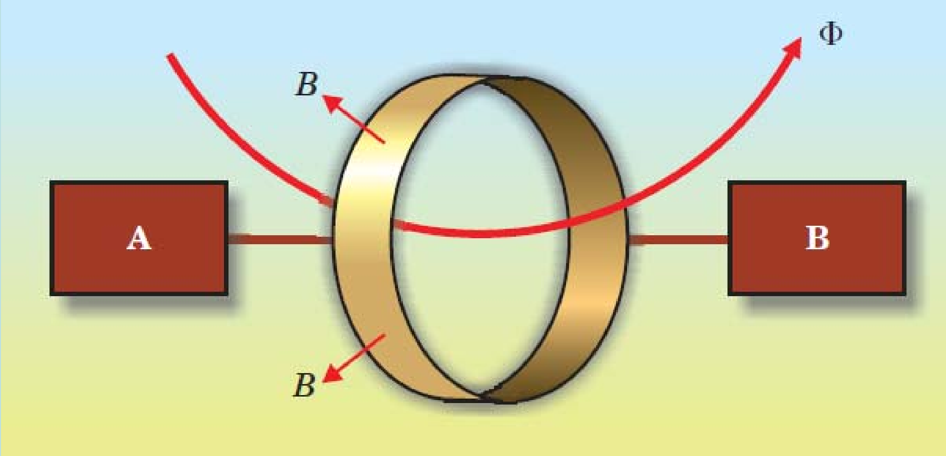

- Hall conductance as the curvature

$$\boxed{Hall\ conductance = \ \hbar c K}$$

- Integrate over a complete band

Hall conductance $\propto \frac{1}{2\pi}\int_S \ KdA = Chern\ number$

$$\boxed{\sigma_{xy} = n\frac{e^2}{h}, \quad \mathrm{n:integer.}}$$

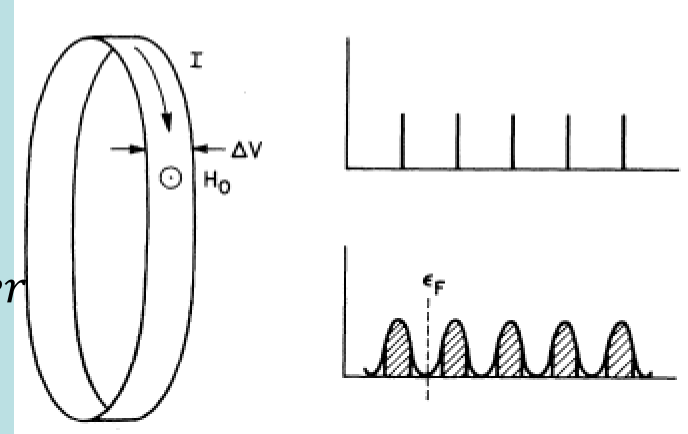

FIG. 1. Left: Diagram of metallic loop. Right: Density of states without (top) and with (bottom) disorder. Regions of delocalized states are shaded. The dashed line indicates the Fermi level.

-- Laughlin, Phys. Rev. B 81’

Surface (Edge) states in a Quantum Hall system

Ideal 2DEG with finite system size
Under high magnetic field

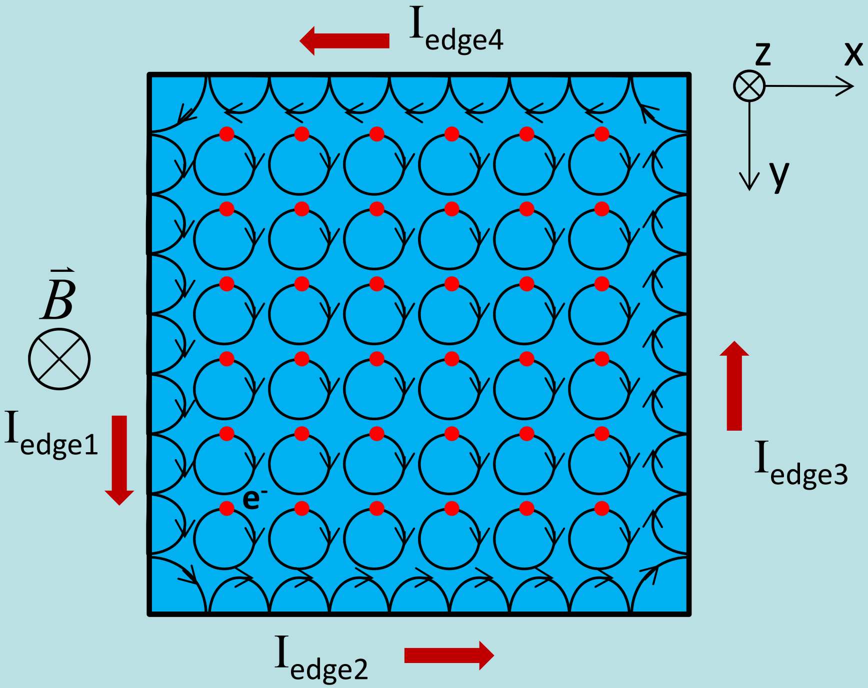

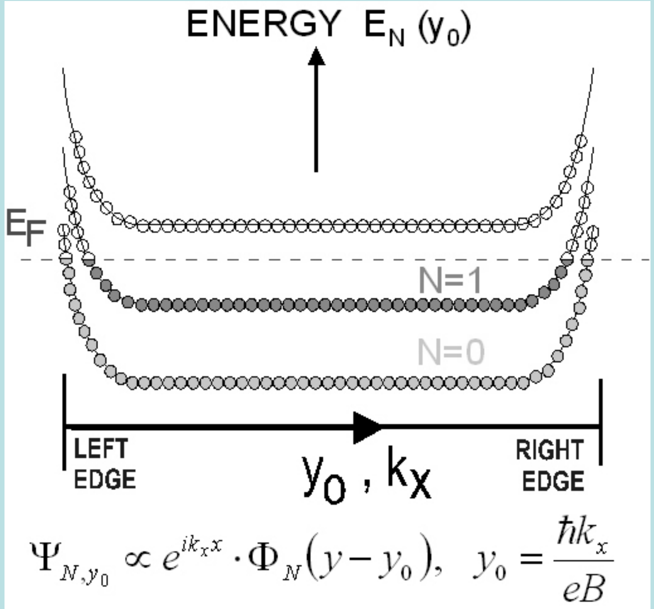

$$\boxed{\vec{j} = \vec{\sigma}\vec{E} + \vec{\alpha}(-\vec{\nabla}T)}$$

- Incompressible when E_F falls in the gap b/w LLs
  $\rho_{xx}=\sigma_{xx} = 0$ and $\sigma_{xy} = ne^2/h$
- In the absence of external bias, no net I_{edge}
- When there is a potential difference δVx, $\delta I_y = I_{edge1} - I_{edge3}$, is quantized.

$$\delta I_y = ne^2/h\,\delta V \rightarrow \sigma_{xy} = ne^2/h$$

- Similarly, for a temperature difference δTx, universal value in α_{xy} ?

$$\alpha_{xy} \equiv J_y/(-\nabla_x T) = (k_B e/h)\ln 2 \approx 2.32\ \text{nA/K}$$

-- Halperin, PRB 82'
-- Girvin *et al.*, PRB 84'
-- Checkelsky *et al.*, PRB 09'

Topological metallic states at the surface (edge)

- Skipping orbitals (chiral) at the edge of a quantum Hall system under intense field

B ≠ 0

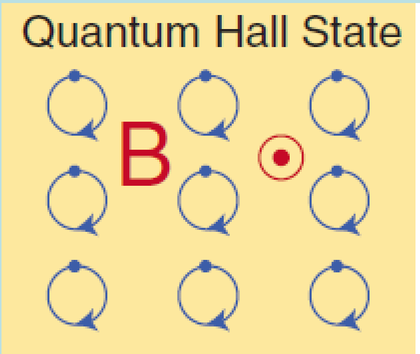

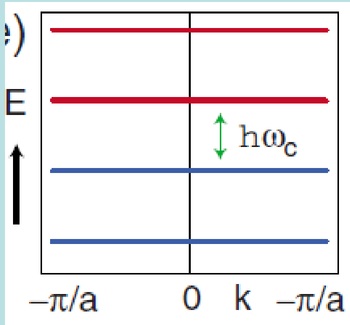

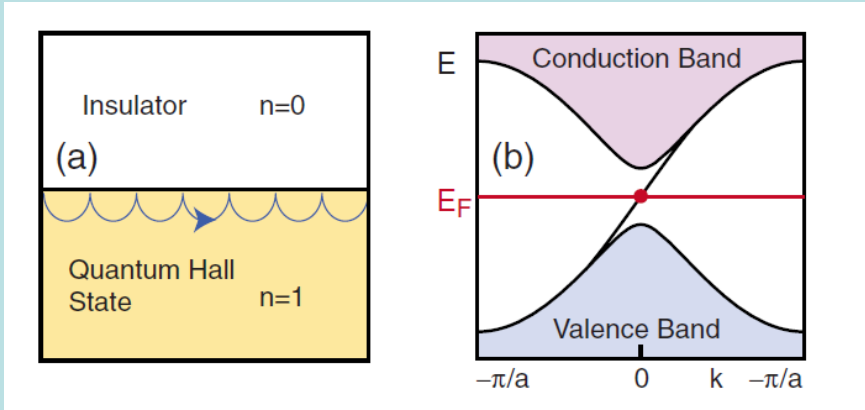

- Counter propagating spin channels at the edge of a quantum spin Hall system in zerc

B = 0 and time reversal symmetric system

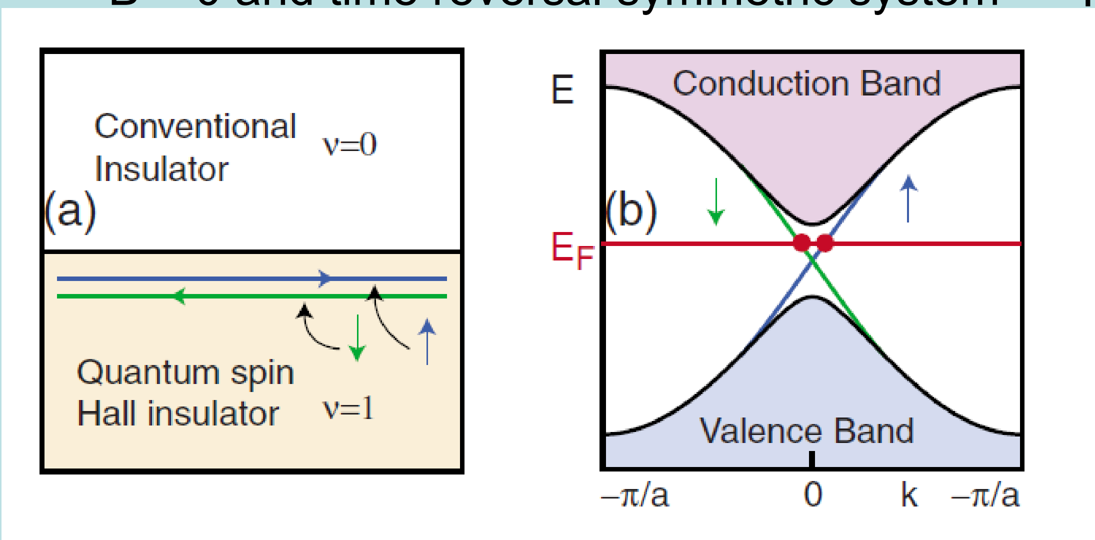

Time reversal sym. prevent gap form

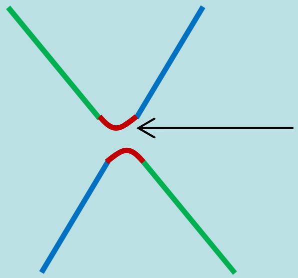

Violate
Kramer's degenercy

helical surface states : Chiral + spin-orbit interaction (SOI)

- Dirac cone and Berry's phase π

$$\mathcal{H}_{surf.} = \hbar v_F \vec{k} \times \hat{n} \cdot \vec{s}$$

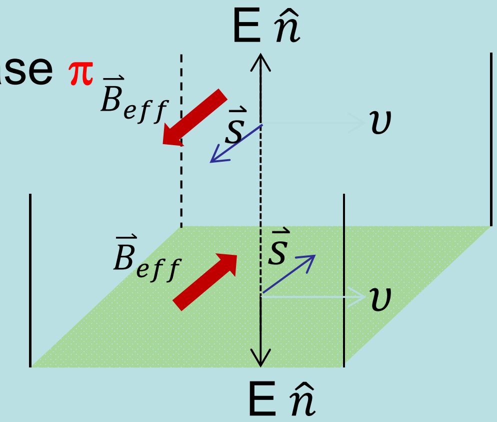

SOI

$$B_{eff} = v \times E\hat{n}$$

Massless Dirac fermion
With opposite chirality on
Opposite surfaces of a TI !

Berry's phase

$$\gamma(C) = \iint_C K \cdot d\vec{S} = \frac{1}{2}\Omega(C) = \pi$$

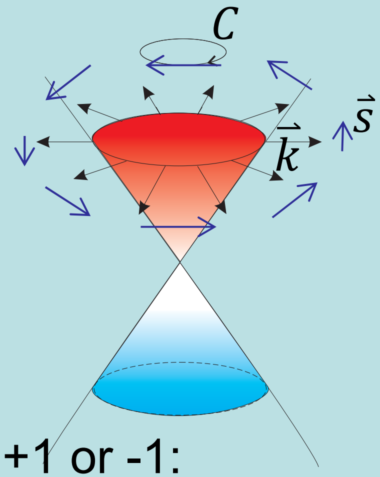

Parallel transport of vector v on curved surface

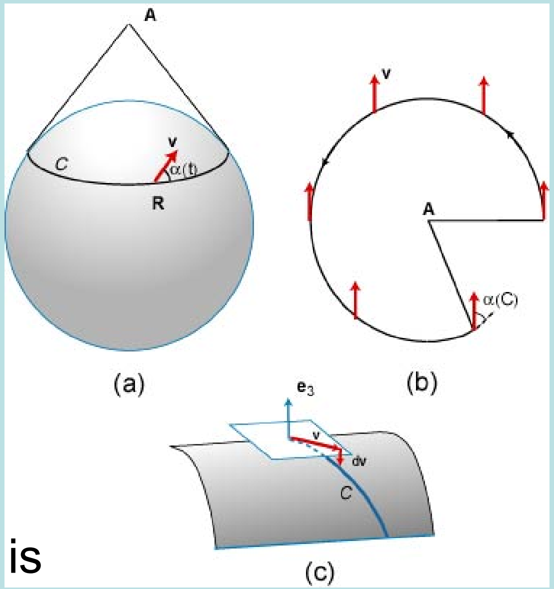

- Well-defined chirality: $\sigma \cdot p = +1$ or -1:

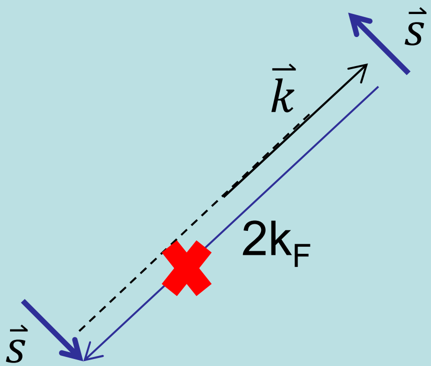

Back-scattering ($2k_F$)
by non-magnetic impurity is
suppressed !!

2-D Quantum Spin Hall Phase

Kane and Mele, PRL '05
Bernevig et al., Science '06
Konig et. al., Science '07

Quantum Spin Hall Effect in Graphene

C. L. Kane and E. J. Mele
Dept. of Physics and Astronomy, University of Pennsylvania, Philadelphia, Pennsylvania 19104, USA
(Received 29 November 2004; published 23 November 2005)

Quantum Spin Hall Insulator State in HgTe Quantum Wells

Markus König,[1] Steffen Wiedmann,[1] Christoph Brüne,[1] Andreas Roth,[1] Hartmut Buhmann,[1] Laurens W. Molenkamp,[1*] Xiao-Liang Qi,[2] Shou-Cheng Zhang[2]

2-D system
Time-reversal symmetry (TRS) + spin-orbit coupled

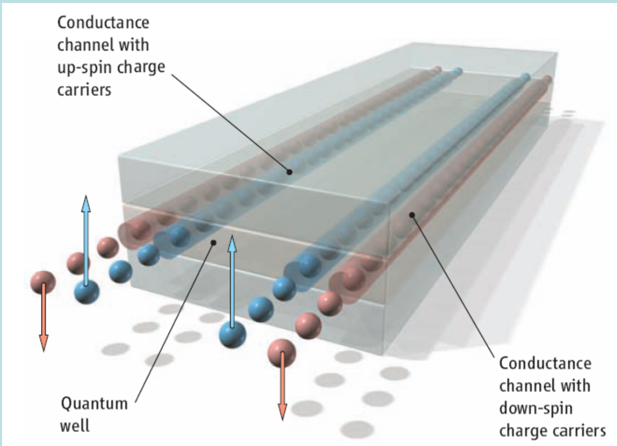

Schematic of the spin-polarized edge channels in a quantum spin Hall insulator.

Backscattering by non-magnetic impurity is suppressed.

CdTe-HgTe-CdTe quantum Well

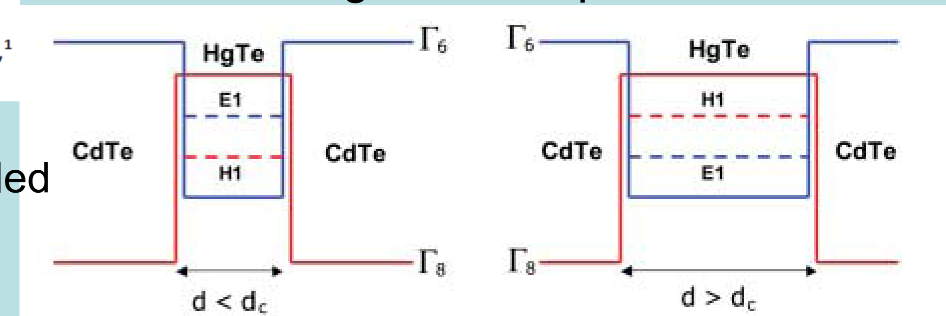

d_c ~ 6.3 nm

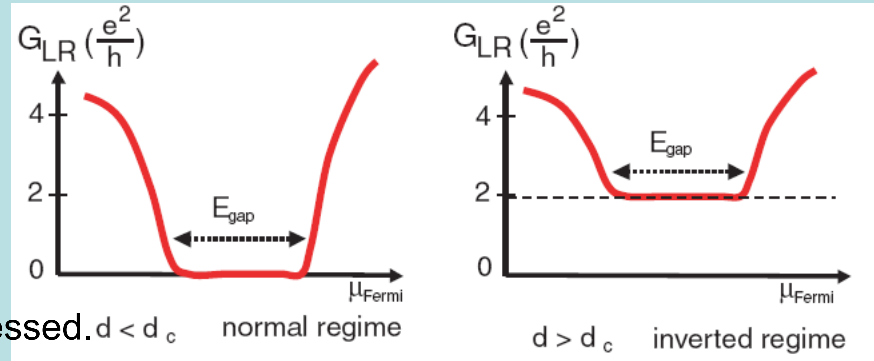

I : d=5.5 nm, II & III & IV : d = 7.3nm

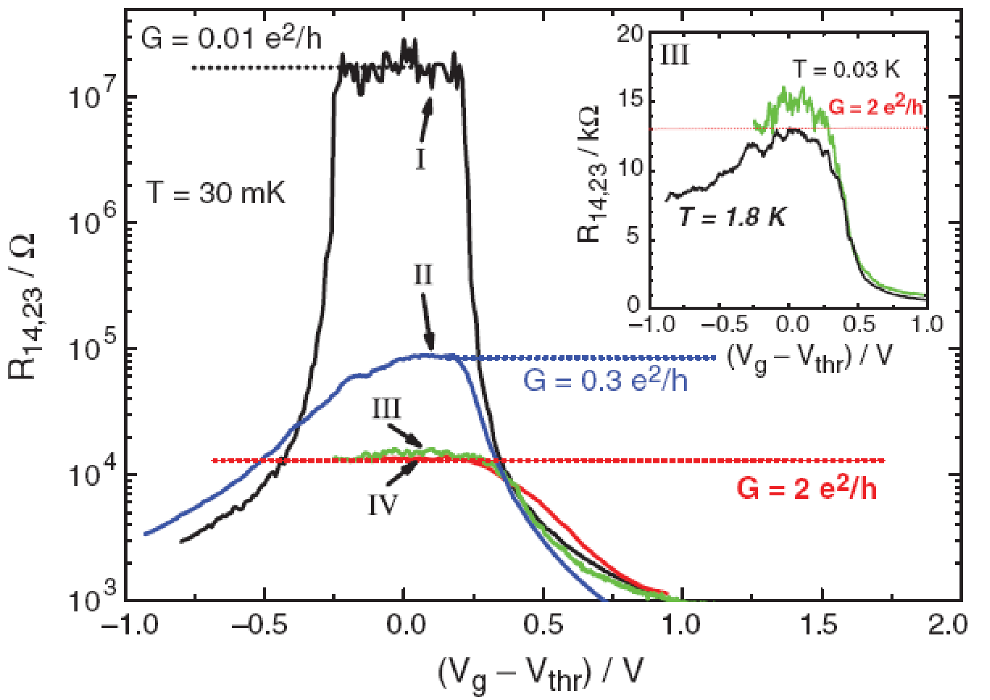

Breaking of TRS by B

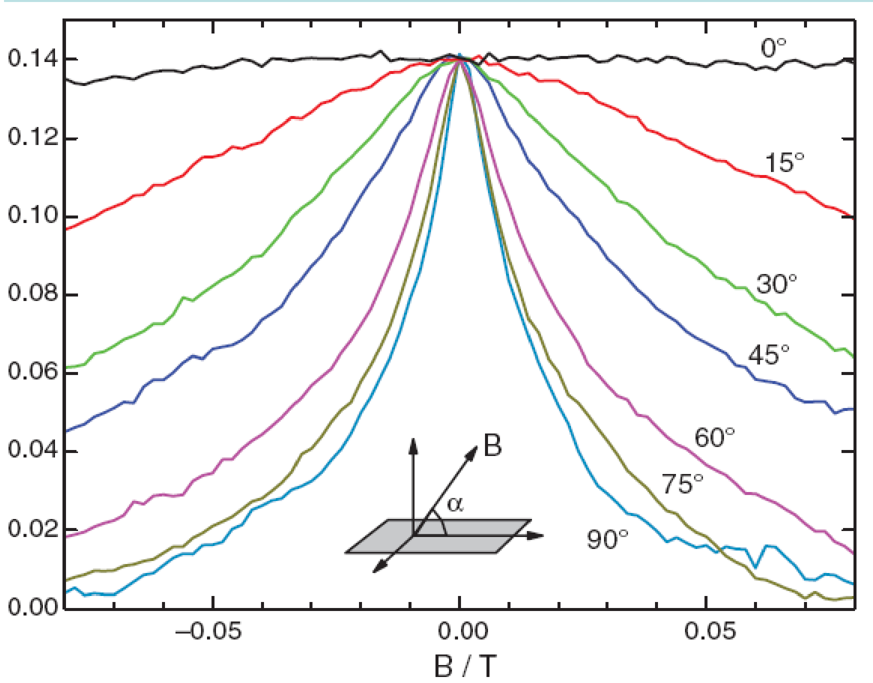

3-D Topological Insulator (TI)

Xia et al., Nature Phys. ’09
Hsieh et al., Nature ’09
Zhang et al., Nature Phys. ‘

$Bi_{0.9}Sb_{0.1}$

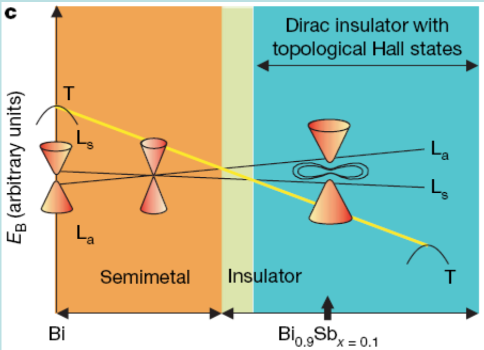

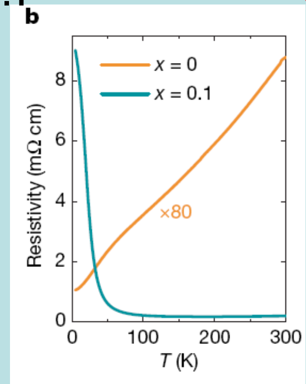

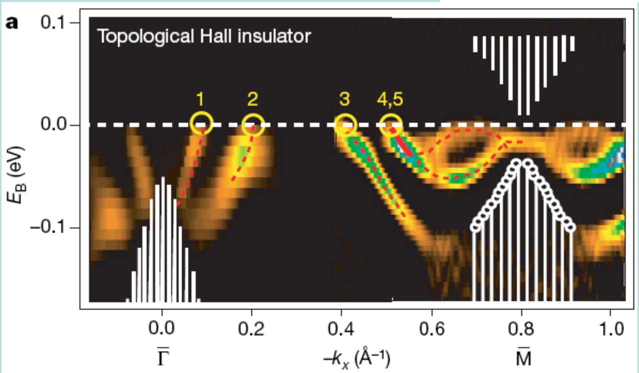

5 crossing points at E_F for surface states
Topological nontrivial (Z_2)

Hsieh et al., Nature ’08
Hsieh et al., Science ‘09

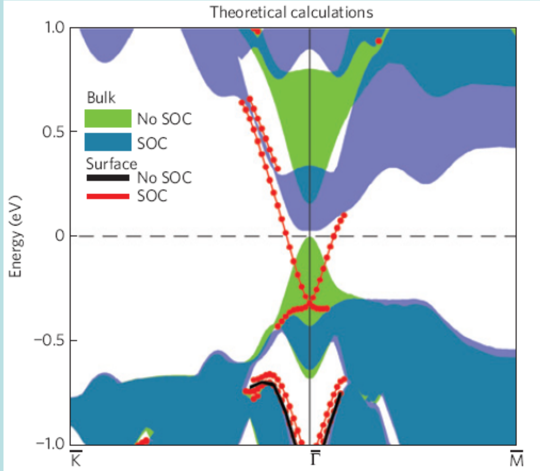

Bi_2Se_3

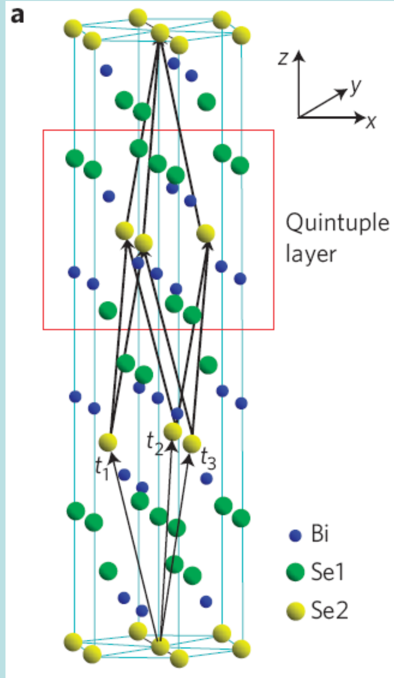

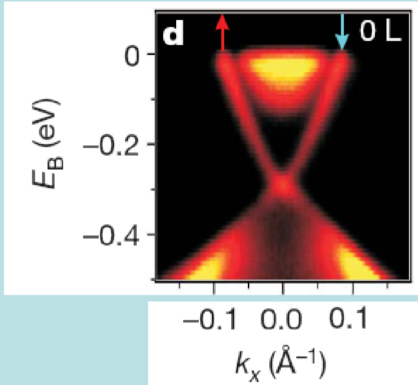

Single Dirac cone and spin-polarized surface states
Same for Bi_2Te_3, Bi_2Te_2Se, Sb_2Te_3, $TlBiSe_2$

Chen et al., Science ’09
Kuroda et al., PRL ’10
Zhang et al., Nature Phys. ’09
Ren et al., PRB ‘10

Hsieh et al., Nature ’09
Sobota et al., PRL ‘12

How to Characterize a TI ?

- An insulator that conducts : gapless surface states
- Angle-resolved photo-emission (ARPES), spin-resolved ARPES :

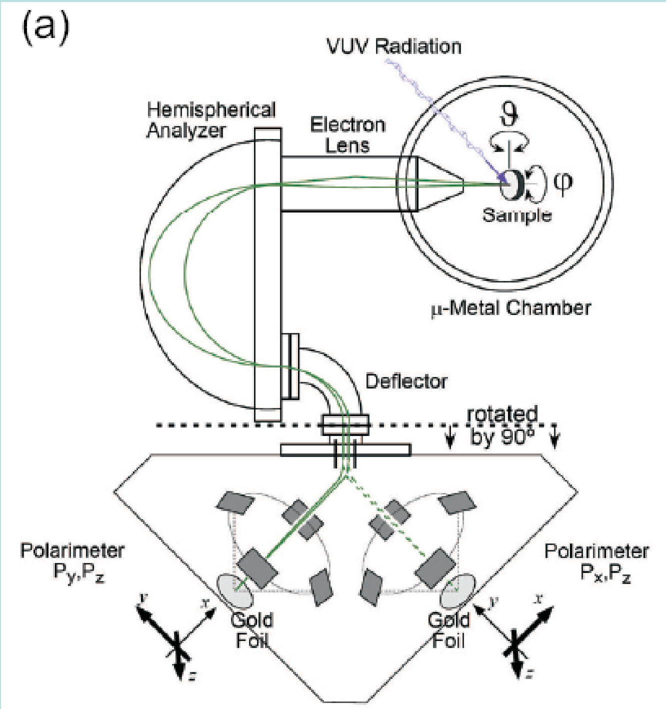

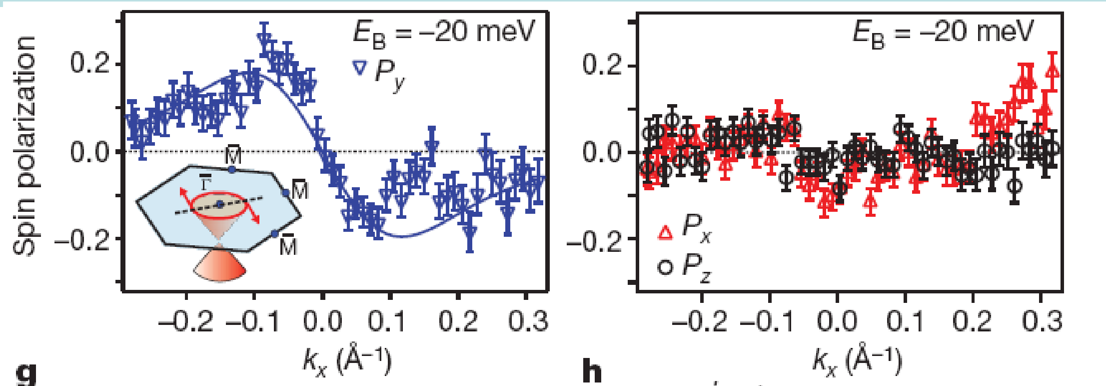

Spin-momentum Locking !

Angular uncertainty ~ ± 10^o

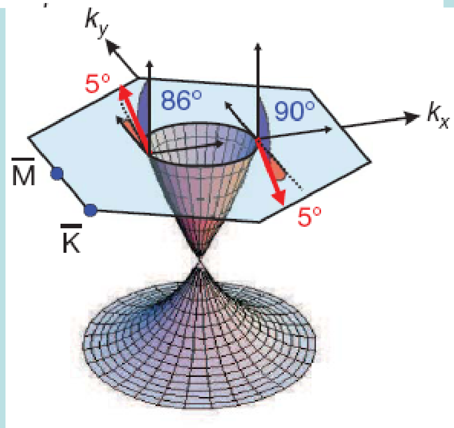

- Time-resolved and Angle-resolved photo-emission (trARPES)

Pump: 1.5eV , 50 fs
Probe: 6eV, 160 fs

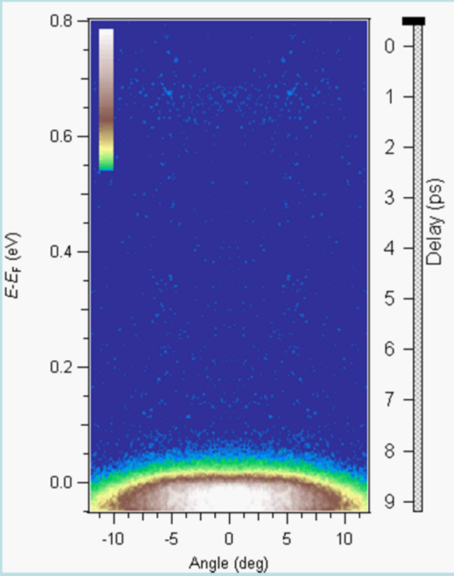

Transient electron dynamics in p-typed Bi2Se3

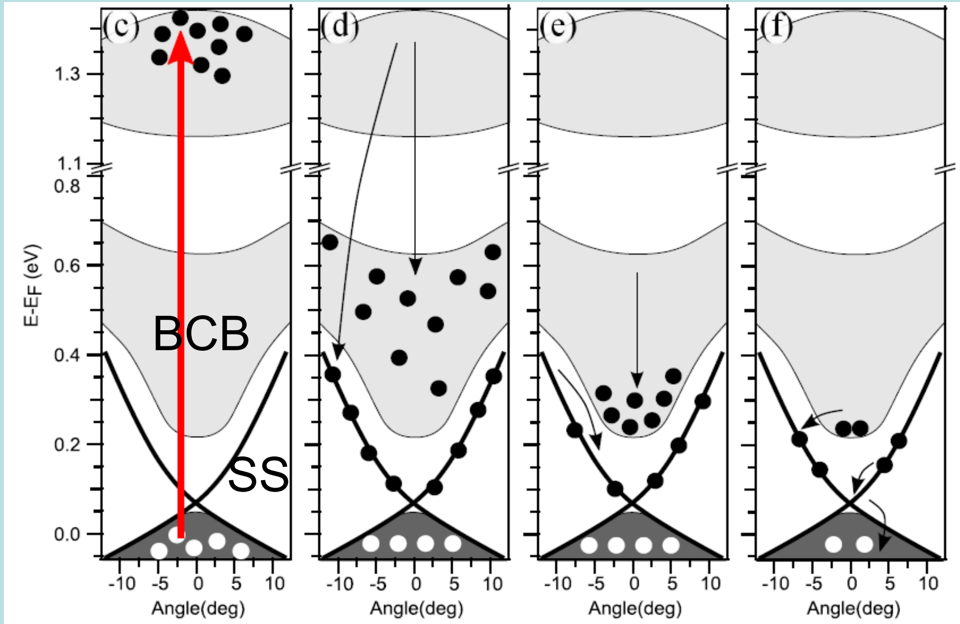

- Filling of SS state from BCB
- Long-lived SS states > 10 ps
- Enhanced ratio of photoexcited surface carriers to bulk carriers (penatration depth ~ 50 nm)
- Ideal for driving transient spin currents without significant bulk contribution

How to Characterize a TI ?

Qu et al., Science '10

- Quantum Oscillation:

Bi_2Te_3

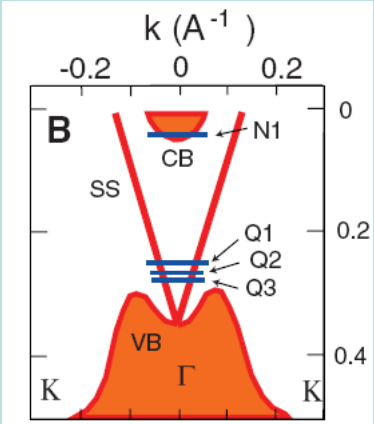

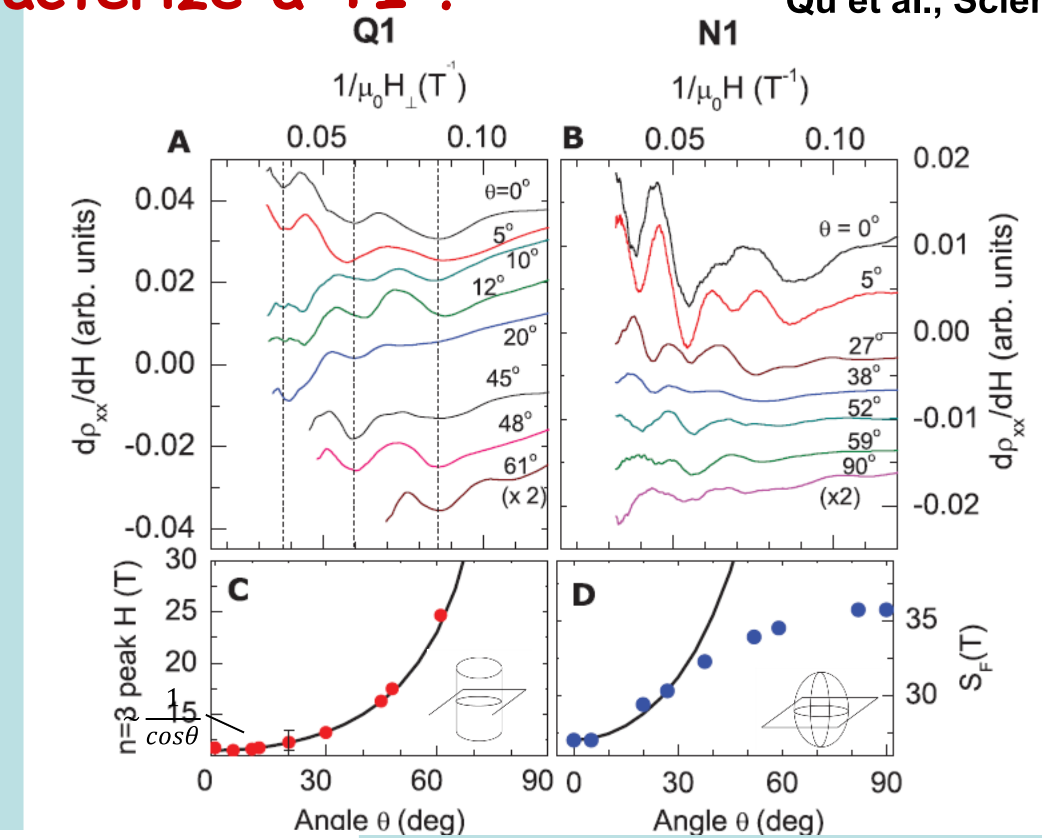

Hall anomaly

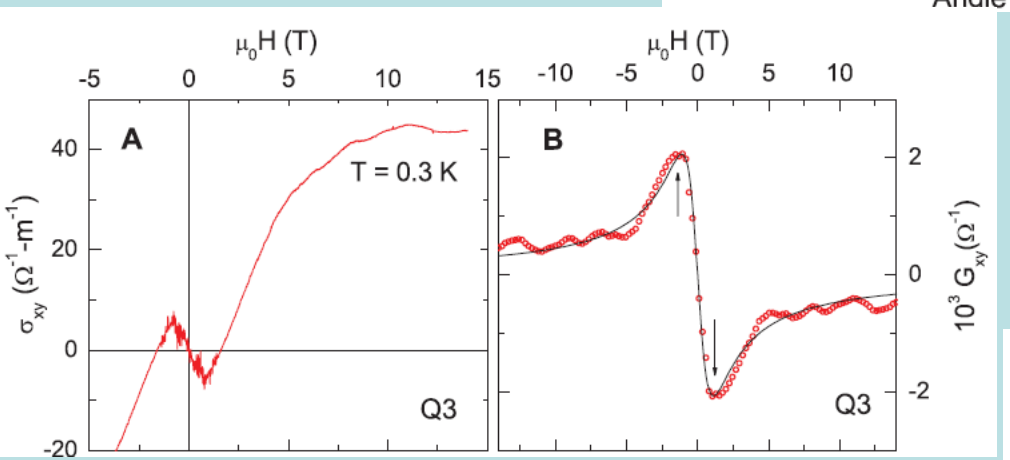

$$\sigma_{xy} = \sigma_{xy}{}^{bulk} + G_{xy}/\mathrm{t}$$

$$G_{xy} = \frac{2\pi e^3}{h^2}\frac{B\ell^2}{[1+(\mu B)^2]}$$

2DEG conductance

units	S_F T	k_F Å^{-1}	E_F meV	$k_F\ell$ —	v_F 10^5 m s^{-1}
Q1	41.7	0.036	94	–	–
Q2	33.3	0.032	84	69	3.7
Q3	28.6	0.030	78	66	4.2
N1	23.3*	0.027	–	–	–

The Challenge of growing TI

Benia et al., PRL ’11
Chen et al., Science ’10
Hsieh et al., Nature ‘09

- Defects in Bi-based TI
  - ➢ Se and Te Vacancies : high vapor pressure
  - ➢ $Bi_{se(Te)}$ anti-sites
  - ➢ Bi intercalation in van de Waals gap
- Chemical instability at the surface :

  Water vapors (H_2Se gas): n-type doping

  Oxygen : p-type doping

Water exposure (L:Langmuir)

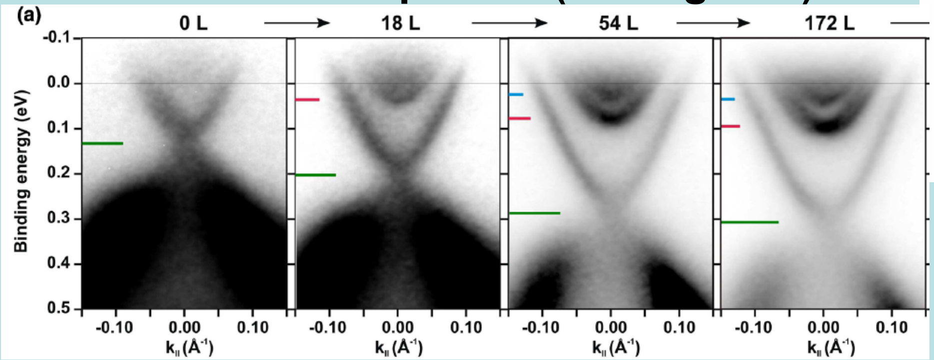

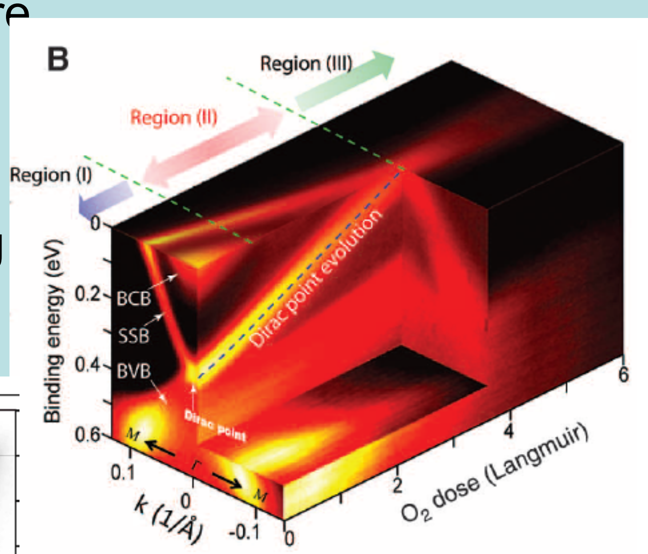

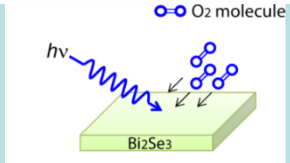

- Surface doping : additional quantum Well states with Rashba splitting
- Aging effect ?

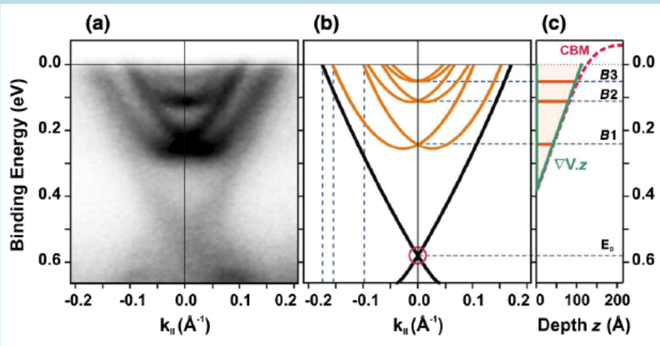

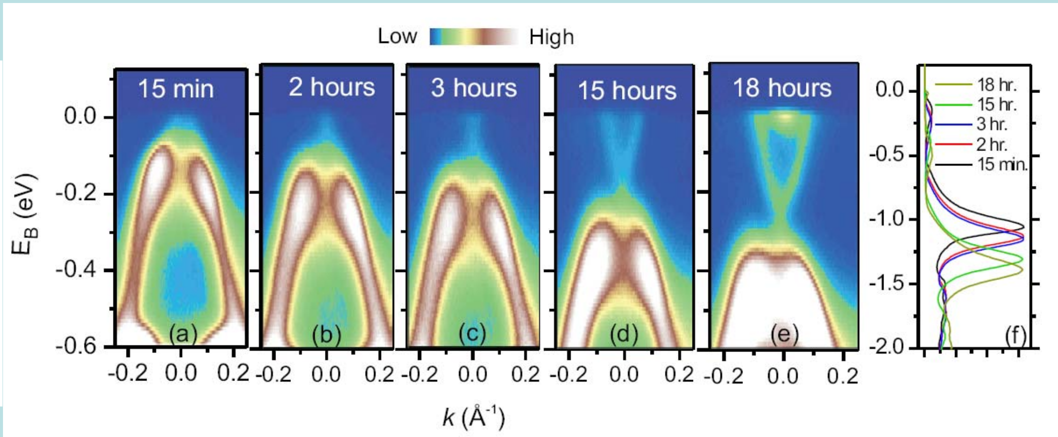

Magnetic Topological Insulator

- Magnetic doped TI : Massive Dirac Fermion at surface

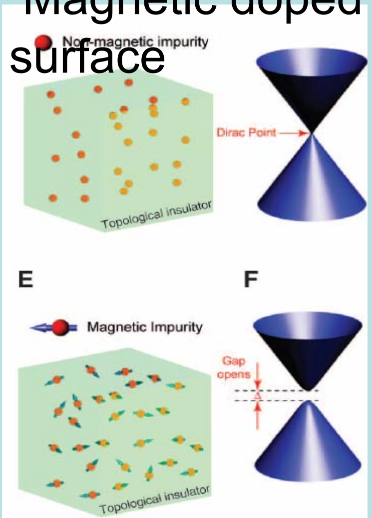

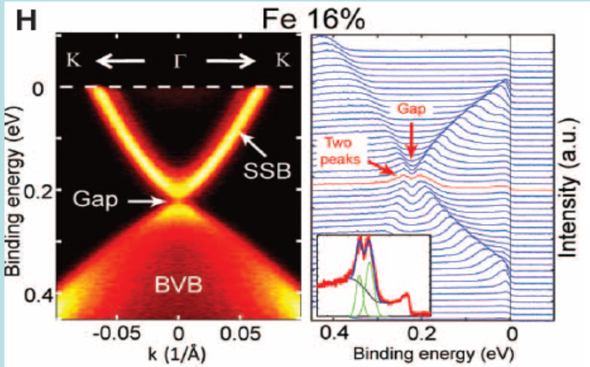

Breaking TRS !

Yu et al., Science '10
Chen et al., Science '10

- Insulating massive Dirac Fermions
- Quantized Anomalous Hall Effect
  $\sigma_{xy} = e^2/h$ at zero field ?
- Topological contribution to Faraday rotation and Kerr effect

…

- Quantized anomalous Hall effect in $Cr_{0.15}(Bi_{0.1}Sb_{0.9})_{1.85}Te_3$ epitaxial film by MBE

Chang et al., Science '13

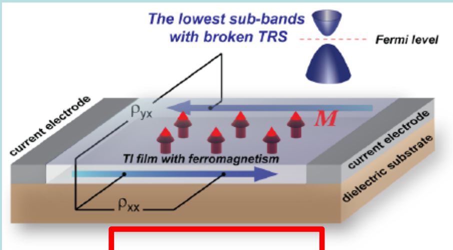

T_c ~ 15 K

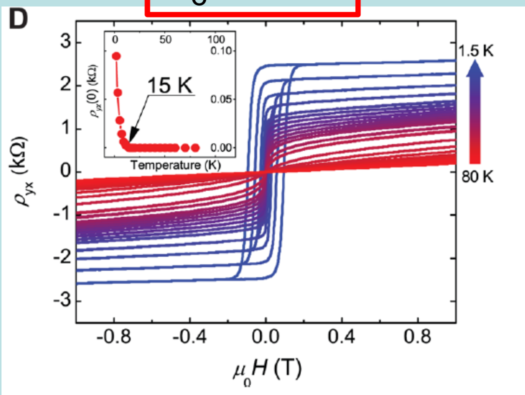

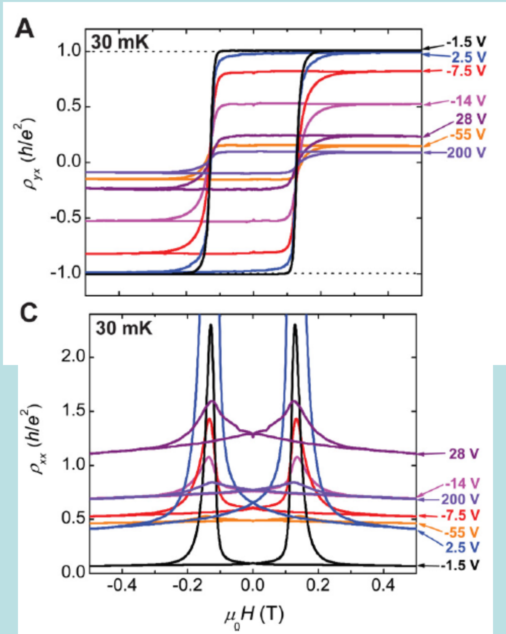

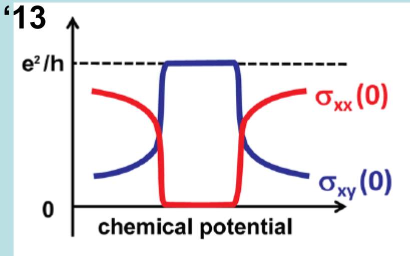

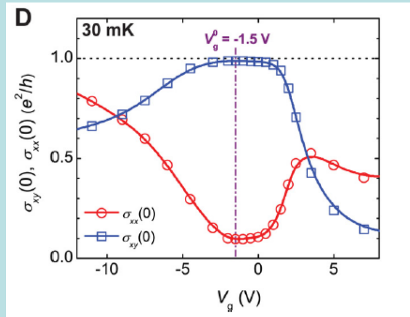

Quantized σ_{xy} in zero field !

Physical property in topological superconductor

- Topological superconductor : $Cu_xBi_2Se_3$

Hor et al., PRL ’10
Kriener et al., PRL ’11
Levy, et al., PRL ’13
Fu et al., PRL ‘11

Cu intercalated Bi_2Se_3

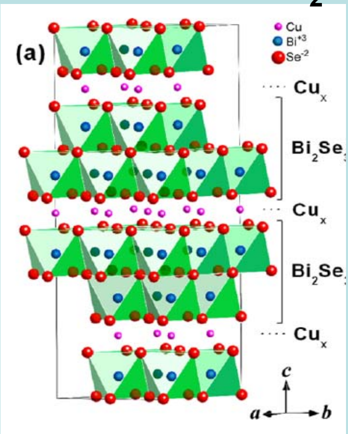

$Cu_{0.29}Bi_2Se_3$

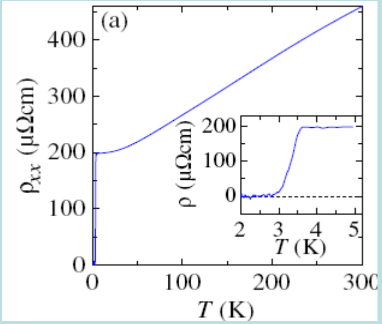

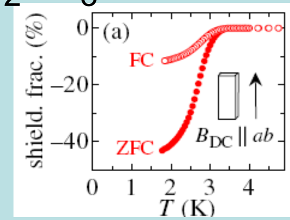

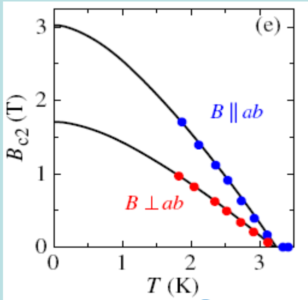

- **Fully Gapped SC**
- **P wave pairing symmetry ?**
- **Possible host for Majorana Fermions ?**
- **Zero-bias conductance peak ? (ZBCP)**

Point Contact experiment

ZBCP ? YES !

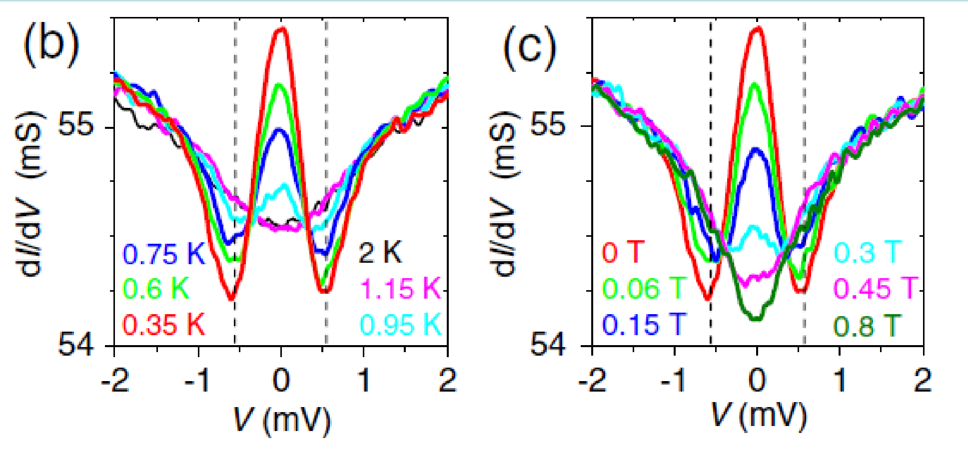

- **Sasaki et al., PRL ’11**
- **Kirzhner et al., PRB ‘12**

Scanning Tunneling experiment

ZBCP ? No !

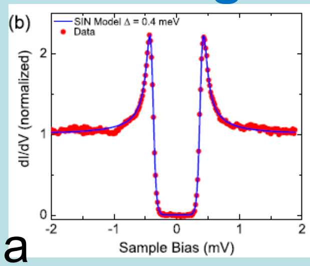

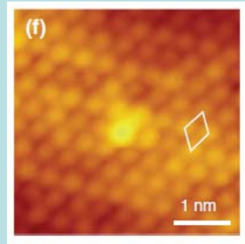

B = 1 Tesla

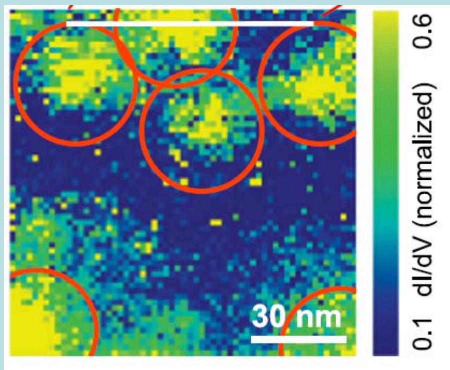

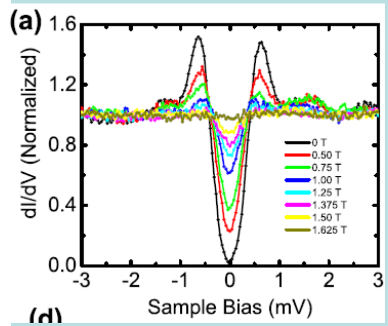

No ZBCP in the vortex core !

Spin-momentum lock in TI ?
100% spin polarization in surface states ?

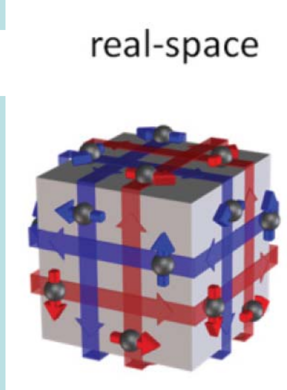

Spin- and angle- resolved photoemission spectroscopy (spin-ARPES)

- Experimental results range from 20% to 85%
- Both k-dependent (helical surface state) and
  k-independent (photoemission-specific effect) spin polarization
  were observed
- Inequivalence of quasiparticle and photoelectron spin in TI.
- Nontrivial spin-orbital texture: reduced spin polarization surface sta
  - ➢ layer-dependent spin-orbital entanglement
  - ➢ Interband scattering between Bulk band and surface state
  - ➢ Hexagonal warping of the band structure due to crystal symmetry
  - ➢ …

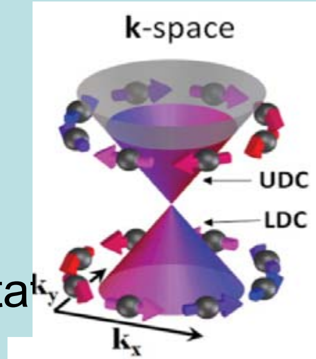

-Jozwiak et al., PRB 11
-Pan et al., PRL 11'
-Zhu et al., PRL 13'

Spin transport and spin valve study in T
More experimental works are needed !

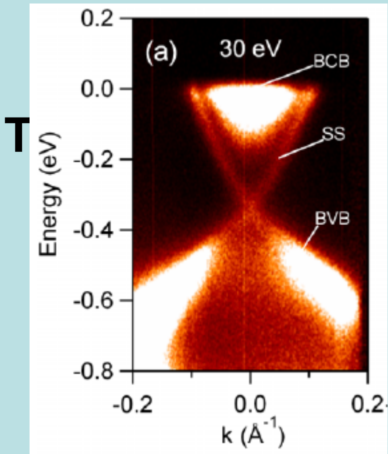

From spin-ARPES

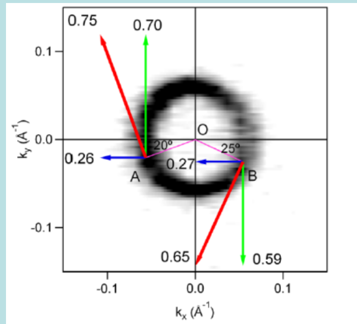

E = -0.1 eV

The pursuit for Majorana Fermions

Ettore Majorana in 1937

- Majorana fermion: particle that is its own antiparticle

$$\gamma_j = \gamma_j{}^{\dagger}, \qquad \{\gamma_i, \gamma_j\} = 2\delta_{ij}$$

A particle that has No charge and No spin !!

- Quasiparticle excitation in a superconductor:

Bogolubov quasiparticle

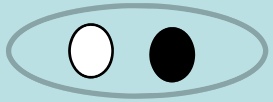

$$d = u\, c_{\uparrow}{}^{\dagger} + v\, c_{\downarrow} \quad \Rightarrow \quad d^{\dagger} = u^{*}\, c_{\uparrow} + v^{*}\, c_{\downarrow}{}^{\dagger}$$

Almost a Majorana fermion by NOT yet !

Now the only problem is the "spin"

- **Majorana bound states (zero modes) in Abrikosov vortices :**

$\gamma_j = c_j{}^{\dagger} + c_j$, only possible in **spin-triplet state** $|\uparrow\uparrow\rangle$

$\Rightarrow$ orbital p wave s wave + Dirac equation(Berry phase π)

"Spinless" p-wave superconductor

Kitaev's toy model

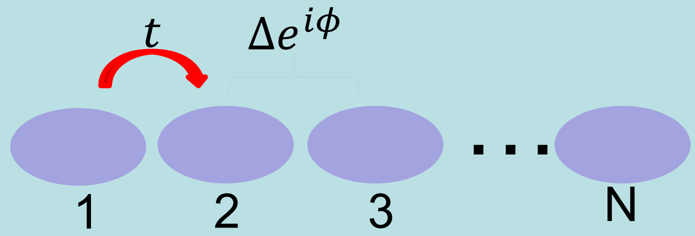

- **1-D** spinless p-wave superconductor

$$\mathcal{H} = -\mu \sum_{x=1}^{N} c_x{}^{\dagger} c_x - \frac{1}{2} \sum_{x=1}^{N} \left(t c_x{}^{\dagger} c_{x+1} + \Delta e^{i\phi} c_x c_{x+1} + H.C. \right)$$

chemical potential　　Spinless fermion operator

- Decomposition of c_x in terms of two Majorana fermions $\boxed{\gamma_{\alpha,x} = \gamma_{\alpha,x}{}^{\dagger}}$

$$c_x = \frac{e^{-i\phi/2}}{2} \left(\gamma_{B,x} + i\gamma_{A,x} \right)$$

$$\mathcal{H} = -\frac{\mu}{2} \sum_{x=1}^{N} \left(1 + i\gamma_{B,x}\gamma_{A,x} \right) - \frac{i}{4} \sum_{x=1}^{N-1} \left[(\Delta + t)\gamma_{B,x}\gamma_{A,x+1} + (\Delta - t)\gamma_{A,x}\gamma_{B,x+1} \right]$$

- In a limiting case of $\mu = 0$ and $t = \Delta \neq 0$,

Zero-energy Majorana modes: $\gamma_{A,1}$ *and* $\gamma_{B,N}$!

$$\boxed{\mathcal{H} = -\frac{it}{2} \sum_{x=1}^{N-1} \gamma_{B,x}\gamma_{A,x+1}}$$

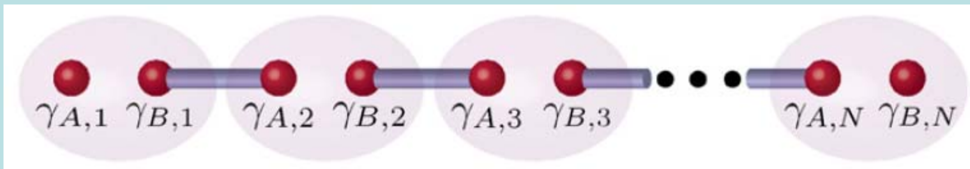

$$f = \frac{1}{2} \left(\gamma_{A,1} + i\gamma_{B,N} \right)$$

Highly non-local zero-energy fermion : non-abelian statistics

PRL **100,** 096407 (2008) PHYSICAL REVIEW LETTERS week ending 7 MARCH 2008

Superconducting Proximity Effect and Majorana Fermions at the Surface of a Topological Insulator

Liang Fu and C. L. Kane

Department of Physics and Astronomy, University of Pennsylvania, Philadelphia, Pennsylvania 19104, USA

(Received 11 July 2007; published 6 March 2008)

We study the proximity effect between an s-wave superconductor and the surface states of a strong topological insulator. The resulting two-dimensional state resembles a spinless $p_x + ip_y$ superconductor, but does not break time reversal symmetry. This state supports Majorana bound states at vortices. We show that linear junctions between superconductors mediated by the topological insulator form a nonchiral one-dimensional wire for Majorana fermions, and that circuits formed from these junctions provide a method for creating, manipulating, and fusing Majorana bound states.

$$\mathcal{H}_{surf.} = \psi^{\dagger}(-iv\vec{\sigma}\cdot\nabla - \mu)\psi + \Delta e^{i\phi}\psi_{\uparrow}{}^{\dagger}\psi_{\downarrow}{}^{\dagger} + \text{H.C.}$$

s-wave superconductor

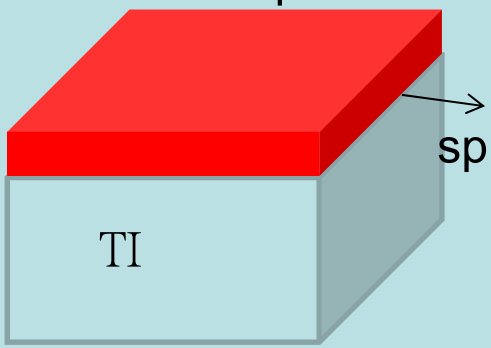

spinless p-wave S.C. at The interface !

Excitation spectrum

$$E_k = \pm\sqrt{\left(\pm v\left|\vec{k}\right| - \mu\right)^2 + \Delta^2}$$

resemble a spinless p_x+ip_y S.C. !!

Majorana Fermions in TI ?

Wilczek Nature Phys. '09
Reed and Green PRB '00
Fu et al., PRL '08

- **Heterostructure TI/*SC* :**

Proximity induced p-wave superconductivity at interface ?

-Wang et al., Science '12

The Coexistence of Superconductivity and Topological Order in the Bi_2Se_3 Thin Films

Mei-Xiao Wang,[1*] Canhua Liu,[1*] Jin-Peng Xu,[1] Fang Yang,[1] Lin Miao,[1] Meng-Yu Yao,[1] C. L. Gao,[1] Chenyi Shen,[2] Xucun Ma,[3] X. Chen,[4] Zhu-An Xu,[2] Ying Liu,[5] Shou-Cheng Zhang,[6,7] Dong Qian,[1†] Jin-Feng Jia,[1†] Qi-Kun Xue[4]

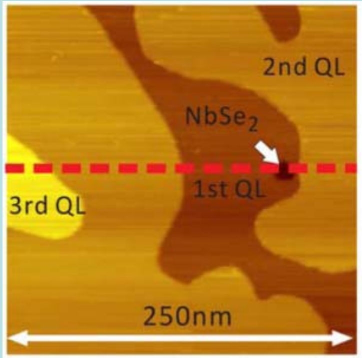

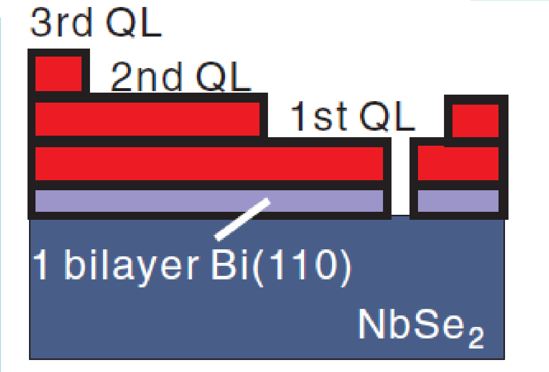

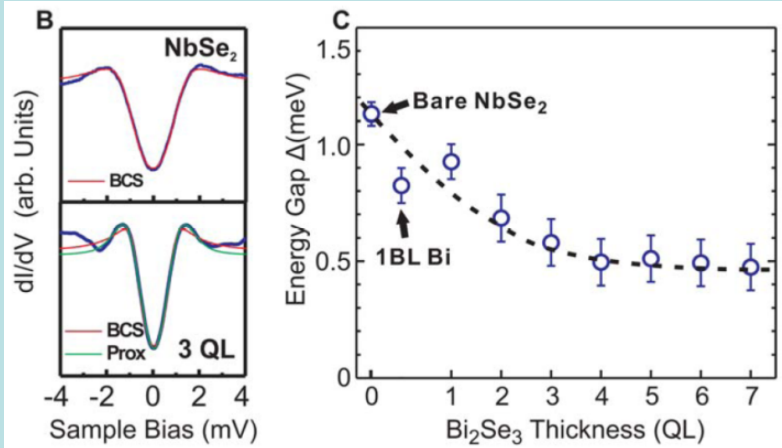

- ***SC/TI/SC* Josephson Junction**

-Williams et al., Arxiv '12

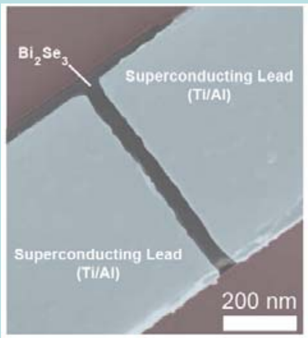

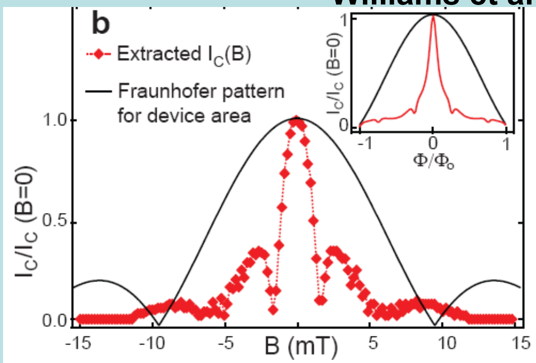

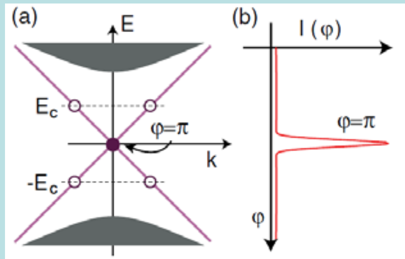

Anomalous peak due to netrual Majorana modes

- Au/InSb/NbTiN (N/NW/SC) junction: zero-bias conductance peak (ZBCP)

Signatures of Majorana Fermions in Hybrid Superconductor-Semiconductor Nanowire Devices

V. Mourik,[1]* K. Zuo,[1]* S. M. Frolov,[1] S. R. Plissard,[2] E. P. A. M. Bakkers,[1,2] L. P. Kouwenhoven[1]†

-Mourik et al., Science '12

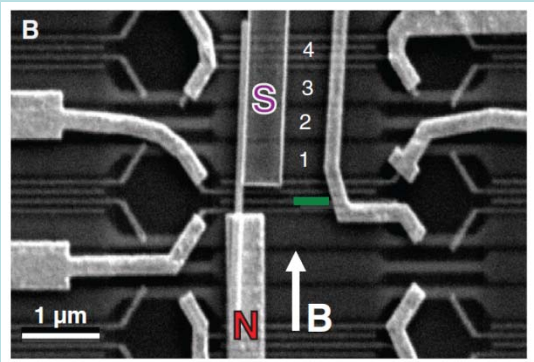

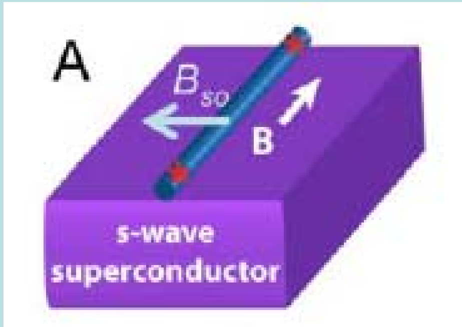

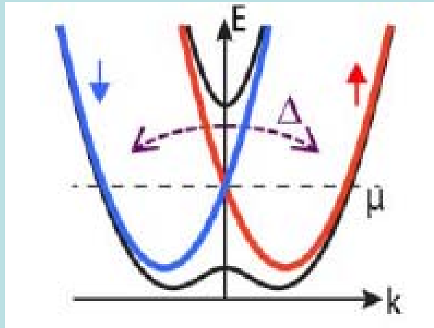

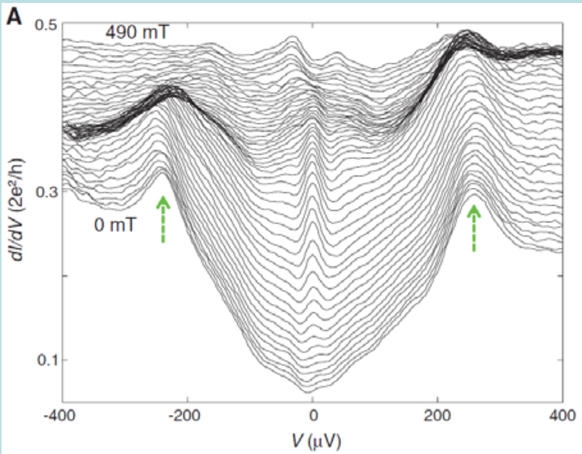

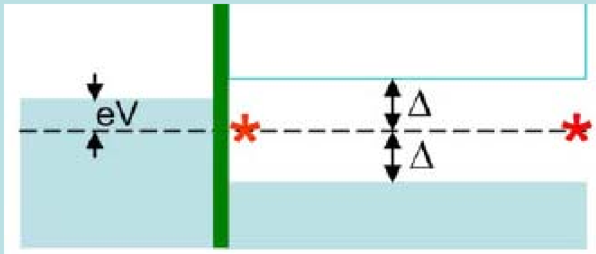

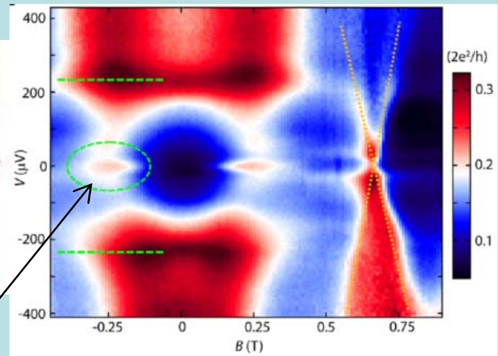

ZBCP is not quantized !

- Liu et al., PRL '12

Part IV: Conclusion

- Band curvature connection to transport phenomena
  - ✓ quantized Hall conductivity
  - ✓ gapless Dirac surface (edge) states
- 2D and 3D examples of topological insulator (TI)
- Magnetic doped (TI)
  - ✓ massive Dirac fermion
  - ✓ quanitzed anomalous Hall effect in zero field
- Superconducting (TI)
  - ✓ Copper doped TI
  - ✓ p-wave pairing mechanism ?
- The search for Majorana fermion in condensed matter
  - ✓ 1-D spinless superconductors
  - ✓ Quantized zero bias conductance peak
- Possible future application
  - ✓ Non-abelian statistics using Majorana bound states
  - ✓ Helical states for IC interconnect material
  - ✓ Helical states for spin eletronics

Summary

0D - Fullerene

- Fullerene structure : C_{20+h*2}
- An example of strongly correlated electronic system
  - Insulator – undoped C_{60}
  - Metallic – Alkali-doped C_{60}
  - Superconductivity – A_3C_{60} (A=K, Rb,CsK,RbCs)
- T_c increase linearly with lattice constant : BCS theory prediction

1D - Carbon nanotube

- Label for a CNT (n,m), 1/3 of the CNTs with random (n,m) is metallic.
- 1-D band structure of CNTs : slicing 2-D band structure of graphene
- Application : CNT FETs, chemical sensors,
  Fuel cell storage medium, mechanical reinforcement

2D - Graphene

- Chiral Fermionic excitation in single layer and bilayer graphene
- Unconventional QHE
- Phase coherent transport at the Dirac point
- Appearance of band gap in graphene nanoribbon, $E_g \sim 1/W$
- Novel phase near CNP at spin-polarized QH regime

Topological insulator

- 3D narrow bandgap semiconductor with strong spin-orbit interaction
- non-trivial band topology gives rise to the gapless surface state
- Surface states contain odd number of Dirac cones